NUCLEONICS VOL. 3, NO. 6, DECEMBER, 1948

An International Journal for Techniques and Applications of Nuclear Science

TECHNICAL CONSULTANTS

John R. Dunning, Clark Goodman, F. C. Henriques, Jr., A. Kalitinsky, R. E. Lapp, W. F. Libby, L. D. Marinelli, C. Rogers McCullough, L. A. Ohlinger, Winfield W. Salisbury, T. I. Taylor, E. O. Wollan

With the cooperation of . . .

THE NETHERLANDS — C. J. BAKKER
DENMARK and SWEDEN — GEORGE HEVESY
FRANCE — F. JOLIOT-CURIE
GERMANY — HANS KOPFERMANN
SWITZERLAND — P. SCHERRER

CONTENTS

Fission of Atomic Nuclei 2
B. C. PURKAYASTHA

Nuclear Physics and Low Temperatures 23
M. E. ROSE

Beta- and Gamma-ray Spectroscopy 32
GERALD J. HINE

Design of An Improved-Yield Discharge Tube 43
JAROSLAV PACHNER

Measurement of P^{32} and I^{131} Radiations with Dental Film 52
F. HERMANN RUDENBERG, RUSSELL F. COWING and CHARLES K. SPALDING

What Can Be Patented and How 70
WILLIAM R. BALLARD

Atomic Energy Commission Publications 73

INDEX to Volume 3 85

NUCLEONIC EVENTS 60
PRODUCTS AND MATERIALS 68
ABSTRACTS 77

Walter M. DeCew . . . . . Technical Editor
Jerome D. Luntz . . . . . Assistant Editor
Ethel Pelzer . . . . . Assistant Editor
Gladys Montgomery . Washington Editor
Keith Henney . . . . . Consulting Editor
E. J. Tangerman . . . . . General Manager

NUCLEONICS (with which is consolidated "Atomic Power" and "Atomic Engineering") December, 1948, Vol. 3, No. 6. Publication Office: 212 East York St., York, Pa. Editorial and Circulation Offices: 330 W. 42nd St., New York 18, N. Y. Published monthly by McGraw-Hill Publishing Company, Inc. Entered as second class matter December 17, 1947, in the Post Office at York, Pa., under the act of March 3, 1879. Copyright 1948 by McGraw-Hill Publishing Company, Inc. All rights reserved. James H. McGraw, Jr., President; J. A. Gerardi, Secretary; Curtis W. McGraw, Treasurer. Allow at least ten days for change of address. All communications about subscriptions should be addressed to J. E. Blackburn, Jr., Director of Circulation, 330 W. 42nd St., New York 18, N. Y. Price per copy $2. Subscription rates: United States and U. S. Possessions $15 a year. Canada and Latin America $20 a year. All other countries $25 a year. Return postage guaranteed. Member A.B.C.

FISSION OF ATOMIC NUCLEI—II

The second in a series of articles reviewing data available on nuclear fission. In addition to the chemistry of plutonium, the transuranates are discussed with the aid of a nuclear chart which demonstrates the usefulness of the isotope number in predicting properties of existing and missing isotopes

By B. C. PURKAYASTHA

Institute of Nuclear Physics, Calcutta University, Calcutta, India

IN THE FIRST article* of this series, the historical background of the discovery of neptunium, plutonium, americium and curium, along with some of their chemical properties, was discussed. Also outlined were the use of ultramicrochemistry in this field and the electronic structure of the actinide series. The present article will concern itself with the details of the chemistry of plutonium and a further discussion of the transuranics. The description of the former is based mainly on publications of the Canadian school [Harvey (*50*, *52*), Harvey, *et al.* (*51*), and Betts (*53*)].

CHEMISTRY OF PLUTONIUM

It has been mentioned previously that plutonium, the most important member of the actinide group, exhibits tri-, tetra-, penta- and hexavalencies and that the lower oxidation states tend to be more stable than in the case of neptunium or uranium. A few typical experiments demonstrating the tri-, tetra- and hexavalent states of plutonium are mentioned below (*51*).

That plutonium is most stable in its tetravalent state was shown by weighing a sample of $Pu(IO_3)_4$ and igniting it to the oxide. The loss in weight agreed exactly with the reaction $Pu(IO_3)_4 \rightarrow PuO_2 + 2I_2 + 5O_2$. That tetravalent plutonium reduces to trivalent state was shown by two typical experiments. In the first, iodine generated in the reaction:

$$Pu^{+4} + nI' \rightarrow Pu^{+(4-n)} + \frac{n}{2} I_2$$

was estimated and the value of n was found to be unity. In the second experiment, the potential of a platinum electrode was measured in solution containing Pu^{+4} and the lower valency state. The potential value was found to satisfy the Nernst equation:

$$E = E_0 + \frac{RT}{nF} \ln \frac{Pu^{+4}}{Pu^{+(4-n)}}$$

when n was set equal to unity. That tetravalent plutonium oxidizes to the hexavalent state was shown by direct permanganate titration.

The detailed information on these valency states has been gathered from the study of electrode potentials, the measurement of absorption spectra in solution and from the chemical properties of the typical compounds.

Electrochemical Study

Polarographic investigations constitute the most important studies made in the field of electrochemistry of plutonium. The usual form of the mer-

* NUCLEONICS **3**, No. 5, 2 (1948).

cury dropping electrode is replaced by a platinum micro-electrode, since, at the potential employed, mercury dissolves anodically. The capillary constriction is replaced by a sintered glass plug. With the micro-electrode a volume of 0.2 ml is sufficient for experiments (*51*).

Figure 5* shows polarograms for plutonium in N HCl, N $HClO_4$ and N H_2SO_4 (*53*). In each case a suitable reference electrode was chosen. Polarographic reduction waves in Pu^{+4} solution were found in a range of +0.75 to +0.95 volts (on the hydrogen scale), the exact value depending on the nature of the acid employed. The slope of the steeply rising portions of these curves corresponds to that for one electron transfer and hence we have the electrochemical reaction: $Pu^{+4} + e \rightarrow Pu^{+3}$. The polarogram for Pu^{+3} is also shown in the same figure. The reaction $Pu^{+3} \rightarrow Pu^{+4} + e$ occurs at nearly the same potential as the reverse reaction: $Pu^{+4} + e \rightarrow Pu^{+3}$. This means that the reaction is reversible ($Pu^{+4} \rightleftharpoons Pu^{+3}$) in an electrochemical sense. A glance at the polarogram will show that above 0.95 volts there is evidence for Pu^{+4} being oxidized to the hexavalent state. It will be further observed from the figure, that the potential value for $Pu(ClO_4)_4$ lies midway between the values for $Pu(SO_4)_2$ and $PuCl_4$. It has been argued that if, as is quite likely, perchlorate ion does not complex with Pu^{+4} or Pu^{+3}, the shift in potential implies that SO_4 complexes with the oxidized form of the couple, Pu^{+4}, whereas Cl′ is in complex combination with the reduced form Pu^{+3} of the couple.

The standard electrode potential of the system $Pu^{+3} \rightleftharpoons Pu^{+4}$ was measured by Harvey, *et al.*, (*51*) by use of the cell:

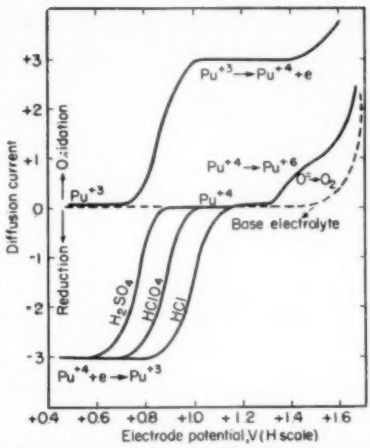

FIG. 5. Polarograms for Pu III and Pu IV (schematic)

It was found that the potential varies linearly with $\log(C_1/C_2)$. The value found for $Pu^{+3} \rightarrow Pu^{+4}$ couple is about −0.72 volts. The value is about the same as that of the well-known $Fe^{+2} \rightarrow Fe^{+3}$ system (−0.75 v). The oxidation-reduction potential values are summarized in Table 5.

It should be mentioned that no direct electrochemical evidence has yet been found for the existence of Pu^{+5}. A glance at the potential values (Table 2) will show that the transitions between Pu^{+3} and Pu^{+6} occur over such a narrow range of potentials that all four valence forms can co-exist in solution under suitable conditions.

Inference from Absorption Spectra

Kasha and Sheline (*54*, *55*) have developed a special method for the study of absorption spectra which is used in determining the amount of plutonium in each valency state. By

$$Hg|Hg_2SO_4(S),\ 1\ N\ H_2SO_4|1\ N\ H_2SO_4|\ \ 1\ N\ H_2SO_4,\ \frac{Pu^{+3}(C_1)}{Pu^{+4}(C_2)}\Big|\ Pt$$

* Numbering of illustrations and tables is continued from Part 1.

this method the co-existence of different valence states (3, 4, 5, 6) of plutonium in a solution of $PuCl_4$ in hydrochloric acid has been thoroughly studied. The authors have shown that the reaction $3Pu^{+4} \rightleftharpoons 2Pu^{+3} + Pu^{+6}$ does actually occur. They measured the value of the equilibrium constant: $K = \frac{[Pu^{+3}]^2[Pu^{+6}]}{Pu^{+4}]^3}$ at different temperatures and HCl concentrations and found values ranging from 1×10^{-4} in 1.5 M HCl to 6.9 in 0.18 M HCl (25° C). At higher temperatures K was much greater. Hence in dilute solutions of hydrochloric acid (M/10), a considerable amount of Pu^{+4} breaks down into Pu^{+3} and Pu^{+6}. During this change of tetravalent plutonium to tri- and hexavalent states in dilute acid, a considerable amount of pentavalent plutonium has been found to be formed by the reaction $Pu^{+3} + 2Pu^{+4} \rightleftharpoons 3Pu^{+5}$. The equilibrium constant $K = \frac{[Pu^{+3}][Pu^{+4}]^2}{[Pu^{+5}]^3}$ of this reaction has also been studied at low acid concentrations. In order to avoid the formation of colloidal Pu^4 at low acidities the authors (*54*, *55*) used mixtures Pu^{+3} and Pu^{+6}. The K was found to have values 8.1 in 0.1081 M HCl and 0.59 in 0.0615 M HCl. The concentration of Pu^{+4} was very small under these conditions. Actually, in very dilute hydrochloric acid, up to 35% of the plutonium present in solution was found to be in the pentavalent state. It has been assumed that pentavalent plutonium exists as an oxygenated monovalent cation PuO_2^+ and this ion appears to be more stable than the analogous UO_2^+ which exists in exceedingly low concentration in equilibrium with UO_2^{++} (*57*). No pentavalent compounds of plutonium have yet been described.

TABLE 5

Standard Oxidation-reduction Potential of Plutonium

Couple	*Acid*	*Potential (Volts)*	*Temp. (°C)*	*Ref.*
Pu^{+3}-Pu^{+4}	1 N H_2SO_4	−0.72	23	*51*
"	1 N $HClO_4$	−0.86	"	*51*
"	1 N HCl	−0.99	30	*51*
"	0.5 N HCl	−0.967	?	*56*
Pu^{+4}-Pu^{+6}	0.5 N HCl	−1.006	?	*56*

Preparation and Chemical Properties of Plutonium Compounds

From the values of the oxidation-reduction potentials one can make a choice of suitable oxidizing or reducing agents to pass from one oxidation state to another. Tetravalent state, the most stable valency state of plutonium, can be reduced to trivalent plutonium by reducing agents like SO_2, hydroxylamine, the uranous ion, mercury in the chloride solution or gaseous hydrogen in contact with a platinum catalyst. It can be oxidized to Pu^{+6} by $Cr_2O_7^{--}$, $S_2O_8^{--}$, BrO_3^- in nitric acid, MnO_4^-, or AgO. It has been observed that perchloric acid at temperatures above about 170° C oxidizes Pu^{+4} completely and rapidly to Pu^{+6} (*58*).

The oxidation of Pu^{+3} to Pu^{+4} requires very mild oxidizing agents such as oxygen. It is also oxidized by nitrate ion on heating or concentrated nitric acid at room temperature. The oxidation by nitrate ion seems to be autocatalytic. The following mechanism has been suggested (*56*):

(*a*) $2Pu^{+3} + NO_3' + 2H^+ \rightarrow 2Pu^{+4} + NO_2' + H_2O$

The liberated NO_2' then reacts with more Pu^{+3} as shown in (*b*)—

(*b*) $Pu^{+3} + NO_2' + 2H^+ \rightarrow Pu^{+4} + NO + H_2O$

The NO formed in reaction (*b*) pro-

duces more NO_2 by scheme (*c*)—

(*c*) $2NO + NO_3' + H^+ + H_2O \rightarrow 3HNO_2$

It is not yet certain which of the two latter reactions controls the rate.

Trivalent plutonium. It has already been mentioned that trivalent plutonium has about same stability towards oxidizing agents as ferrous ion, just as $Fe(OH)_2$, the insoluble $Pu(OH)_3$, absorbs oxygen rapidly. The solutions are slowly oxidized by air. But unlike the corresponding valency state of uranium it does not reduce water, so that its solutions are stable in an inert atmosphere.

The co-precipitation of trivalent plutonium with BiOCl or $Cb_2O_5 \cdot x\,H_2O$ is much less incomplete than in the case of tetravalent plutonium. The basic strength of the trivalent plutonium has therefore been assumed to be stronger than that of the tetravalent state (*50, 59*). The reagents such as phenyl arsenic acid or picrolonic acid, which are characteristic precipitants of tetravalent ions, do not precipitate trivalent plutonium (*51*).

The chloride, the nitrate, and the sulfate of trivalent plutonium are soluble. The sulfate crystallizes well from the sulfuric acid solution. The double sulfates (*59, 60*) of the general formula $RPu(SO_4)_2 4H_2O$, where R stands for Cs, Rb or NH_4, have also been prepared from respective salt solutions by precipitation with methyl alcohol. Cs and Rb salts are lambent blue in color, whereas ammonium salts are somewhat pale blue. In air these double salts oxidize slowly at the rate of about 3% per hour. Compounds of similar compositions, such as $NH_4LA(SO_4)_2 4H_2O$ are well known in the lanthanide series. The double sulfates of the type $R_4Pu(SO_4)_4$, where R may be K or Tl, have also been prepared.

Tetravalent plutonium. The solution of tetravalent plutonium salts is red-brown in color. The color of the nitrate solution (yellowish green in dilute nitric acid and bright green in concentrated nitric acid) seems to be an exception. It has already been mentioned that $Pu(OH)_4$ is a weaker base than $Pu(OH)_3$. As a consequence aqueous solutions of the salts undergo ready hydrolysis and form colloids. Due to this colloidal behavior, it adsorbs appreciably on to the glass surface and can be partly separated from solution by centrifugation (*61*). As a typical tetravalent ion it complexes with almost all anions of strong acids. Evidences of complex formation with oxalate, carbonate and thiocyanate have also been set forth (*51*).

The most important insoluble salts of plutonium are hydroxide, fluoride, iodate, peroxide, *m*-nitrobenzoate and phenylarsonate.

The only oxide described to date is PuO_2. It can be prepared by heating hydroxide, iodate or nitrate. It is a dark-colored substance which can be redissolved slowly in acids. But when ignited to a high temperature, fuming with sulfuric acid or even bisulfate fusion may be required.

The anhydrous sulfate prepared by heating hydroxide or iodate with sulfuric acid is light pink in color. From a solution of the sulfate in dilute H_2SO_4, red-brown crystals of $Pu(SO_4)_2 4H_2O$ separate.

The peroxy compounds of tetravalent plutonium open up an interesting phase of study. The addition of hydrogen peroxide to an acidic solution (not too acidic) of tetravalent plutonium produces first a red-brown coloration and then the green flocculent precipitate of a peroxide appears. The precipitation is most complete in the pH range 3 to 4.5. The presence of sulfate ion appears to favor the reaction (*51*). The peroxide precipitated from the sulfate has the composition $Pu_2O_7 nSO_4$ (n = about $\frac{2}{3}$). At room temperature this decomposes with the formation of

$PuO_3 \frac{1}{2} SO_4$. These two compounds resemble the peroxides of thorium $Th_2O_7SO_4$ and ThO_3, the latter being formed by the decomposition of the former at room temperature (*52*).

On the other hand the hexavalent plutonium is reduced by H_2O_2. In 0.5 M HCl the hexavalent plutonium is first reduced to pentavalent state and then there starts a series of oxidation-reduction processes as stated previously. As a result probably all four valence forms can co-exist, and under this condition the tetravalent plutonium is also reduced by H_2O_2. So the main product of reaction in 0.5 M HCl is the formation of trivalent plutonium.

Another interesting fact reported by Harvey (*52*) from a declassified document (*62*) is the formation of two soluble complexes—one brown and another red. According to the report, if only very small amounts of H_2O_2 are added to a solution containing tetravalent plutonium, no peroxide is precipitated, but first a brown complex is formed, and then, on the addition of more H_2O_2, a red complex. The equilibrium involved in this complicated system have been elucidated by means of absorption spectra. The following alternative structures for the brown and the red complexes have been suggested:

Brown Complex:

$$[Pu—OO—Pu—OH]^{+5} \qquad (1a)$$

or

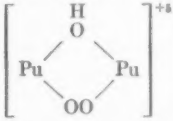

(1*b*)

Red Complex:

$$[HO—Pu—OO—Pu—OOH]^{+5} \qquad (2a)$$

or

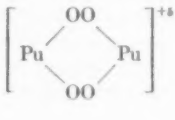

(2*b*)

It should be mentioned that the present writer has not read the declassified document containing this particular interesting aspect. But certain apparent anomalies in the proposed structure as depicted should be pointed out. In the structure 1*b* one of the plutonium atoms should be connected to the hydroxyl group by a secondary valency bond. In the structure 2 for the red complex in order to retain the pentavalent nature as pictured for the complex peroxy ion we should assume that the two atoms of plutonium in question must exist in different valency states. A combination of tri- and hexa- or penta- and tetravalence states can account for the valency of the complex peroxy ion as depicted. So the proposed scheme should be clarified as follows:

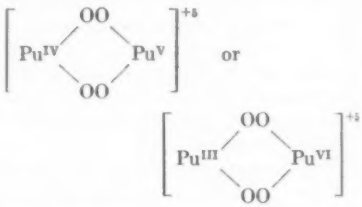

The instances for the co-existence of different valency states in the same compound are not very rare. Uranium pentachloride serves as a typical example. The suggested constitution for the chloride is:

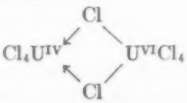

It should be mentioned that, in the case of plutonium, as the observation goes, the extent of co-existence of different valency states depends upon the nature of the anion in combination with plutonium, and on the acidity and nature of the anion in combination with the acid in question. Even the reaction with H_2O_2 seems to be dependent

on these factors. But in the report no experimental details are given. It may also be that the red peroxy ion is tetravalent but has been depicted as pentavalent because of a typographical error.

The reactions of tetravalent plutonium with organic reagents are shown in Table 7.

Hexavalent plutonium. Because of the similarity of the compounds of plutonium to those of uranium, plutonium in this valence state, analogous to the corresponding uranyl ion (UO_2^{++}), has been assumed to exist as a divalent plutonyl ion (PuO_2^{++}). This assumption has been verified both from physical and preparative points of view.

The well-defined absorption bands observed in a solution of hexavalent plutonium in nitric and perchloric acids are similar to the characteristic band system attributed to the vibration of the U—O bond of the uranyl ion. It can therefore be concluded that analogous to uranium, plutonium also exists as an oxy ion in solution (*55, 63*).

It has been observed that plutonyl nitrate is isomorphous with uranyl nitrate (*50*), $UO_2(NO_3)_2 6H_2O$, and sodium plutonyl acetate forms mixed crystals with $NaUO_2Ac_3$ (*64*).

The plutonyl oxinate has the same percentage composition as uranyl oxinate so these two are expected to have analogous structure. Plutonyl nitrate can be extracted with ether from a saturated solution of NH_4NO_3 (*50*).

The addition of alkalies precipitates the sparingly soluble plutonates which are analogous to uranates. Sodium and ammonium salts are slightly soluble; the precipitation as barium plutonate has therefore been recommended for the removal of hexavalent plutonium. After aging for 14 hours the solubility of barium plutonate is 12 mg per liter (*65*). No oxide of hexavalent plutonium has been reported. Probably the oxide formed by heating ammonium plutonate decomposes to PuO_3.

The solutions of the hexavalent plutonium salts are pink in color. In solution, PuO_2^{++} undergoes a slow process spontaneous reduction. The reduction is due to strong α radiation (138×10^6 α particles per minute per mg) coming out of plutonium. The reaction kinetics of the process have also been studied by Kasha and Sheline (*54*).

In Table 6 the chemical properties of plutonium with simple anions have been summarized, and in Table 7 the reaction of plutonium with a few organic reagents has been shown. The organic complexes which can be extracted by suitable solvents may find application in separation and purification of plutonium provided the condition is found such that the reagent in question becomes specific for plutonium.

By recalling the properties of plutonium compounds, one will find that trivalent plutonium behaves as one of the lanthanides, tetravalent compounds resemble corresponding compounds of uranium and thorium whereas hexavalent plutonium has the closest resemblance to the corresponding valency state of uranium. The difference lies in order of stability of the valencies in question. These behaviors can only be accounted for by the actinide theory proposed for the group.

Estimation of plutonium. Plutonium can be estimated by counting the α particles. It can be weighed as PuO_2, $Pu(SO_4)_2$, or $Pu(IO_3)_4$. The oxidation of Pu^{+4} to PuO_2^{++} by warm permanganate is used for the volumetric estimation of plutonium. It is also determined by reducing a solution of plutonium in sulfuric acid to the trivalent state by zinc amalgam and then oxidizing back to tetravalency by ceric sulfate, the end point being read by a potentiometer (*66*).

TABLE 6

Properties of a Few Compounds of Plutonium with Simple Anions

Compounds	*Pu III*	*Pu IV*	*Pu VI*
Color of the solution of soluble salts	Bright blue	Red-brown (exception nitrate)	Pink (exception nitrate)
Chloride	Soluble, not isolated probably complexes with Cl' ion	Soluble, not isolated	Soluble, not isolated
Nitrate		Solution bright green, not isolated	Soluble, at low pH the solution appears pink, with increase in pH the color becomes orange; can be extracted by ether in saturated NH_4NO_3 solution, isomorphous with $UO_2(NO_4)_2 6H_2O$
Sulfate	Soluble, bright blue crystals	$Pu(SO_4)_2$ a light pink substance, $Pu(SO_4)_2 4H_2O$ red-brown crystals	
Double sulfate	R $Pu(SO_4)_2 4H_2O$ (R = Cs, Rb, or NH_4; cf. La) $R_5Pu(SO_4)_4$; (R = K, Tl)		
Double acetate			$NaPuO_2Ac_3$ forms mixed crystals with $NaUO_2Ac_3$
Fluoride	Insoluble in dil. acids, large excess Cl' inhibits co-precipitation	Insoluble in dil. acids, dissolves in ammonium carbonate and oxalates	Soluble

Transuranates

In this section the nuclear chart (Fig. 6) of Saha, Sirkar and Mukherjee (*67*) and M. N. and A. K. Saha (*68*) will be used for discussion of the nuclear properties of the transuranates. Other radioactive nuclei are included since treatment of the transuranates is inseparably connected with them.

By this arrangement each isotope has been given a position with reference to its mass, charge and isotopic number. A glance at the chart will show how a nuclear reaction mechanism can be studied and how predictions as regards syntheses of new nuclei can be made. Use of the horizontal line representing I is very interesting. It was observed by the authors (*67*, *68*) that regularities as regards stability and nature of activity are found among nuclei with the

TABLE 6 (Continued)

Compounds	*Pu III*	*Pu IV*	*Pu VI*
Double fluorides*	$NaPuF_4$, hexagonal crystals isomorphous with $NaLaF_4$	KPu_2F_9, orthorhombic crystals, isomorphous with KM_2F_9 (M = Th, V or Np) and $RPuF_5$ (R = Na, K or Rb) rhombohedral crystals isomorphous with RMF_5(R = Na or K; M = Th or U)	
Oxalate	Insoluble in acid, dark-green anisotopic crystals, can be removed by hot ammonium oxalate from the La carrier (in between cerium and Yt earths)	Insoluble in acids but readily dissolves in ammonium oxalate solution (cf. Th)	
Iodate		$Pu(IO_3)_4$ precipitates as a voluminous pale pink substance (cf. Th)	
Hydroxide	Insoluble dirty blue substance	Insoluble pale green gelatinous	Insoluble ammonium plutonate (cf. U)
Oxide		PuO_2, a dark colored substance	
Peroxide		$Pu_2O_7 \cdot xSO_4$, a bulky green precipitate, decomposes to PuO_3 $\frac{1}{3}$ SO_4 (cf. Th)	

same value of I and this regularity divides the nuclei into two classes—nuclei with even values of I and those with odd values of I. As a result, the following rules for stability have been empirically deduced by the authors.

RULE 1 (I even)—

When I is even and >2, we get alternation of stable and active nuclei. Stable nuclei are obtained for even values of Z, and active nuclei are obtained for odd values of Z.

For $I = 2$, the first stable nucleus is $Z = 8$, O^{18}, after which the rule of alternation holds good.

RULE 2 (I odd)—

In these groups we first find β^--active

* NOTE ADDED IN PROOF: The study of double fluorides of the actinide elements by X-ray diffraction methods has recently been published (74). The results are summarized here.

TABLE 7

Reactions of Plutonium with Some Organic Reagents (*52*)

Ion	*Reagent*	*pH Range*	*Reaction*
Pu IV	Acetylacetone	2–10	Complex extractable in benzene
Pu IV	Benzoylacetone	3	Complex extractable in benzene
Pu IV	Monofluoracetylacetone	3	Complex extractable in benzene
Pu IV	Trifluoracetylacetone	2–4	Complex extractable in benzene
Pu IV	*p*-Dimethylaminobenzene-azophenylarsonic acid	4	Orange precipitate
Pu III	*p*-Dimethylaminobenzene-azophenylarsonic acid	4	No precipitate
Pu IV	*p*-Dimethylaminobenzene-azophenylarsinic acid	4	Orange-red precipitate
Pu III	*p*-Dimethylaminobenzene-azophenylarsinic acid	4	No precipitate
Pu IV	3-Nitro-4-hydroxyphenyl-arsonic acid	2.5	Pale greenish-buff precipitate. Pu carried down on Zr salt
Pu III	3-Nitro-4-hydroxyphenyl-arsonic acid	2.5	No precipitate. Pu not carried down on Zr salt
Pu IV	*m*-Nitrophenylarsonic acid	2.5	Pale greenish-buff ppt. Pu carried down on Zr salt
Pu III	*m*-Nitrophenylarsonic acid	2.5	No ppt. Pu not carried down on Zr salt
Pu IV	Phenylarsonic acid	2	Pale greenish-buff ppt. Pu carried down on Zr salt
Pu III	Phenylarsonic acid	2	No ppt. Pu not carried down on Zr salt
Pu IV	*n*-Propylarsonic acid	2	Pale greenish-buff ppt. Pu carried down on Zr salt
Pu III	*n*-Propylarsonic acid	2	No ppt. Pu not carried down on Zr salt
Pu IV	*m*-Nitrobenzoic acid	1.5	Pale greenish-buff ppt. Pu carried down on Zr salt
Pu III	*m*-Nitrobenzoic acid	1.5	No ppt. Pu not carried down on Zr salt
Pu IV	Sebacic acid	1–2	Pu carried down on Zr salt
Pu III	Sebacic acid	1–2	Pu poorly carried down on Zr salt
Pu IV	5-*p*-Acetamidophenylazo-8-hydroxyquinoline	4	Complex extractable in amyl acetate. Insol. in water
Pu IV	8-Hydroxyquinoline	4–8	Purple-brown ppt. extractable in amyl acetate

nuclei and then arrive at a number of succeeding stable nuclei. These are followed by K-capturing and β^+-active nuclei. (The number of intermediate stable nuclei has been found sometimes as small as 3, sometimes as large as 12;

TABLE 7 (Continued)

Ion	*Reagent*	*pH Range*	*Reaction*
Pu VI	8-Hydroxyquinoline	4–8	Orange-brown ppt. extractable in amyl acetate
Pu IV	1′-Sulfonaphthalene-4′-azo-5:8-dihydroxyquinoline	3	Purple precipitate
Pu IV	Anthranilic acid	3	Complex extractable in amyl acetate
Pu IV	Cinnamic acid	2.5–4.5	Complex extractable in amyl alcohol
Pu IV	Cresotinic acid	2.5–4.5	Complex extractable in amyl acetate
Pu IV	2:4-Dihydroxybenzoic acid	3	Complex extractable in methyl isobutyl ketone
Pu IV	2:4-Dinitrosalicylic acid	3	Complex extractable in amyl acetate
Pu IV	Salicylic acid	2–3	Complex extractable in amyl acetate. Pu carried down on Th, La or Zr salts
Pu IV	Benzoic acid	2	Green-yellow ppt.
Pu IV	Citric acid	1–11	Soluble complex
Pu IV	Dihydroxytartaric acid	1	Pu carried down on Th salt
Pu III	Dihydroxytartaric acid	1	Pu poorly carried down on Th salt
Pu IV	3:5-Dinitrobenzoic acid	3	Complex extractable in amyl acetate
Pu IV	Phthalic acid	2	Pu carried down on Zr salt
Pu III	Phthalic acid	2	Pu not carried down on Zr salt
Pu IV	Tartaric acid	1–11	Soluble complex
Pu VI	Tartaric acid	1–11	Soluble complex
Pu IV	Thiobarbituric acid	2	Pu carried down on Th, Zr and La salts
Pu III	Thiobarbituric acid	3	Pu poorly carried down on Th, Zr, and La salts
Pu IV	Cupferron	0.5–2	Complex extractable in chloroform or carbon tetrachloride
Pu IV	Ethylenediamine	—	Brown ppt. insol. in water and organic liquids
Pu IV	α-Nitroso-β-naphthol	2	Complex extractable in methyl isobutyl ketone
Pu IV	Sodium benzenesulfinate	2	Buff ppt. not extractable in amyl acetate
Pu VI	Sodium benzenesulfinate	2	Complex extractable in amyl acetate
Pu VI	Sodium diethyldithiocarbamate	3	Purple-brown complex extractable in amyl acetate and amyl alcohol

usually the nucleus in the midst of the stable group appears to be most stable though there are some exceptions).

The great merit of the chart is its use in predicting the properties of missing nuclei and giving clues to the syntheses

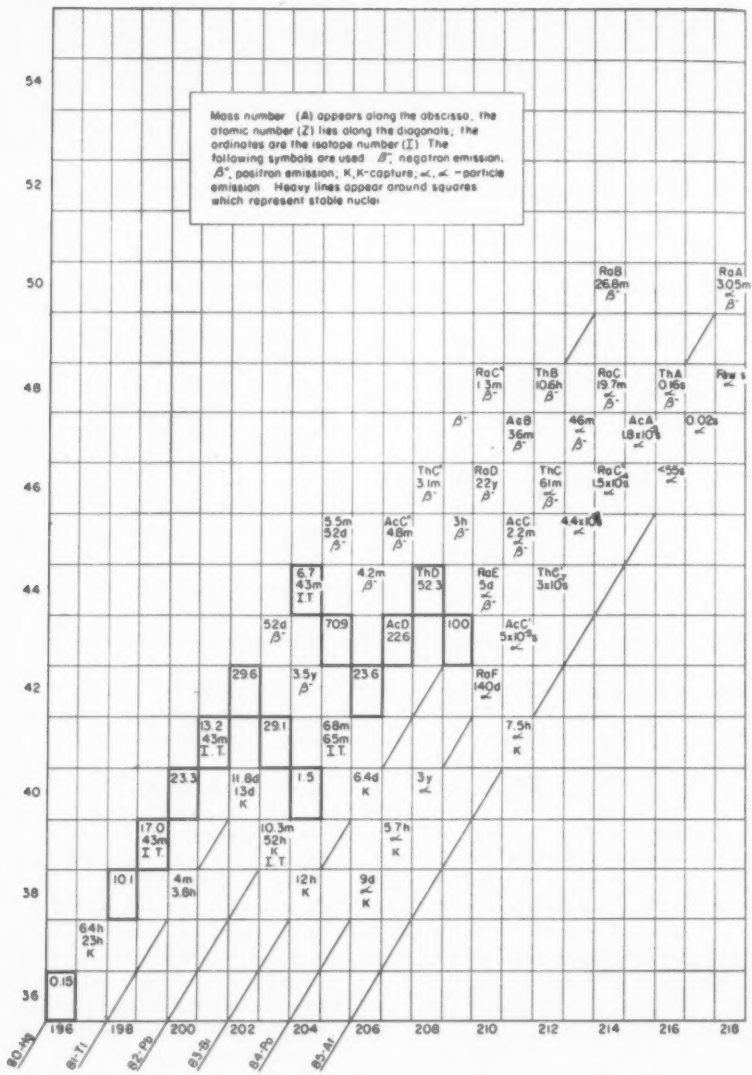

FIG. 6. Nuclear chart

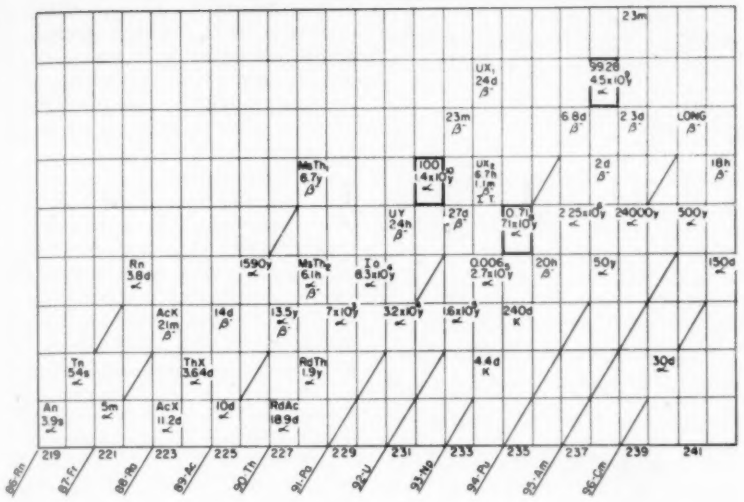

of those missing ones. It should be pointed out that α-active nuclei have been considered as stable from the β-stability viewpoint.

The explanation of the above rules of stability, with a quantitative expression for the energy release in β-emission and K-capture processes, is given by the β-energetics formulas by M. N. Saha and A. K. Saha (*68*). Further studies of β-energetics in natural radioactive and transuranic regions have been done by Biswas and Mukherjee (*69*).

The formulas for energy release in β^- and β^+ emissions are

$$E^- = A^- + x(Z+1,A) - x(Z,A)$$
$$E^+ = A^+ + x(Z-1,A) - x(Z,A)$$

where

$$A^- = 0.766 + \frac{4\beta(I-1)}{A} - \frac{0.58(A-I+1)}{A^{1/3}} \text{ Mev}$$

$$A^+ = -1.788 - \frac{4\beta(I+1)}{A} + \frac{0.58(A-I-1)}{A^{1/3}} \text{ Mev}$$

$x(Z,A)$ etc. are spin-dependent terms. The value of β varies from 17.4 Mev to 19.5 Mev, the average value being 18.9 Mev (*69*).

The energy release in the K-capture process is

$$E^K \simeq E^+ + 2m$$

Hence K-capture is possible even if E^+ is negative and lies between 0 and -1 Mev.

For each I-group, A^- and A^+ curves are drawn with A as the abscissa. In I = even groups,

(a) For even-even nuclei [Z = even, N (number of neutrons) = even].

$$E^- = A^- + x(Z+1,A) < A^-$$
$$E^+ = A^+ + x(Z-1,A) < A^+$$

since $x(Z,A)$ is negative when Z is odd;

(b) For odd-odd nuclei (Z = odd, N = odd)

$$E^- = A^- - x(Z,A) > A^-$$
$$E^+ = A^+ - x(Z,A) > A^+$$

since Z is odd, $x(Z,A)$ is negative.

In I = odd groups,

$$E^- \simeq A^-,\ E^+ \simeq A^+$$

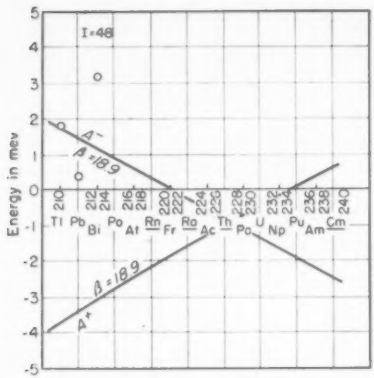

FIG. 7. A^- and A^+ curve for I = 48

A glance at Fig. 6 shows that the lowest value of I for which transuranate nuclei appear is 48. A discussion of the group with $I = 48$ is given below.

I = 48

The group $I = 48$ extends from $_{81}Tl^{210}$ to $_{96}Cm^{240}$ with a number of important gaps as shown in the chart. As far as β-stability is concerned, the rule of alternate stability holds good with the apparent exceptions of $_{82}Pb^{212}$ (ThB) and $_{84}Po^{216}$ (ThA). The odd-odd nuclei are all β-active (or K-capturing) as expected. The even-even nuclei are generally β-stable with the two exceptions mentioned above. Still unknown nuclei of this group are $_{87}Fr^{222}$, Ac^{226}, Pa^{230}, U^{232}, Pu^{236} and Am^{238}. From the formulas stated above the A^- and A^+ curves from this group are drawn (Fig. 7). The energetics of still unknown nuclei can be predicted with their help.

Tl^{210} (RaC″)—This well-known β^--active nucleus emits 1.8 Mev β^--rays. A high energy γ-ray, like that of ThC″, is expected, because the energy release E^- should be greater than the A^- value in Fig. 7.

Pb^{212}(ThB)—This nucleus is situated in the flank of the group. Although even-even, it is β^--active similar to $_6C^{14}$ which is discussed in a paper by M. N. Saha and A. K. Saha (*68*). As expected E_β^- is small, 0.36 Mev ($< A^-$). A low energy γ-ray is present, but its energy is not given.

$_{83}Bi^{214}$(RaC)—RaC is both α- and β^--active. We have $E^- = 3.15$ Mev which is as large ($> A^-$) as expected.

$_{84}Po^{216}$(ThA)—The small β^--activity is due to its position in the flank of the group. As expected, α-activity is predominant ($\sim$100%) and β^--activity is weak (only 0.014%). The energy of β^--rays is not measured. It is expected to be very small. The calculated β^--emission life is about 20 min and E^- is said to be very small, as expected.

$_{85}At^{218}$—This is obtained from the β^--decay of $_{84}RaA^{218}$. It has been found to emit α-rays of energy 6.63 Mev with a life of several seconds. This nucleus is expected to be very weakly β^--active, but it has not been reported so far.

$_{86}Rn^{220}$(Tn)—This is α-active, having a half-life of 54 s. No β^--activity is expected or found.

$_{87}Fr^{222}$—This nucleus cannot be prepared at present due to want of suitable target. This nucleus is expected to be β^--active.

$_{88}Ra^{224}$(ThX)—This is a 3.64-day half-life, α-active nucleus. No β^--activity is expected or found.

$_{89}Ac^{226}$—This isotope is as yet unknown. It can be prepared by using Ra as the target in the reactions $Ra^{226}(d,2n)Ac^{226}$, $Ra^{226}(p,n)Ac^{226}$. This is expected to decay by K-capture to $_{88}Ra^{226}$, and may also show feeble β^--activity.

$_{90}Th^{228}$ (RaTh)—This is known to be α-active with a 1.9-year half-life. It is β-stable.

$_{91}Pa^{230}$—This is not yet known. It can be prepared from $Pa^{231}(n,2n)Pa^{230}$ reaction. From the A^+ curve (Fig. 7), this is expected to decay by K-capture

to Io^{230}. It is expected to be α-active as well.

$_{92}U^{232}$—This should be a β-stable but α-active nucleus. To date a U^{232} isotope has not been discovered in nature. The non-existence of U^{232} may be due to its strong α-activity. Another cause of non-occurrence of U^{232} may be its strong spontaneous fissionable property, for according to the calculations of Bohr and Wheeler (*29*) and of Turner (*70*), it is more fissionable than U^{235} or U^{238}. It is worthwhile to try to prepare U^{232} and study its properties. The suggested reactions are $Pa^{231}(d,n)U^{232}$; $Th^{230}(\alpha,2n)U^{232}$; $Th^{232}(\alpha,4n)U^{232}$; $Pa^{231}(n,\gamma)Pa^{232} \xrightarrow{\beta^-} U^{232}$.

Np^{234}—The 4.4-day K-capture activity assigned to this nucleus is in agreement with the stability rules and the A^+ curve. This isotope has been prepared by the bombardment of 22-Mev deuterons and 44-Mev α-particles in the following reactions: $U^{235}(d,3n)Np^{234}$ and $U^{235}(\alpha,p4n)Np^{234}$. γ-rays from this nucleus have been detected but the energy measurements have not been given (*37*).

Pu^{236}—Nothing is reported as yet about this nucleus. Np^{236}, which is a 20-h β^--emitting nucleus, will decay to Pu^{236}. Also, Pu^{236} is formed in the α-emission of Cm^{240} which has a half-life of 30 days. According to the A^- and A^+ curves for $I = 48$, Pu^{236}, being "even-even," will be β-stable and α-active. The α-decay product of Pu^{236} is U^{232}. This isotope is expected to have high fissionability. The convenient means of production is from U^{235} by the reactions $U^{235}(d,n)Np^{236} \xrightarrow{\beta^-} Pu^{236}$ and $U^{235}(\alpha,3n)Pu^{236}$.

Am^{238}—This nucleus is not yet known. From the A^+ curve this is expected to show β^+-activity, decaying to Pu^{238}. This can be verified by artificially producing this isotope by the reactions $Pu^{239}(d,3n)Am^{238}$; $Pu^{239}(\alpha,p4n)Am^{238}$; $Np^{237}(\alpha,3n)Am^{238}$.

Cm^{240}—This is the last known nucleus belonging to this group. From the A^- and A^+ curve, this nucleus seems to be at least β^--stable. It is α-active with a half-life of 30 days and has been prepared in the reaction $Pu^{239}(\alpha,3n)Cm^{240}$ (*37*).

$_{97}X^{242}$—The group $I = 48$ can be extended beyond the last known isotope $_{96}Cm^{240}$ by producing element 97. This is possible because of the isolation, in weighable amounts, of Am^{241} which has been used as a target for producing Am^{242} by the reaction $Am^{241}(n,\gamma)Am^{242}$. With Am^{241} as the target in an $(\alpha,3n)$ reaction as in the case of Cm^{240}, the new element 97 can be obtained. This nucleus is expected to decay by β^+-activity and K-capture to Cm^{242}.

I = 49

This group at present extends from $_{87}Fr^{223}$ to Np^{235}. The extension of the group to the left flank is not possible because of want of suitable targets. On the right flank its extension to 97^{243} seems probable. As is characteristic of odd groups, nuclei 87^{223} to Ac^{227} are β^--active; then we have a group of β-stable but α-active nuclei, Th^{229} to U^{233}, which are followed by K-capturing and β^+-active nuclei. Only one K-capturing nuclei, Np^{235}, is known beyond U^{233}. Thus, as far as is known, the stability rule is well satisfied. The A^- and A^+ curves of this group are given in Fig. 8. The nuclei of this group are discussed below.

$_{87}Fr^{223}$(**AcK**)—This β^--active nucleus emits β^--rays of 1.2 Mev. This is in agreement with the A^- curve ($A^- \sim E^-$) but the reported γ-ray of high energy, >3 Mev, does not seem probable from energetics considerations.

Ra^{225}—One of the new $(4n + 1)$ nuclei recently obtained by English, et al (*71*) and Hagemann, et al (*72*). It is reported to be only β^--active, with $E_{\beta^-} \sim 0.2$ Mev and a half-life of 14 d.

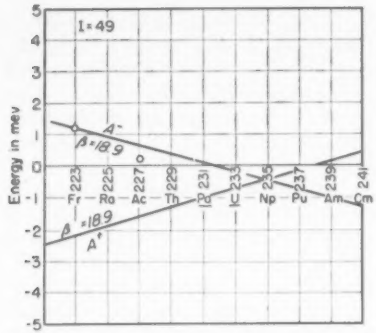

FIG. 8. A⁻ and A⁺ curve for I = 49

Ac^{227}—Ordinary actinium. It was for long supposed to be only β^--active ($E^- = 0.22$ Mev, half-life = 13.5 y), but in 1939, Perey discovered weak α-activity (1%), the decay product being AcK.

Th^{229}—One of the new $(4n + 1)$ nuclei showing α-activity only. It is β-stable in accordance with Fig. 8.

Pa^{231}—Ordinary protoactinium. This is β-stable, as given in Fig. 8, but α-active.

U^{233}—This nucleus has been prepared from thorium in the reaction $Th^{232}(n,\gamma)Th^{233} \xrightarrow{\beta^-} Pa^{233} \xrightarrow{\beta^-} U^{233}$. This long-lived ($1.6 \times 10^5$ y) U^{233} isotope is a member of the $(4n + 1)$ radioactive series which has been recently completed. As reported by Seaborg, et al (*73*) a weighable amount of U^{233} has been isolated and high fissionability has been observed. No β-activity is expected or reported.

Np^{235}—A 240-day K-capturing Np^{235} has been prepared from the reactions $U^{235}(d,2n)Np^{235}$; $U^{235}(\alpha,p3n)Np^{235}$ (*37*). This activity is in agreement with the A^+ curve since A^+ is -0.5 Mev. This may also be α-active.

Pu^{237}—Not yet known. This may be prepared from the reactions $U^{235}(\alpha,2n)Pu^{237}$; $Np^{237}(d,2n)Pu^{237}$; and $Np^{237}(\alpha,p3n)Pu^{237}$. This isotope is expected to decay by K-capture to Np^{237}.

Am^{239}—The possible methods of production of this nucleus are $Np^{237}(\alpha,2n)Am^{239}$; $Pu^{239}(d,2n)Am^{239}$; and $Pu^{239}(\alpha,p3n)Am^{239}$. This is expected to decay by K-capture and β^+-activity to Pu^{239}.

Cm^{241}—The possible methods of production are $Am^{241}(d,2n)Cm^{241}$ and $Pu^{239}(\alpha,2n)Cm^{241}$. This is expected to decay by β^+-emission to Am^{241} which is known and is α-active.

97^{243}—This new element presents an interesting possibility of production by the use of Am^{241} and bombardment with α-rays in the reaction $Am^{241}(\alpha,2n)97^{243}$. It is expected to decay by β^+-activity.

No further extension of the group appears possible at present.

The above discussion, based on values of I, is an illustration of how the nuclear chart of Fig. 6 serves as a guide for studying the properties of isotopes, and predicting the existence and the nature of activity of the missing ones. Entirely different characteristics of even groups and odd groups are illustrated in the discussion of one even and one odd group. However, for a general discussion of isotopes of elements, use of the Z line as a basis for study seems convenient. Uranium is the first element which will be so discussed.

Uranium

Three isotopes of uranium occur in nature, *viz.*, U^{234}, U^{235} and U^{238}. All these isotopes satisfy the stability rules. Other known and expected isotopes of U are discussed below.

U^{231}—The lightest isotope of U is moved to U^{231} by the reaction $Pa^{231}(d,2n)U^{231}$, since Pa^{231} has already been used as a target. The expected activity of this isotope is K-capture, decaying to $_{91}Pa^{231}$.

U^{232}—Already discussed.

U^{233}—Already discussed.

U^{236}—This isotope of uranium is not

yet known. The difficulty in producing it is that U^{235}, when bombarded by slow neutrons, transforms into U^{236} which instantly undergoes fission. Other reactions, *viz.*, $Np^{237}(\gamma,p)U^{236}$ and $Pu^{239}(n,\alpha)U^{236}$, do not appear promising because of high fissionability of the targets. If, however, U^{236} can be prepared without undergoing fission, it is expected to be α-active.

U^{237}—This 7-d β^--active isotope has been obtained from an $(n,2n)$ reaction on U^{238}, *viz.*, $U^{238}(n,2n)U^{237}$. The stability rule is obeyed by this nucleus. No α-activity has been reported (*37*).

U^{239}—A 23-m β^--active isotope is obtained by resonance capture of neutrons by U^{238}. This is the only known nucleus in the group $I = 55$. More nuclei are required to verify the stability rule in this last group.

Neptunium

So far, six isotopes of Neptunium, 234 to 239, are known. The most stable is Np^{237} (α-active of half-life 2.25×10^6 y). The isotopes 234 and 235 exhibit K-capture, and 236, 238 and 239 β^--activity. As seen in Fig. 6, all these isotopes satisfy the stability rules already referred to. They have been prepared by bombardment with deuterons and α-particles of energies 22 Mev and 44 Mev, respectively (*37*). The activities and reactions are given in Table 1.*

The possibility of production of lighter and heavier isotopes is discussed below.

Np^{232}—The discovery and isolation of $_{92}U^{233}$ in weighable amounts open up a possibility of artificial production of lower isotopes utilizing U^{233} as the target. As Np^{234} has been produced by $U^{235}(d,3n)Np^{234}$ reaction, Np^{232} can be obtained from the reaction $U^{234}(d,3n)Np^{232}$.

This isotope is expected to decay by β^+-activity to U^{232}, which will be β-stable and α-active as we have discussed before. This reaction is important from the point of view that two new isotopes Np^{232} and U^{232} can be obtained and their properties can be verified.

Np^{233}—U^{233} can be utilized in preparing this unknown isotope by the reaction $U^{233}(d,2n)Np^{233}$. The expected activity of Np^{233} is K-capture.

Np^{240}—The isotopes higher than Np^{239} are difficult to prepare because of the lack of suitable targets. With U^{238} as the target, Np^{240} can be obtained by the rather doubtful reaction $U^{238}(\alpha,pn)Np^{240}$. This isotope will be β^--active, decaying to Pu^{240} which is β-stable and α-active.

Np^{241}—As in the case of Np^{240}, this isotope can be prepared from $U^{238}(\alpha,p)Np^{241}$. This reaction, though common for low energy α-particles, is doubtful at the high energy required for bombardment in the transuranic region. This isotope is expected to be β^--active, decaying to Am^{241} in the chain $Np^{241} \xrightarrow{\beta^-} Pu^{241} \xrightarrow{\beta^-} Am^{241}$.

Production of isotopes higher than Np^{241} does not seem probable at present.

Plutonium

Three isotopes of plutonium, Pu^{238}, Pu^{239} and Pu^{241}, are known. Pu^{238} is 50-y α-active; Pu^{239} is 24,000-y α-active; and Pu^{241} is long-lived β^--active. Of these the long-lived Pu^{239} is the most important isotope at present which has been utilized for atomic energy production. All these isotopes obey the stability rules. The methods of production by high-energy particles (*37*) are given in Table 1.

The production of isotopes of Pu lower than Pu^{238} seems probable, as discussed below.

Pu^{234}—The lowest probable isotope of Pu can be moved down to Pu^{234}

* Nucleonics **3**, No. 5, 8 (1948).

utilizing U^{233} as the target, as in the case of Np. The probable method of formation of Pu^{234} is from the reaction $U^{233}(\alpha,3n)Pu^{234}$. Because of the stability rule and the position of this isotope in the extreme right flank of the group $I = 46$, it should show K-capture. Pu^{234} should have high fissionability and may be α-active also.

Pu^{235}—It is possible to prepare this isotope by using U^{233} or Np^{237} as targets in the following reactions: $U^{233}(\alpha,2n)Pu^{235}$ and $Np^{237}(d,4n)Pu^{235}$. The probable activity of this isotope is β^+-emission.

Pu^{236}—Already discussed ($I = 48$).

Pu^{237}—Already discussed ($I = 49$).

Pu^{240}—This isotope can be obtained from the reactions $U^{238}(\alpha,2n)Pu^{240}$; $Np^{237}(\alpha,p)Pu^{240}$; and $Pu^{239}(d,p)Pu^{240}$. But Pu^{240}, formed by neutron capture of Pu^{239}, instantly undergoes fission. This isotope, if it is prepared, will be α-active, decaying to U^{236}, which is again α-active.

$$Pu^{240} \xrightarrow{\alpha} U^{236} \xrightarrow{\alpha} Th^{232}$$

These isotopes, Pu^{240} and U^{236}, will thus be predecessors of Th^{232} in the $4n$ series.

Isotopes of Pu heavier than Pu^{241} can not be prepared by transmutation because suitable targets are not available.

Americium

Two isotopes of americium, Am^{241} and Am^{242}, are known at present. Isolated in weighable amounts, 500-y α-active Am^{241} has been used as a target in nuclear reactions. This, as well as 18-h β^--active Am^{242}, satisfies the stability rules. The reactions employed for the production of these isotopes are given in Table 1.

Other probable isotopes with their expected activities are discussed below.

Am^{237}—This is the lightest isotope of Am which it is possible to prepare by transmutation of Pu^{239} in the reaction $Pu^{239}(d,4n)Am^{237}$. It is expected to disintegrate by β^+-emission to Pu^{237} which again will decay by K-capture to Np^{237}.

Am^{238}—Already discussed ($I = 48$).

Am^{239}—Already discussed ($I = 49$).

Am^{240}—This may be obtained by the reactions $Pu^{239}(d,n)Am^{240}$ and $Np^{237}(\alpha,n)Am^{240}$. From the stability rule this nucleus is expected to decay to β^--activity.

Isotopes of Am, heavier than the known Am^{242}, can not be expected with the known reactions because of lack of suitable targets.

Curium

Only two short-lived isotopes of Cm are known at present. These are Cm^{240}(30-d α-active) and Cm^{242} (150-d α-active). These two even-even isotopes are β-stable and α-active in conformity with the stability rule. The methods of production (*37*) are given in Table 1.

Other isotopes of Cm may be obtained by transmutation as discussed below.

Cm^{239}—This is the lightest isotope that can be prepared using Am^{241}. Am^{241} has already been used as a target in nuclear transmutation. The reaction is $Am^{241}(d,4n)Cm^{239}$. Cm^{239} is expected to give high-energy β^+-emission, decaying to Am^{239} which again is expected to decay by β^+-activity to Pu^{239}.

Cm^{241}—Already discussed in group $I = 49$.

Cm^{243}—This nucleus does not appear to be convenient to prepare with known reactions and available targets. It can be prepared by the rare reaction $Am^{241}(\alpha,pn)Cm^{243}$. If it is ever prepared, it is expected to be α-active.

Cm^{244}—Using Am^{241} as a target this isotope can be prepared by the reaction $Am^{241}(\alpha,p)Cm^{244}$. But it is rather doubtful whether the (α,p) reaction occurs appreciably, because high-energy

α-particles are required for transmutation in the transuranic region.

Other isotopes of Cm do not seem probable at present.

Element 97

Since the two known isotopes of Cm are rather shortlived, they cannot be used as targets for producing elements 97 and 98 by deuteron and α-particle bombardment. But since Am^{241} is moderately long-lived and has already been isolated in weighable amounts and used as target material in the $Am^{241}(n,\gamma)Am^{242}$ reaction, it can be utilized in preparing element 97 by high-energy α-particle bombardment. The reactions (α,n), $(\alpha,2n)$, $(\alpha,3n)$ will give corresponding isotopes of element 97.

$$_{95}Am^{241}(\alpha,n)_{97}X^{244};$$
$$Am^{241}(\alpha,2n)_{97}X^{243};$$
$$Am^{241}(\alpha,3n)_{97}X^{242}$$

These reactions are interesting since they may take us one step further in the transuranic element region.

When a sufficiently long-lived Cm isotope is known and isolated in weighable quantity, it will be possible to use this as a target, and syntheses of elements 97 and 98 as well may be made possible.*

The nuclear reactions and properties are summarized in Table 1. The predicted isotopes are marked with asterisks. All the transuranium nuclei, without any exception, known to date have been found to obey Saha-Sirkar's rule of stability (*67*).

It is of interest to note that bombardments with energetic alpha and deuteron nuclei have opened up an interesting and fascinating chapter in nuclear chemistry and its application to nuclei other than heavy ones also promises a great advance in this branch of study.

(4n + 1) SERIES AND NATURAL TRANSURANATES

The discovery of transuranium elements has brought up many fascinating questions. The naturally occurring elements which undergo radioactive changes fall into three groups

1. the thorium series, $4n$
2. the uranium series, $4n + 2$
3. the actinium series, $4n + 3$

In addition to the elements comprising these groups, potassium and rubidium were known to show β-activity which has been traced to K^{40} and Rb^{87}, and samarium also exhibits α-radioactivity, now traced to the isotope Sm^{152}. The three groups mentioned above are termed respectively, $4n$, $4n + 2$ and $4n + 3$ series where n is a multiple of α-particles.

Evidently the $4n + 1$ radioactive series seems to be missing among naturally occurring elements. Only recently the $4n + 1$ radioactive series has been discovered in the process of laboratory syntheses and the decay products of the whole series up to its stable member, $_{83}Bi^{209}$, have been traced (*71*, *72*).† Figure 9 represents the members of the decay chain. Unlike the other three series, it ends in an isotope of bismuth. It also differs from the other series in that it doesn't contain a rare gas, or emanation, member. Of the members, Np^{237} has the longest half-life (2.3×10^6 y) and the series has therefore been designated as the neptunium series. A glance at the nuclear chart (Fig. 6) will show that all the members of the neptunium series fit in well in the chart in accordance with the rules of stability already mentioned (*67*, *68*).

* NOTE ADDED IN PROOF: The fact that Cm^{242}(150 d) has been isolated in weighable amounts (*49a*) is significant in that it opens up the way to syntheses of elements 97 and 98 by the same type of nuclear reactions in which other transuranium nuclei have been used as targets (Table 1).

† NOTE ADDED IN PROOF: A review which includes historical details of the $(4n + 1)$ radioactive series has been published (*76*).

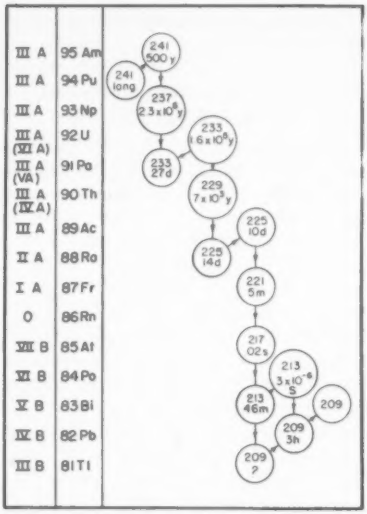

FIG. 9. Neptunium series ($4n + 1$). The vertical arrows denote α-ray transformations, diagonal arrows β-ray transformations

But the life of Np^{237} is very short in comparison with the age of the earth and if it is formed along with other elements, no weighable fraction can still remain undecomposed. From another angle the three natural radioactive series, namely, thorium, uranium and actinium, may be considered as remnants of the series which once may have included any number of transuranates. The mother transuranates might have been extinct due to their comparatively short lives. Thus the absence of the $4n + 1$ radioactive series in nature may be more due to the absence of at least one member with a long life in the series than to its lesser probability of formation along with other elements. It may be that among higher transuranates some representative of the series with a very long half-life might have been formed along with other elements in a very scanty amount, but this has escaped detection because of a lack of knowledge of the chemistry of transuranium elements.

It is also suspected that the $4n + 1$ radioactive series might have once existed at least in its present form in nature but is now extinct because of the short life of its members. The stable nucleus it can produce is Bi^{209}, and the presence of bismuth in radioactive minerals may have its origin in radioactive decomposition of the $4n + 1$ series which is now extinct.

A glance at the nuclear chart (Fig. 6) will show that each of the four series mentioned above has its generators in transuranium nuclei. But mere laboratory syntheses and the establishment of a genetic chain in the laboratory do not prove that transuranium elements were formed along with other elements. For example, U^{235} may be formed in the general way in nature but its mother $_{94}Pu^{239}$ and still higher transuranates may not be formed in the natural process of syntheses of elements.

The question of whether transuranium elements occur in nature and in what possible minerals they occur arises at this point.

It has already been stated that the existence of a series in nature depends upon the fact that at least one of the members must have a long half-life. But the choice of a mineral in which a particular radioactive isotope may occur depends upon whether it is a radioactive decay product of some other element or a primary product of natural synthesis. In the case of primary formations the long-lived isotopes of Np and Pu can be found in association with minerals where uranium occurs in tetravalent state or in association with tetravalent thorium. Samarskite, monazite and pitchblende can be cited as examples. The last named mineral, pitchblende, contains both hexa- and tetravalent uranium. The higher members, from $_{95}Am$ up to element 103, the last rare earth, will be found in associ-

ation with trivalent minerals. Still higher members, say, elements 104 and 105, which are, respectively higher homologues of Hf and Ta, should be looked for, respectively, in the zircon- and niobium-tantalum group of minerals. But in the case where a particular isotope of an element has been formed as a result of radioactive decay, its chemical property will not be of use in determining the mineral in which it exists. The mineral must be investigated in accordance with the chemical properties of its originator. For example, consider a quest for a long- or short-lived Np isotope. If it originates from a long-lived isotope of element 104, it will be found in the zirconium-hafnium group of minerals, and if the original mother is an isotope of element 105, the niobium-tantalum group of minerals will be the most suitable source of exploitation. But it has already been mentioned that elements with charge numbers above 100 are expected to be highly unstable. However, existence of long-lived isotopes of neptunium and plutonium in nature is probably not beyond the realm of possibility.

Search for Natural Transuranates

To date, the search for transuranium elements in various minerals has brought discouraging results. Early in 1942, Seaborg (*40*) and M. L. Perlman, in Berkeley, undertook a search for these elements in pitchblende ore.* About 0.5 kg of the ore was completely dissolved and subjected to an exhaustive chemical process designed to separate and isolate the elements neptunium and plutonium. A small quantity of α-radioactivity was found in this transuranium fraction and the investigators attributed it to the plutonium isotope, Pu^{239}. The amount of plutonium in the pitchblende corresponded to about one part in 10^{14}. The relatively short life of Pu^{239}, compared to the age of the earth, makes it necessary to assume that it is being continuously produced in uranium minerals by the well-known (n,γ) reaction upon U^{238} with the production of U^{239} (23 m), which is converted to Pu^{239} by successive β-disintegration. The neutron available for the purpose has been assumed to be derived from spontaneous fission of uranium and also from the (α,n) process upon light nuclei such as Li, B, Be, F, O, *etc.*, in the pitchblende.

A further search for transuranium elements in nature was made during the summer of 1942. The radioactive ore, carnotite, was chosen for the purpose, the investigation being carried out by C. S. Garner, N. R. Bonner and Seaborg (*40*). A transuranium fraction which would contain neptunium and plutonium was carefully isolated from the completely dissolved carnotite ore, about 5 kg being used in this case. An α-radioactivity was found, the concentration of the corresponding $_{94}Pu^{239}$ being comparable to that found in the pitchblende. Seaborg also assumes the formation of some Np^{237} (2.25×10^6 y) by an $(n,2n)$ process upon U^{238}. However, its quantity will be much smaller than Pu^{239}. He also expects the formation of americium and curium isotopes by α-bombardment but the quantity will be still less. It should be pointed out that the source of natural neutrons or α-particles is so scanty that we cannot expect any transuranium element in weighable amounts if transuranium elements are only formed by the above-mentioned nuclear reactions. However, the failure to detect long-lived isotopes of neptunium and plutonium in only two minerals does not exclude their probable existence in nature.†

* NOTE ADDED IN PROOF: Details of the chemical procedure have recently been published (*76*).

† NOTE ADDED IN PROOF: A preliminary note, claiming the isolation of a naturally occurring α-emitter with a charge number above 92 has recently been published (*77*).

(*Continued on next page*)

BIBLIOGRAPHY

For convenience, references *29, 37, 40* and *49a* have been repeated from the first paper in this series. MDDC refers to Manhattan District Declassified Documents.

29. N. Bohr, J. A. Wheeler, *Phys. Rev.* **56,** 426 (1939)
37. G. T. Seaborg, *Science* **104,** 379 (1946)
40. G. T. Seaborg, *Chem. Eng. News* **25,** 358 (1947)
49a. I. Perlman, *J. Chem. Education* **25,** 273 (1948)
50. B. G. Harvey, *Proc. Conf. on Nuclear Chem.*, McMaster University, Canada, Part 1, 60 (1947)
51. B. G. Harvey, H. G. Heal, A. G. Maddock, E. L. Rowley, *J. Chem. Soc.* 1010 (1947)
52. B. G. Harvey, NUCLEONICS **2,** No. 4, 30 (1948)
53. R. H. Betts, *Proc. Conf. on Nuclear Chem.*, McMaster University, Canada, Part 1, 68 (1947)
54. M. Kasha, G. E. Sheline, MDDC 392
55. M. Kasha, MDDC 591
56. R. E. Connick, W. H. McVey, MDDC 337
57. W. E. Harris, I. M. Kolthoff, *J. Am. Chem. Soc.* **67,** 1484 (1945)
58. M. Kahn, MDDC 391
59. R. E. Connick, W. H. McVey, G. E. Sheline, MDDC 339
60. H. H. Anderson, MDDC 1128
61. E. L. King, MDDC 393
62. R. E. Connick, W. H. McVey, MDDC 619
63. R. H. Betts, unpublished work, information from ref. *52*
64. R. E. Connick, et al MDDC 587
65. R. E. Connick, W. H. McVey, MDDC 335
66. H. E. Boas, P. Numerof, H. A. Potratz, W. H. Throckmorton, MDDC 279
67. M. N. Saha, S. C. Sirkar, K. C. Mukherjee, *Proc. Natl. Inst. Sci. India* **6,** 45 (1940)
68. M. N. Saha, A. K. Saha, *Trans. Natl. Inst. Sci. India* **2,** 193 (1946)
69. S. Biswas, A. Mukherjee, *Ind. J. Phys.* **22,** 80 (1948)
70. L. A. Turner, *Revs. Modern Phys.* **17,** 293 (1945)
71. A. C. English, T. E. Cranshaw, P. Demers, J. A. Harvey, E. P. Hincks, J. V. Jelley, A. N. May, *Phys. Rev.* **72,** 252 (1947)
72. F. Hagemann, L. I. Katzin, M. H. Studier, A. Ghiorso, G. T. Seaborg, *Phys. Rev.* **72,** 252 (1947)
73. G. T. Seaborg, J. W. Gofmann, R. W. Stoughton, *Phys. Rev.* **71,** 378 (1947)
74. W. H. Zachariasen, *J. Am. Chem. Soc.* **70,** 2147 (1948)
75. G. T. Seaborg, *Chem. Eng. News* **26,** 1902 (1948)
76. G. T. Seaborg, M. L. Perlman, *J. Am. Chem. Soc.* **70,** 1571 (1948)
77. B. Gysae, H. Korsching, *Z. Naturforsch* **2a,** 475 (1947); *Chem. Abstracts* **42,** 2864 (1948)

Future Energy Needs

Practically all energy is of atomic origin. Most of it comes —or came—from atomic processes in the sun. Some of the solar energy that reached the earth many milleniums ago still exists today, in the form of "stored sunlight"—coal, petroleum, natural gas, shale oil.

Estimates of ultimate resources of these sources vary tremendously. The highest and lowest estimates were taken for each fuel, and stated in terms of the number of years they alone would satisfy the present annual energy requirement (12-trillion hph).

Coal—maximum 1,700 years, minimum 170 years; petroleum—maximum 16 years, minimum 5 years; natural gas—maximum 12 years, minimum 5 years; shale oil—maximum and minimum both 13 years; total—maximum 1,741 years, minimum 193 years.

These figures, of course, are based on a constant energy requirement at the present level. It is estimated that demand will increase about 50% every 50 years. On that basis, demand would be 27-trillion hph 100 years from now, instead of the present 12-trillion.

—From a Business Week *(Nov. 13, 1948) report on a talk by Eugene Ayres of Gulf Research and Development Co. at the 28th Annual Meeting of the American Petroleum Institute.*

NUCLEAR PHYSICS AND LOW TEMPERATURES

A survey of some recent developments in nuclear physics and low temperatures describing certain problems of common interest and the adoption of new techniques in these two fields

By M. E. ROSE

Oak Ridge National Laboratory, Oak Ridge, Tennessee

ALL NUCLEI are endowed with a random thermal motion by virtue of the finite temperature of the medium in which they are embedded. For almost all nuclear phenomena which have been the subject of extensive study during the past two decades, this thermal motion was not of great importance because the thermal energy (about $\frac{1}{40}$ electron volt at room temperature) was small compared to nuclear energies involved in most experiments.* Where it was not small, as in thermal neutron collisions, corrections for the nuclear motion (referred to as Doppler effect) could easily be made. For the purposes which have hitherto been of concern, it was sufficient to carry out nuclear investigations at room temperatures and, in the few exceptional cases where liquid nitrogen or even liquid hydrogen temperatures were used, the techniques of the modern cryogenic laboratory were not required.

In contrast to this situation, several nuclear physics laboratories are now embarked on projects wherein not only liquid helium temperatures (between 1° and 4.2° K) will be utilized but also it is hoped nuclei cooled to temperatures of order 0.01° K will be possible. Supplementing these developments is the widening interest on the part of workers in low-temperature phenomena in the techniques of nuclear physics.

The reason for this recent rapprochement between the two fields is to be found in the necessity for introducing new techniques in response to the demands imposed by the widening investigation of basic problems.

For the nuclear physicist the interest in low temperatures lies in the fact that the investigation of certain nuclear properties, of prime importance for the problem of nuclear forces, involves the study of small effects that would be entirely masked except at the very low temperatures cited above. A specific example is the behavior of the magnetic (or spin) properties of the nucleus. A large number of nuclei (all those with an odd mass and, in addition, a few others with even mass and odd numbers of both neutrons and protons) possess an intrinsic or spin angular momentum and a magnetic moment (*1*). Ordinarily, these elementary magnets are random in direction and their effects cancel out. In order to determine the role of the magnetic character of nuclear constituents in nuclear structure, it is necessary to magnetize the sample so that there will be a net moment in some direction. Since the thermal motion promotes the random distribution and since the nuclear particles have very weak moments ($\sim 10^{-23}$ esu), low temperatures are needed. Other

* An exception is the scattering of neutrons by ortho- and parahydrogen where the scatterer and neutrons must be cold. For this experiment liquid hydrogen temperatures (20° K) were sufficient. *Cf.*, for example, references *1* and *10*.

applications of low temperatures will be discussed below.

For the low-temperature physicist the interest lies in the possibility of connecting the peculiar behavior of liquid helium below the lambda point (2.19° K) with the nuclear properties of He^4. It is well known that in this temperature range a new liquid phase, referred to as He II, exists in the so-called superfluid state with highly anomalous properties: for example, practically zero viscosity and ideal thermal conductivity (*2*). There is some reason to believe that the superfluidity of He^4 is connected with the fact that the nucleus contains four particles and is therefore described by Bose statistics.* This point of view is refuted or confirmed according to whether or not He^3 exhibits superfluidity. Up to now experiments to decide the question have not been entirely conclusive because of the difficulty of obtaining a sufficiently concentrated sample of He^3 by nonnuclear means. The superfluidity problem is cited as an example, albeit an important one. Many other problems of importance in low-temperature work can be most effectively studied with the aid of nuclear techniques. For example, liquefaction of He^3 under a given temperature and pressure may be investigated directly by bombardment with neutrons. Again, there exists the possibility, discussed by Simon (*3*), of attaining temperatures as low as 10^{-6}° K by adiabatic demagnetization of nuclear spins. In this case one would presumably produce nuclear ferromagnetism.

It is reasonable to expect that the overlapping of interests in nuclear physics and low temperatures will result in advances of mutual benefit to workers in both fields.

In the following sections some of the problems connected with the production and utilization of nuclear spin alignment are discussed in greater detail.

* The statistical mechanics description of quantum systems containing identical particles is always one of two types: Fermi or Bose statistics. Particles of the former type behave as though their identity gives rise to a repulsion between them while those of the latter behave as though an attraction exists. The neutron and proton obey Fermi statistics (fermions). Systems with even (odd) numbers of fermions obey Bose (Fermi) statistics. See further, F. London, "The Present State of the Theory of Liquid Helium," *Physical Society Cambridge Conference Report*, p. 1 (1947).

ALIGNMENT OF NUCLEAR SPINS

Clearly, the two questions which must be considered in this connection are (1) by what method may one attempt to produce aligned nuclei, or nuclear paramagnetism and (2) what are the experiments which could be carried out to yield useful information once the aligned nuclei are obtained? Under (1), consideration must be given to the problems of heat transfer from the sample containing the nuclei and to the question of relaxation times involved in reaching a state of equilibrium.

Production of Aligned Nuclei

The most direct method involves the application of a large magnetic field to a sample at low temperatures. Just how large the field and how low the temperature depends on the amount of alignment or polarization required. For this purpose we introduce the polarization factor for the nuclei

$$f_N = \bar{I}_s/I \qquad (1)$$

where I is the nuclear spin in units of $h/2\pi$ and I_s is the component of spin in the direction of the applied field. Then f_N has the meaning "fraction of nuclei lined up in the direction of the field." The bar in Eq. 1 means that an average over all nuclei must be taken remembering that, in a field H at temperature T, the probability that a nu-

cleus has energy W is given by the Boltzmann factor $e^{-W/kT}$, where $k = 1.38 \times 10^{-16}$ erg/deg is the Boltzmann constant. In this case $W = -\mu H I_z/I$, where μ is the magnetic moment of the nucleus. Since $I_z = -I, -I+1, \ldots I-1, I$, one finds

$$f_N = \frac{2I+1}{2I}\coth\frac{2I+1}{2I}\frac{\mu H}{kT} - \frac{1}{2I}\coth\frac{1}{2I}\frac{\mu H}{kT} \quad (2)$$

Fig. 1 shows f_N vs $\mu H/kT$ for various spins I (numbers affixed to the curves). Generally, one will be on the straight portion of the curves near the origin. Then we have more simply

$$f_N \approx \frac{1}{3}\frac{I+1}{I}\frac{\mu H}{kT} \quad (2a)$$

For most purposes a polarization of 20% would be adequate. On this basis, Table 1 shows the magnetic field in kilogauss required for various nuclei if a temperature of 0.01° K is attained. For other temperatures the corresponding fields are given at once by Eq. 2*a*. In Table 1 the magnetic moment μ is given in units of the nuclear magneton (5.05×10^{-24} esu-cm). Of course, the larger the magnetic moment and the smaller the spin the easier it is to obtain a given polarization, the former factor being somewhat more important. Production of fields appreciably larger than 40 kilogauss and temperatures in the 0.005–0.01° range may not be immediately feasible. However, polarization of nuclei for which smaller values of H/T are required offers a reasonable hope of success. Temperatures as low as 0.004°K, it is interesting to note,

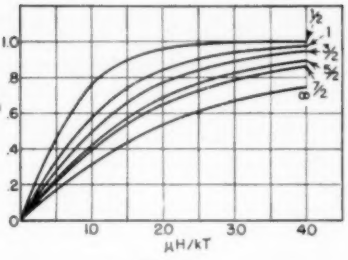

FIG. 1

have been reached recently by de Klerk with adiabatic demagnetization of potassium-chrom alum (*4*).

In any case it will be realized that polarization of nuclei by direct application of external fields represents an experimental problem of nontrivial proportions. It is, therefore, worth considering the possibility of using the rather strong magnetic fields produced at the position of the nucleus by the magnetic moment of the orbital electrons. These fields may be of order 50–200 kilogauss. In this case one would line up the electronic moments almost to saturation. This would require a reasonably small field since the electronic moments are of an order 1000 times larger than the nuclear moments. Low temperatures will still be needed. How low a temperature will depend on the hyperfine structure (hfs) multiplet splitting which is directly dependent on the field produced by the atomic electrons.

It must be recognized that this method of spin alignment can apply only to

TABLE 1

	H^1	H^2	Li^6	Li^7	Co^{59}	In^{115}
I	½	1	1	3/2	7/2	9/2
μ	2.79	0.86	0.82	3.25	2.3	5.49
H (kilogauss)	19	92	96	29	54	23.5

atoms with bound electrons in incomplete shells—thus to rare earths, transition elements including the transuranic elements, and in general to strongly paramagnetic substances. It is clear that, for those solids in which the valence electrons or all electrons other than those in closed shells go into the quasi-continuous band structure, there can be no question of appreciable electron alignment. These electrons form a highly degenerate Fermi gas and the field to be applied must be such that $\mu_e H \sim$ Fermi energy, $H \sim 10^8$ gauss. With practical fields only the very few electrons near and over the top of the Fermi distribution can be polarized.

For the rare earths and transition elements the feasibility of the hfs coupling depends, of course, directly on the over-all hfs multiplet splitting in the ground state. If this is ΔW, the nuclear polarization is

$$f_N \approx \frac{1}{3} f_e \frac{I+1}{I} \frac{J_e}{2J_e+1} \frac{\Delta W}{kT}, \quad J_e \geq I$$

$$f_N \approx \frac{1}{3} f_e \frac{I+1}{2I+1} \frac{\Delta W}{kT}, \quad J_e \leq I \quad (3)$$

Here f_e is the electron polarization (percent saturation) and J_e is the electronic angular momentum. Since the numerical factor multiplying $\Delta W/kT$ is of order ½ to ⅙, a 20% nuclear polarization requires $\Delta W/kT \sim 0.5$ to 1.0. Rough estimates of ΔW for the rare-earth ions, based on spectroscopic data for screening constants and average radius of the 4*f* shell (0.5 A.U.), indicate a ΔW varying from a few tenths to a few hundredths wave number. This, therefore, gives the temperature range required, ~ 0.01 to 0.1° K. Since these estimates are perhaps too rough to rely on, measurement of these splittings would be desirable.

Relaxation times. When the magnetic field is applied to the nuclei, the equilibrium distribution corresponding to the aligned state is reached only after a finite time. The alignment of a fraction f_N of N nuclei involves the release of magnetic energy equal to $\mu H f_N N$ and this energy must be removed by some mechanism from the spin system. This energy, which amounts to about 10^1 ergs for a typical case, may be transferred to the surroundings in which the nuclei are embedded by virtue of whatever interactions may act on the nuclear spins. These various mechanisms have been considered by E. M. Purcell (*5*) who concludes that the most efficient means of energy removal is that one in which the energy is transferred to conduction electrons in a metal. The characteristic time for this process has been estimated by Heitler and Teller (*6*) to be about one second at 0.1° K. This has been confirmed by measurements of Rollin and Hatton (*7*). Since the relaxation time should vary inversely as the temperature, this would indicate a time of about 10 sec for reaching equilibrium which would be quite reasonable.

Heat transfer. The internal magnetic energy which has been transferred to the conduction electrons of the metal in which the sample is embedded must be conducted away in order to maintain the temperature at the desired low level. Additional energy arising from work done by the external field on the induced nuclear moments is released. These together, constituting the total energy liberated, are equal to the temperature times the entropy change ΔS. At most the entropy change for N nuclei is $Nk \log (2I + 1)$ so that about 10^6 ergs must be removed by conduction.

The problem of heat conduction is not quite straightforward since the amount of information available about thermal conductivity at very low temperatures is rather meager. This question has been discussed by H. B. G. Casimir (*5*) who has pointed out that, whereas heat transfer was relatively simple in the liquid-helium temperature range of 1° to 4° absolute, many problems were

encountered below 1° K. Examining the process of heat conduction by nonmagnetic insulating crystals, metals, superconductors, liquid helium, and by radiation, one finds that only metals retained a reasonably good heat-transfer coefficient at the very low temperature of 0.01° K. This is due to the fact that the electronic specific heat C_v goes down only linearly with temperature giving $C_v = 10$ erg/deg cc at 0.01° K. This C_v may seem small compared to customary room temperature values, but it is still one hundred thousand times larger than that of an insulating crystal like KCl at the same temperature. This large C_v leads to a heat transfer coefficient of 10^5 cgs. Assuming the amount of heat to be transferred at 0.01° K to be of the order of 10^6 ergs, thermal equilibrium would be attained to within 0.01° K within 100 to 1000 seconds. These times would be very convenient for experiments on nuclear alignment.

From the foregoing it would appear that a feasible arrangement for the alignment process might involve a paramagnetic salt (*8*), for carrying out the adiabatic demagnetization, in contact with a metal strip that terminates some distance away in a piece of metal in which is embedded the nuclei whose spins are to be aligned.

EXPERIMENTS WITH ALIGNED NUCLEI

Nuclear Forces

It is now firmly established that nuclear forces are spin-dependent; that is, the interaction between two nuclei depends on the relative orientation of their spins. The quantitative investigation of this spin-dependence is usually carried out by means of scattering experiments. Thus, in the case of hydrogen, one wishes to measure separately the triplet and singlet scattering cross sections at all energies—or at least up to about 12 Mev above which *P*-scattering (involving neutrons with orbital angular momentum equal to $\hbar/2\pi$) sets in (*1*). This information, that is, scattering for both possible spin orientations of neutron and nucleus, is available at present only for thermal neutrons from the ortho-parahydrogen scattering experiments or, for other nuclei as well, from the diffraction of neutrons by crystals (*9*). The fact that the spin dependence can be investigated in these cases depends on the special circumstances that one can separate ortho- and parahydrogen, and that, in the case of crystal diffraction, one can measure coherent and incoherent scattering separately.

Nevertheless, with exception of scattering in hydrogen where some theoretical information can be used, the scattering data obtained with unpolarized nuclei are incomplete. In addition, in order to deduce nuclear forces (shape of well) from scattering data, that is, from observed phase shifts (*1*), these data must be known for all energies for which the cross section is appreciable. In principle, this information is obtainable from scattering with polarized nuclei. This also implies production of polarized neutrons at all energies up to 12 Mev. This raises the question of obtaining polarized neutrons at all energies. A possible method will be discussed below.

In the general case of scattering of an *S*-neutron, orbital angular momentum zero, by a nucleus with spin I, the interaction is described in terms of two phase shifts η_0 and η_1 which correspond to the case of total angular momenta $J = I - \frac{1}{2}$ and $I + \frac{1}{2}$ for the combined system. These are defined so

UNIVERSITY OF MICHIGAN LIBRARIES

that the scattering cross sections for these two J values are

$$\begin{aligned} \sigma_{I-\frac{1}{2}} &= 4\pi\eta_0^2/k^2 \qquad |\eta_0|,\ |\eta_1| \ll 1 \\ \sigma_{I+\frac{1}{2}} &= 4\pi\eta_1^2/k^2 \qquad \text{or} \qquad |\pi - \eta_\delta| \ll 1 \end{aligned} \tag{4}$$

where k is the wave number of the neutrons (not to be confused with the Boltzmann constant). For neutrons with velocity v, $k = M_n v/\hbar$, where M_n is mass of the neutron and $\hbar = h/2\pi$. It is convenient to introduce the scattering amplitudes

$$\begin{aligned} a &= \frac{4\pi}{k}\,\frac{I\eta_0 + (I+1)\eta_1}{2I+1} \\ b &= 2\,\frac{4\pi}{k}\,\frac{\eta_1 - \eta_0}{2I+1} \end{aligned} \tag{5}$$

In the case of unpolarized nuclei, a^2 and b^2, respectively, give the coherent and incoherent scattering by a crystal. The b gives the effect of spin dependence. This is also clear when one realizes that the interaction energy between neutron and nucleus can be written in the form (*10*):

$$V = -\frac{\hbar^2}{2M_n}(a + b\,\mathbf{I}\cdot\mathbf{s})\delta(\mathbf{r}_n - \mathbf{r}_{nuc}) \tag{6}$$

Here $\mathbf{s}$ = spin of neutron, because $2\mathbf{I}\cdot\mathbf{s}$ equals I for $J = I + \frac{1}{2}$ and equals $(I+1)$ for $J = I - \frac{1}{2}$. So

$$V = -\frac{\hbar^2}{2M_n}\frac{\eta_1}{k}\delta \quad \ldots \quad \text{and}$$

$$V = -\frac{\hbar^2}{2M_n}\frac{\eta_0}{k}\delta \quad \ldots$$

in these two cases.

In addition to the polarization factor for nuclei, f_N, introduced in Eq. 1, we define the polarization factor for neutrons in a similar way

$$f_n = \frac{C_+ - C_-}{C_+ + C_-} \tag{7}$$

where C_+ and C_- are proportional to the intensity of neutrons with spin parallel and opposite to the net nuclear moment.

Scattering above thermal energies. When the neutron wavelength, equal to $2\pi/k$, is appreciably smaller than the lattice spacing in the scatterer, each nucleus scatters independently. In this case, the scattering cross section with nuclei and neutrons polarized is

$$\sigma = \sigma_0(1 + \rho) \tag{8}$$

where $\sigma_0 = \frac{1}{4\pi}\left[a^2 + \frac{1}{4}I(I+1)b^2\right]$ is the unpolarized cross section and

$$\rho = If_nf_N\,\frac{\frac{b}{a}\left(1 - \frac{1}{4}\frac{b}{a}\right)}{1 + \frac{1}{4}I(I+1)\frac{b^2}{a^2}} \tag{8a}$$

For H this gives $(b/a = -6.9)$

$$\rho = -0.95f_nf_N \tag{8b}$$

And in general $\rho \lesssim f_nf_N$. Neutron polarizations up to 40% have been obtained (*11*). Thus, if one can obtain 25% nuclear polarization the effect of polarization is to reduce the cross section by 10%.

It can be shown that the cross section depends on η_0^2 and η_1^2 only, even in the polarized scattering. However, by measuring the scattering with and without polarization, the extra datum is just sufficient to get both $\sigma_{I\pm\frac{1}{2}}$. In fact,

$$\begin{aligned} \sigma_{I-\frac{1}{2}} &= \sigma_0\left(1 - \frac{I+1}{I}\,\frac{\rho}{f_nf_N}\right) \\ \sigma_{I+\frac{1}{2}} &= \sigma_0\left(1 + \frac{\rho}{f_nf_N}\right) \end{aligned} \tag{9}$$

in which the cross sections are expressed entirely in terms of measurable quantities, although measurement of the polarization factors would not be simple. The sign of the ratio of b/a could be determined also but only if this ratio happens to fall in the interval 0 to 4, i.e., $\rho > 0$.

Crystal diffraction. Since all cross sections involving only nuclear scattering are given as bilinear forms in the two phase shifts η_0 and η_1, it is impossible from scattering measurements to fix both within a common sign. However, the relative sign of the phase shifts, which is important to know, can be determined by diffraction of slow polarized neutrons by polarized nuclei in

crystals. The diffraction and consequent interference effects occur when the neutron wavelength becomes comparable with the lattice spacing, that is, for neutron energies in the neighborhood of the thermal region (~ 0.01 ev).

The essential advantage over the scattering by single nuclei is that one can measure the coherent and incoherent scattering separately. Expressing the cross sections as before

$$\sigma_c = (\sigma_0)_c(1 + \rho_c); \qquad \sigma_i = (\sigma_0)_i(1 + \rho_i) \quad (10)$$

where σ_c and $(\sigma_0)_c$ are coherent cross sections per solid angle with and without polarization and σ_i, $(\sigma_0)_i$ are incoherent cross sections per nucleus with and without polarization, one finds for a monoisotopic lattice

$$\rho_c = \frac{f_N^2 b^2 I^2}{4a^2}\left(1 + 4\,\frac{f_n}{I f_N}\,\frac{a}{b}\right) \quad (10a)$$

$$\rho_i = -f_N \frac{f_N I + f_n}{I + 1} \quad (10b)$$

The occurrence of the term in f_N^2, which indicates a change in scattering even without neutron polarization, is due to what may be called spin correlation between different scattering centers in the crystal. Even if the neutrons are unpolarized, the scattering involves interference effects and, therefore, depends on whether or not pairs of nuclei have correlated spin directions.

It is recognized, of course, that the incoherent scattering may be due in part to temperature motion, multiple scattering, etc. However, since polarizing the nuclei and/or neutrons affects only the spin-dependent part of the incoherent scattering, this part (σ_{si}) may be determined by observations with and without polarization and by a knowledge of f_N, f_n and, therefore, of ρ_i.

$$\sigma_{si}(1 + \rho_i) = \sigma_i - (\sigma_0)_i \quad (11)$$

From the form of the coherent factor ρ_c it is seen that the sign of a/b and, therefore, of η_0/η_1 can be determined by observing the *direction* in which the coherent scattering changes when the neutron polarization is reversed, or is turned on. This is essentially the additional information which one obtains from diffraction with polarization. Similar, although somewhat more involved, considerations apply to lattices containing more than one nuclear species.

An idea of the order of magnitude of the effects can be obtained from Table 2, referring to H, in which $f_N = 0.2$ was assumed.

TABLE 2

f_n	0.3	−0.3	0
ρ_c	−0.088	0.328	0.120
ρ_i	−0.080	0.040	−0.013

The case of H is somewhat more favorable than most others since $|b/a|$ is large in this case, thus promoting large ρ_c.

Angular Momentum of Compound Nuclear Levels

Another rather interesting experiment would involve the resonance absorption of polarized neutrons by polarized nuclei. By a qualitative observation, viz., the observation of the direction in which the absorption cross section changes when the neutron polarization is turned on, one can determine directly the angular moment of levels of compound nuclei. For example, consider the case of In^{116}. This nucleus has a spin of 9/2 in the ground state. A strong resonance absorption at a neutron energy of 1.44 ev exists. This level of the compound nucleus In^{116} corresponds either to $J = 4$ or $J = 5$. If $J = 4$, then neutrons completely polarized parallel to In^{115} nuclei, also completely polarized, would not be absorbed at all. In the more practical case of partial polarizations the cross sections for well-separated levels are:

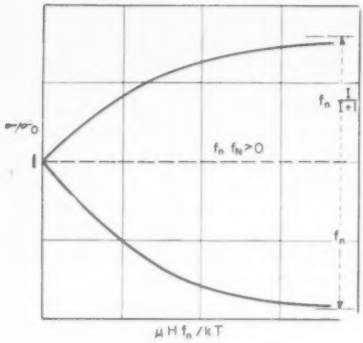

FIG. 2

If $J = I + \frac{1}{2}$

$$\sigma = \sigma_{I+\frac{1}{2}} \left(1 + f_n f_N \frac{I}{I+1}\right)$$

If $J = I - \frac{1}{2}$

$$\sigma = \sigma_{I-\frac{1}{2}}(1 - f_n f_N)$$

(Here $\sigma_{I+\frac{1}{2}}$ refers to the cross sections without polarization; σ_0 is used below as a generic symbol for these cross sections).

Thus, with parallel polarization, an increase in σ upon turning on the neutron polarization gives $J = I + \frac{1}{2}$; a decrease directly implies $J = I - \frac{1}{2}$. For the numbers cited, the change in cross section on reversing the neutron polarization is about 12% in either case and this should be easily detectable. The behavior of the cross section as a function of field strength, temperature, or neutron polarization is shown schematically in Fig. 2 for the case of neutrons and nuclei polarized in the parallel sense. These results also indicate a method of measuring nuclear polarization whenever the two levels corresponding to the two possible orientations of angular momentum vectors are well separated; therefore, one measures the scattering or absorption of each level separately. It is only necessary to measure the cross sections with and without polarization but these must be measured rather accurately for small nuclear polarizations. The neutron polarization can be measured by comparison of transmissions through an iron plate with and without magnetization. Alternatively, one simply measures the product $f_n f_N$.

Polarization of Neutrons

The experiment just described assumes that one can produce polarized resonance neutrons. However, this experiment itself suggests a way of producing them since the absorption depends on the spin orientation of the neutrons. With unpolarized neutrons incident on a polarized absorbing target, the polarization in the beam transmitted through a thickness x is

$$f_n = -\tanh \frac{I}{I+1} N\sigma_{I+\frac{1}{2}} f_N x; \qquad J = I + \frac{1}{2}$$

or

$$f_n = \tanh N\sigma_{I-\frac{1}{2}} f_N x; \qquad J = I - \frac{1}{2}$$

The signs simply express the fact that the polarization in the transmitted beam is opposite to that of the nuclei when $J = I + \frac{1}{2}$ because in this case the neutrons with spin parallel to the nuclei are absorbed more strongly. In a similar fashion, the fact that the polarizations are parallel when $J = I - \frac{1}{2}$ can be understood. The essential limitation on neutron polarization is seen to be one of neutron intensity and detection sensitivity.

It is to be understood that the directions of the magnetic fields in the polarizing sample and in the target, or analyzer, can be independently changed. Otherwise, one is restricted to working at thermal energies for which polarization by transmission through magnetized iron can be used.

Angular Distribution of Emitted Radiation

This problem has been discussed by Spiers (*12*). As Spiers points out,

the establishment of a preferred direction in space, say, the direction of the magnetic field polarizing the nuclei, implies that the emission of any type of radiation from excited states of polarized nuclei will no longer be isotropic. Instead there will be a certain angular distribution with the magnetic field as a symmetry axis. The angular distribution will depend on the angular momenta involved in the transition so that one can hope to use such observations to supplement the other data of nuclear spectroscopy.

For an electric dipole transition of emitted γ-rays, the departure from spherical symmetry may lie between 3 and 30% for $T = 0.01°$ K, $\mu = 3$ nuclear magnetons, and a field of 100 kilogauss. The angular distribution of dipole photons is of form $1 + \beta \cos^2 \vartheta$ where ϑ is the angle between the emitted radiation and the magnetic field. The effect, i.e., the constant β varies directly with f_N^2, or $(\mu H/kT)^2$. The numbers given correspond to f_N between 30 and 60% (angular momentum of the initial level J between infinity and 1, respectively), extreme values corresponding to $J = 1$. For $\beta < 0$, $\Delta J = 0$, while $\Delta J = \pm 1$ gives $\beta > 0$. Similar calculations for the angular distribution of quadrupole radiation emitted by polarized nuclei show that the anisotropy in this case is of the same order of magnitude but its sign is reversed. Only when $\Delta J = 0$ do the γ-rays come out preferentially in the direction of the magnetic field. In the cases $\Delta J = \pm 2$, emission in the antiparallel direction is preferred.

It will be understood, of course, that an experimental program aiming at obtaining polarized nuclei will be beset by many difficult problems which have not been mentioned here. However, there is every reason to believe that these problems are capable of solution and that it will be possible to carry out experiments of the type described. Experiments not involving the use of strong magnetic fields, such as those referred to in the introduction, may be carried out quite readily and it is perhaps in this direction that one may look for new developments in the near future.

BIBLIOGRAPHY

1. M. E. Rose, NUCLEONICS **2**, No. 6, 57 (1948); **3**, No. 1, 57 (1948)
2. K. K. Darrow, *Revs. Modern Phys.* **12**, 257 (1940)
3. F. Simon, "Le Magnetisme," Vol. III, Collection Scientifique, Institut International de Cooperation Intellectuelle (1940)
4. D. de Klerk, "Onderzoekingen Over Adiabatische Demagnetisatie," doctorate thesis, Leyden (1947)
5. Oak Ridge Low Temperature and Nuclear Physics Conference, Oak Ridge National Laboratory, Oak Ridge, Tenn., Aug. 7, 1948
6. W. Heitler, E. Teller, *Proc. Roy. Soc.* **A155**, 629 (1936)
7. B. V. Rollin, J. Hatton, *Phys. Rev.* **74**, 346 (1948)
8. See, *e.g.*, H. B. G. Casimir, "Magnetism and Very Low Temperatures" (Cambridge University Press, New York, 1940)
9. E. O. Wollan, C. G. Shull, NUCLEONICS **3**, No. 1, 8 (1948)
10. J. Schwinger, E. Teller, *Phys. Rev.* **52**, 286 (1937)
11. D. J. Hughes, J. R. Wallace, R. H. Holtzman, *Phys. Rev.* **73**, 1277 (1948)
12. J. A. Spiers, *Nature* **161**, 807 (1948)

BETA- and GAMMA-RAY SPECTROSCOPY—I*

A review of methods and instruments used to investigate energies and intensities of beta rays emitted by radioisotopes. The results of Fermi's theory of beta decay are reported and the shape of the continuous beta-ray spectrum is discussed for various values of maximum energy of the beta rays, charge of the disintegrating nucleus, and its half-life

By GERALD J. HINE

Department of Physics, Sloan-Kettering Institute for Cancer Research
New York, New York

THE TRANSMUTATION of one nucleus into a neighboring one by the emission of a primary electron or positron is called beta decay (*1*, *2*). If the product nucleus is left in an excited state its excess energy will be released as gamma radiation (photons). The nuclear gamma radiation accompanying the decay of a radioactive isotope can consist of zero, one, or any number of discrete lines of different energies and intensities. Their investigation will be discussed in Part II of this paper. This portion of the paper deals with the experimental and theoretical determination of the nuclear beta radiation.

The beta radiation of all radioisotopes shows a continuous energy distribution, covering all energies up to a maximum energy. The shape of the beta-ray spectrum is of paramount importance. A theory will be reported which gives the form of the continuous beta-ray spectrum as a function of its maximum energy and the atomic number of the radioisotope. This theory given by Fermi has been found to check with most but not all beta-ray spectra investigated so far.

Study of the energy distribution of radiation emitted by different isotopes is not only of theoretical interest. The application of radioactive elements as tracers (*3*) and therapeutic agents (*4*) depends on both the quality and intensity of the emitted radiation.

Absorption Method

The different experimental methods which give some information concerning the maximum energy and the shape of the continuous beta-ray spectrum will be reported first. The simplest setup used in beta- and gamma-ray spectroscopy permits the determination of the fraction of incident radiation that is absorbed per unit mass by different elements (*1*). Different absorbers of various thickness are placed between the radioactive source and the radiation detector, which is usually a Geiger-Müller counter.

Besides its simplicity, the absorption method has the advantage that some information, at least concerning the most energetic component of the radiation can be obtained rather quickly. For those radioisotopes which have a short half-life of only a few minutes or less, the analysis of the radiation often depends completely on its absorption curve. The absorption method is also the most convenient one in cases where

* This work was supported in part by the Office of Naval Research under contract N6-ORI-99.

only small amounts of a radioactive material are available.

Very accurate data for energies and intensities of radiation can hardly be obtained from absorption curves. The relative amount of scattered (secondary) radiation detected in addition to the primary rays depends on the energy of the radiation and the geometrical arrangements of radioactive source, absorber and detector. Fig. 1 gives a self-explanatory illustration of how widely the absorption curve for the P^{32} beta rays can vary under different experimental conditions. Nevertheless valuable information concerning the maximum energy as well as the shape of the continuous beta-ray spectrum can sometimes be obtained from careful investigations of beta-ray absorption curves (*1, 5*).

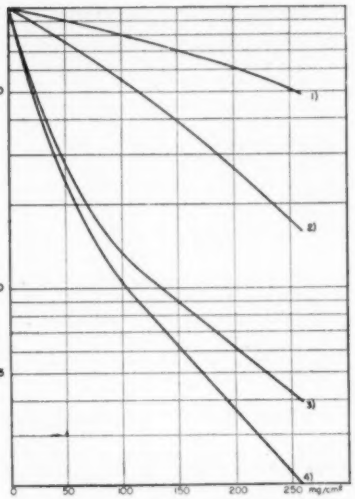

FIG. 1. Absorption of P^{32} electrons in aluminum
1) intensity loss by ionization only (calculated)
2) standard P^{32} absorption curve from reference (*5*); only a fraction of the electrons scattered in the Al absorber can reach the counter
3) attenuation of collimated P^{32} beta-ray beam by scattering only (scattering angle $> 10°$); follows from curve 4 plus curve
4) experimental absorption curve for a collimated P^{32} beta-ray beam; intensity loss by ionization and scattering (determined with a thin end-window counter)

Wilson Cloud Chamber

The first information concerning the continuous nature of beta-ray energy distribution was obtained with the cloud chamber as demonstrated by C. T. R. Wilson in 1911. For many years the cloud chamber was the only instrument for investigating beta-ray spectra. By this method, single tracks of ionizing particles are observed following the expansion of a gas saturated with water and alcohol vapor. The ions produced along the path of the ionizing particle provide centers of condensation for the supersaturated vapor. If a homogeneous magnetic field is applied perpendicularly to the top and bottom plate of the chamber, the kinetic energy of the beta rays inside the chamber can be determined from the curvature of their tracks. The number of tracks counted per energy interval determine the energy distribution curve.

An electron moving in a plane perpendicular to the magnetic field H will describe in the same plane a circular path, if the energy loss by ionization is assumed to be negligible. The magnetic force $e[H \times v]$ on each beta particle is then balanced by the centrifugal force mv^2/ρ. Therefore

$$Hev = mv^2/\rho \qquad (1)$$

where the charge e equals 1.6×10^{-20} emu, the magnetic field H is expressed in gauss, and the radius of curvature is ρ cm. The *kinetic energy* E of the beta particles will be calculated as a function of the magnetic field H and radius ρ of the circular path.

The relativistic mass dependence of the electron mass m on the velocity v of the electron is

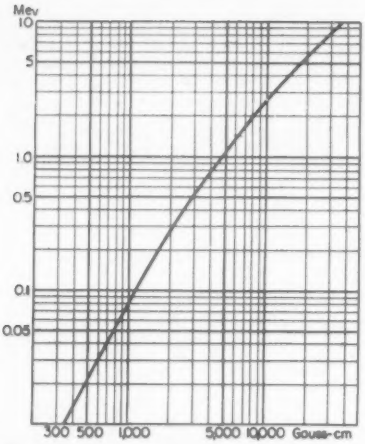

FIG. 2. ($H\rho$) in gauss-cm as a function of the kinetic energy (E) of the electron in Mev

$$m = \frac{m_0}{\sqrt{1-\beta^2}} \qquad (2)$$

where $\beta = v/c$ (c is the velocity of light) and m_0 is the rest mass ($v = 0$) of the electron. The *total* energy W of an electron, that is, its kinetic energy E plus its rest energy m_0c^2, is determined by the relativistic equation

$$W = mc^2 = E + m_0c^2 \qquad (3)$$

By combining Eqs. 1 and 2,

$$eH\rho = mv = m_0v\frac{1}{\sqrt{1-\beta^2}} \qquad (4)$$

From Eqs. 2 and 3,

$$E = m_0c^2\left(\frac{1}{\sqrt{1-\beta^2}} - 1\right) \qquad (5)$$

Combining Eqs. 4 and 5 the velocity v of the electron can be eliminated, giving finally,

$$eH\rho = \frac{1}{c}(E^2 + 2m_0c^2E)^{1/2} \qquad (6)$$

or $$H\rho = \frac{10^4}{3}(E^2 + 1.02E)^{1/2}$$

where E is given in Mev.

Since $eH\rho$ is the momentum of the electron (Eq. 4), the final equation (6) is the frequently used relationship between the kinetic energy E of an electron and its momentum.* This energy-momentum relationship is represented graphically in Fig. 2, where E is given in Mev and $H\rho$ in gauss-cm.

From cloud chamber pictures (see Fig. 3), the radii of curvature ρ and therefore $H\rho$ can be determined accurately, if there is no scattering of the beta particles in the chamber gas. In a cloud chamber filled with hydrogen, the scattering (elastic and inelastic) of the electrons is somewhat reduced. Several procedures have been developed for the determination of the "correct" radius of curvature, but the accuracy attainable is always limited by multiple scattering (*6*). The large number of photographs necessary for each investigation necessitates tedious work. But even with several thousand tracks measured, the statistical error still remains significant.

For these reasons the cloud-chamber method is no longer used for the investigation of beta-ray spectra. However,

* Since $eH\rho = p$, the momentum of the electron, and $E = W - m_0c^2$ (Eq. 3) from Eq. 6 follows the well-known relativistic correlation between momentum and total electron energy, $p^2c^2 = W^2 - (m_0c^2)^2$. The momentum given in relativistic units of m_0c is $\eta = p/m_0c$ and the total energy in units of m_0c^2 is $\epsilon = W/m_0c^2$. Then Eq. 6 becomes $\eta^2 = \epsilon^2 - 1$ and Eq. 4 in these relativistic units becomes:

$$\eta = \frac{eH\rho}{m_0c} = \frac{H\rho\ (\text{gauss-cm})}{1704.2}$$

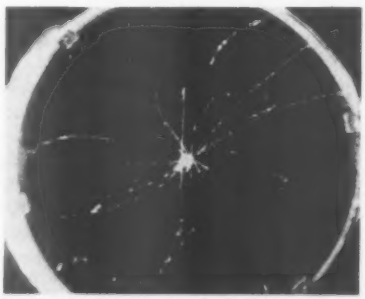

FIG. 3. Cloud chamber tracks of beta rays in a magnetic field; UX-source at the center of the Wilson chamber

the instrument is still a very useful tool in nuclear research, e.g., for studying the different types of particles involved in nuclear reactions, their angular distribution, etc.

The most accurate results today are obtained with the various types of magnetic beta-ray spectrometers. Scattering effects are minimized by the low pressure existing in these instruments.

Semicircular Beta-ray Spectrograph

During recent years several different types of magnetic beta-ray spectrometers have been developed. The oldest, using the semicircular (180°) focusing method is characterized by its great resolving power. The electron energies are determined on the same principle already described for the cloud-chamber measurements. The radius of curvature is fixed in the 180° spectrometer and can, therefore, be determined very accurately. The intensities of the beta radiation at different energy intervals are investigated by varying the magnetic field H.

The fundamental idea of the semicircular method is illustrated in Fig. 4. Only a small fraction of the electrons emitted from the radioactive source (filament) at S can pass the aperture AB. A highly uniform magnetic field H is directed perpendicularly to the plane of Fig. 4. All beta rays with a particular kinetic energy, i.e., with the same velocity v, will move on a circular path of diameter 2ρ. The two circles of radius ρ through S,A and S,B intersect at C, while the central circle cuts SC at D (see Fig. 4). Monochromatic beta rays leaving a point source S through AB will, therefore, be focused between C and D, producing a diffuse image with a sharp outside edge at D.

The interval $CD = \Delta\rho$ is the *width of the image*. It follows from Fig. 4 that $SC = 2\rho \cos \alpha$ and that $SD = 2\rho$. Therefore, the width of the image $\Delta\rho$

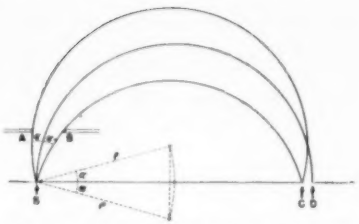

FIG. 4. Focusing principle of the semicircular method

becomes

$$\Delta\rho = 2\rho(1 - \cos \alpha) \qquad (7)$$

For an *extended* source with width s, the width of the image is

$$\Delta\rho = s + 2\rho(1 - \cos \alpha) \qquad (8)$$

The *resolving power* R of the spectrometer is defined as

$$R = \frac{\Delta(H\rho)}{H\rho} = \frac{\Delta\rho}{\rho} = \frac{s}{\rho} + 2(1 - \cos \alpha) \qquad (9)$$

for any constant magnetic field H. The resolving power of the beta-ray spectrometer given in Eq. 9 is independent of the beta-ray energies. The resolution is only a function of the width of the source s, the radius of curvature ρ, and the angular aperture 2α.

In order to obtain a high resolving power (small R), the radius of curvature should be kept large ($\rho \geq 10$ cm).* Large dimensions of the instrument provide two additional advantages. An adequate baffle system can be placed along the path of the beta rays to decrease the number of scattered electrons that will be registered in addition to the focused beta particles. Furthermore, if the isotope emits a strong gamma radiation, the beta-ray detector

* A reduction of only one of the two terms in Eq. 9 would cause an unnecessary reduction of the transmission of the spectrometer without reasonable gain in the resolving power. The optimum ratio between "light" intensity and resolving power occurs, according to the results given by Siegbahn (7), when

$1 - \cos \alpha = s/2\rho$ or $\alpha = \sqrt{s/\rho}$

The above equations hold even for a two-dimensional source of width s and length $2l$ under the condition that $2l \leq 2\pi\sqrt{s\rho}$

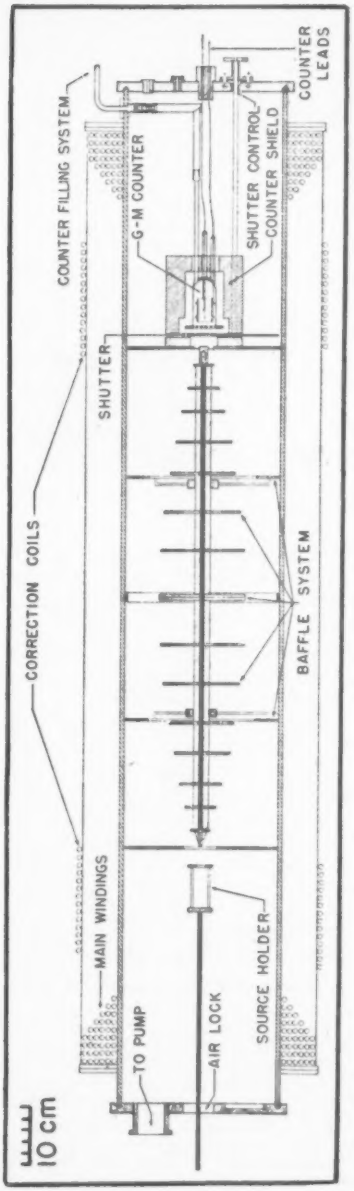

FIG. 5. Solenoidal electron lens spectrometer constructed by Witcher

in a large instrument can be shielded sufficiently against the gamma rays by a thick layer of lead placed between the filament and detector.

A number of difficult problems arise with the construction of a very uniform magnetic field extended over a large area. With a *radially inhomogeneous* magnetic field instead of the uniform one, Langer and Cook (*8*) have recently overcome many of the difficulties involved in the construction of a 180°-focusing spectrometer. Excellent geometric focusing is provided by a magnetic field of the proper inhomogeneity obtained by using a graduated pole face profile. Their instrument combines a high resolving power with a good transmission by using a large mean radius of curvature of 40 cm, a source and a counter slit 0.4 cm wide and 2.54 cm high. Under these conditions the transmission is about 0.1% of the total solid angle and the resolution 0.5%.

Electron Lens Beta-ray Spectrometers

In this short review of beta-ray spectrometers, three other types of instruments should also be mentioned. The application of an electron lens for focusing the beta rays offers the possibility of building instruments with increased transmission.

Fig. 5 shows the *solenoidal* type of electron lens beta-ray spectrometer constructed by Witcher (*9*). A homogeneous magnetic field is produced by a long solenoid together with correction coils compensating for the finite length of the solenoid. The radioactive source, a baffle system 82 cm long, and the detector, a Geiger-Müller counter, are placed inside the coils. At a particular magnetic field strength, electrons with a certain kinetic energy are focused on the detector after they have made exactly one revolution in a helical path

perpendicular to the magnetic field. The solenoid spectrometer combines a high geometric efficiency of about 1% with a good resolution of about 1%, even if the effective source area is very large. Therefore, very thin radioactive sources of rather low activity can be investigated with this instrument.

The *thin magnetic lens* spectrometer represents a different type of instrument, which utilizes the chromatic aberration of a short magnetic electron lens (*10*).

Finally Svartholm and Siegbahn (*11*) have constructed an *inhomogeneous ring-shaped* magnetic field spectrometer for two-directional focusing of electrons. Their apparatus combines the advantageous properties of the semicircular and the magnetic lens methods.

Limitations by Counter Window and Filament

Though today there exists a number of well-designed and thoroughly investigated instruments, the number of reliable measurements of continuous beta-ray spectra is still small but rapidly increasing. In most cases the *low* energy part of the beta-ray distribution curve is subject to distortions.

The beta particles have to penetrate the counter window which separates the Geiger-Müller tube from the evacuated spectrometer chamber. The absorption of the very low energy electrons is considerable, even if the counter window consists of the extremely thin Zaponlac foils (0.3 μ or ~ 0.03 mg/cm^2) recently used by a number of investigators (*8*, *12*). Electrons with energies as low as 3 kev are able to penetrate such foils, but only at a considerable diminution of intensity. Only for beta particles with energies of > 25 kev is the absorption in those counter windows negligible.

Recently attempts have been made to accelerate the low-energy particles (*8*) by applying a difference of potential between the detecting slit and the G-M counter. A rapid increase of the counting rate at potentials above 25 kev has limited the utility of this method so far.

Corrections for the absorption in the counter window can be taken into account to a certain extent. But at the very low-energy region other effects cause additional deformations of the experimental intensity distribution. For example, some of the low-energy beta rays will be absorbed in the sample; others will lose part of their kinetic energy in leaving the sample, even if the amount of radioactive material weighs only ~ 0.5 mg/cm^2 and is mounted on a 0.02 mg/cm^2 Zapon film. Furthermore, the primary beta radiation will expel secondary electrons of lower energies from the radioactive source as well as from its substratum. The "backscattering" of low-energy beta particles from the source increases the intensity at the low energy part of the beta-ray spectrum considerably.

The distortion of the experimental beta-ray spectra in the low-energy region makes comparison with the theoretical distribution curves a difficult task. The best results can be expected from investigations where sources of high specific activity (ratio of sample activity to weight of filament), spread over a relatively large area, can be used for spectrometers with high transmission.

Before discussing some of the experimental results, the theoretical aspect of beta disintegration must be presented first, to enable a comparison between experimental and theoretical data.

The Neutrino and Mass-energy Balance

The numerous electron and positron spectra observed with the different methods, described in the last paragraphs, show a *continuous* distribution in energy covering all values from zero up to a maximum energy E_0.* Since

* Fig. 6 shows four beta-ray spectra with the same upper limit ($E_0 = 1.5$ Mev) for elements of different atomic number Z.

the mass of the nucleus is so large compared with the mass of the beta particle, the kinetic energy of the recoil nucleus is negligible. The initial and final nuclei, however, have *definite* energy levels. Their energy difference has been proved to be equal to the *maximum* beta-ray energy, when no gamma rays are emitted.

On the other hand, calorimetric measurements have shown that the energy released in the decay and absorbed in the calorimeter is equal to the number of disintegrating nuclei times the *average* energy of the beta-ray spectrum. For example, the electron-emitter RaE, which has no gamma rays, has an upper limit of the beta-ray spectrum $E_0 = 1.17$ Mev, and the calorimetric measurements (*13*) give an average energy of $E_{av} = 0.320$ Mev per disintegration.

From these two facts, one has to conclude that in beta decay energy is carried away by some kind of radiation, which is not absorbed in the calorimeter, so that the energy release is always given by the maximum beta-ray energy. In order to conserve charge, this "particle" must have zero charge; this fact excludes its detection by any ionization process. Furthermore, a number of experiments (*14*) show that the rest mass of this particle, if it is not zero, must be small compared to the mass of the electron. This hypothetical particle, introduced by Pauli, is therefore appropriately called the *neutrino* (denoted by ν).

In beta decay a nucleus with a certain mass and charge Z is transformed into another nucleus with the same mass but with a charge of $(Z + 1)$ in the case of electron (β^-) decay, and a charge of $(Z - 1)$ in the case of positron (β^+) emission. For example:

$$_6C^{14} \rightarrow {}_7N^{14} + \beta^- + \nu$$
$$_7N^{13} \rightarrow {}_6C^{13} + \beta^+ + \nu$$

The final neutral atom has one additional orbital electron in the case of β^--decay and one orbital electron less than the initial atom in the case of β^+-decay. Since m_0c^2 is the rest energy of an electron, the *differences in atomic energy* ΔE_{at} involved in beta disintegration are

$$\Delta E_{at} = \Delta E_{nuc} - m_0c^2 \quad \text{(for } \beta^-\text{-decay)}$$
$$\Delta E_{at} = \Delta E_{nuc} + m_0c^2 \quad \text{(for } \beta^+\text{-decay)} \qquad (10)$$

The *change in nuclear energy* ΔE_{nuc}, assuming the neutrino mass to be zero, is the sum of the maximum beta-ray energy and the rest energy of the emitted electron or positron

$$\Delta E_{nuc} = E_0 + m_0c^2 \qquad (11)$$

From Eqs. 10 and 11, it follows that

$$\Delta E_{at} = E_0(\beta^-) \quad \text{(for } \beta^-\text{-decay)} \qquad (12)$$
$$\Delta E_{at} = E_0(\beta^+) + 2m_0c^2 \quad \text{(for } \beta^+\text{-decay)}$$

$E_0(\beta^-)$ and $E_0(\beta^+)$ are the maximum kinetic energies of the beta rays, if the final nucleus is formed in the ground state. If it is left in an excited state, the energy difference emitted as gamma radiation is included in $E_0(\beta^-)$ and $E_0(\beta^+)$.

The mass difference between the radioactive and the final neutral atom has to account for the atomic energy difference expressed in Eq. (12). On an energy basis, for positron emission to occur, the mass M of the initial atom has to be greater than that of the final one by more than $2m_0c^2 = 1.02$ Mev. The conditions for beta decay can be expressed, therefore, as

$$M(Z) > M(Z + 1) \quad \text{(for } \beta^-\text{-decay)}$$
$$M(Z + 1) > M(Z) + 2m_0c^2 \quad \text{(for } \beta^+\text{-decay)} \qquad (13)$$

These two conditions do not exhaust all possibilities. If

$$M(Z) < M(Z + 1) < M(Z) + 2m_0c^2 \qquad (14)$$

then neither β^- nor β^+-decay can occur. A possible process, however, is the capture of an orbital electron, for which it is only necessary that

$$M(Z+1) > M(Z) + \phi$$

where ϕ is the binding energy (positive) of the orbital electron. An example for K-capture is the decay of

$$_{26}Fe^{55} \rightarrow {}_{25}Mn^{55} + \nu$$

The emitted neutrino carries away the energy difference

$$[M(Z+1) - M(Z)]c^2 - \phi.$$

Fermi's Theory of Allowed Transitions

Beta disintegration is regarded as a complex transformation of a neutron ($_0n^1$) into a proton ($_1p^1$) or vice versa, with the simultaneous emission or absorption of an electron and neutrino. β^- and β^+-decay can be expressed therefore as

$$_0n^1 \rightarrow {}_1p^1 + \beta^- + \nu$$
$$_1p^1 \rightarrow {}_0n^1 + \beta^+ + \nu$$

In his theory of beta decay, Fermi (*15*) considers the neutron and the proton as two different states of one "nucleon." The heavy particles (nucleons) are supposed to be the sources and sinks of the light particles (beta particles and neutrinos). The electron (or positron) and the neutrino (or antineutrino)* are created at the moment when the transition takes place, i.e., during the disintegration of the nucleus. This process is thought to be analogous to the creation of a photon when an atomic shell electron makes a quantum jump during light emission. An interaction is postulated between the nucleons and the two light particles (electron and neutrino), analogous to the interaction between charges (electrons) and the electromagnetic field (light) in quantum electrodynamics.

The probability for the emission of a beta particle with an energy in the interval ϵ to $(\epsilon + d\epsilon)$, accompanied by the emission of a neutrino with an energy between $(\epsilon_0 - \epsilon)$ and $(\epsilon_0 - \epsilon - d\epsilon)$, is given by Fermi as

$$P(\epsilon)d\epsilon = \left(\frac{G^2}{2\pi^3}\right)\frac{m_0c^2}{\hbar}|M|^2F(Z,\epsilon)(\epsilon_0 - \epsilon)^2(\epsilon^2 - 1)^{1/2}\epsilon d\epsilon \quad (16)$$

where ϵ is the total energy (kinetic energy plus rest energy) in units of (m_0c^2), and ϵ_0 is the maximum total energy in the same relativistic units.

The shape of the beta-ray spectrum is mainly determined by the statistical factor for the emission of an electron-neutrino pair, included in Eq. 16,

$$(\epsilon_0 - \epsilon)^2(\epsilon^2 - 1)^{1/2}\epsilon d\epsilon$$

for which the rest mass of the neutrino is taken to be zero.

The dimensionless constant G is given by

$$G = \frac{g}{m_0c^2}\left(\frac{m_0c}{\hbar}\right)^3$$

where g is called the "Fermi constant." This coupling constant measures the strength of the interaction between the nucleons and the electron-neutrino field; it has to be determined by experiments.

The Fermi function $F(Z,\epsilon)$ describes the influence of the nuclear Coulomb field; it is given as

$$F(Z,\epsilon) = \frac{4}{[\Gamma(1+2s)]^2}\cdot\left(\frac{1+s}{2}\right)\cdot(2\eta R)^{2s-2}\cdot e^{\pi\alpha Z\epsilon/\eta}\left|\Gamma\left(s + i\frac{\alpha Z\epsilon}{\eta}\right)\right|^2 \quad (17)$$

where $s(Z) = \sqrt{1 - (Z\alpha)^2}$

$\alpha = e^2/\hbar c = 1/137$

$\eta = (\epsilon^2 - 1)^{1/2}$ the momentum of the beta particle in units of m_0c

R = the nuclear radius in units of $\hbar/m_0c$

For $Z = 0$, $F(0,\epsilon) = 1$, and for light elements $F(Z,\epsilon) \approx 1$. The Coulomb field, therefore, has an insignificant effect on the shape of the beta-ray spectrum of light nuclei, while its influence increases for heavier elements. Fig. 6 shows the four calculated energy-distribution curves for elements with $Z = 0$, ± 27, and $+82.2$. The repulsion of the positrons in the nuclear Coulomb field is evident, as is also the increase of attraction of the low-energy

* The neutrino when emitted with a positron is often called an antineutrino.

UNIVERSITY OF MICHIGAN LIBRARIES

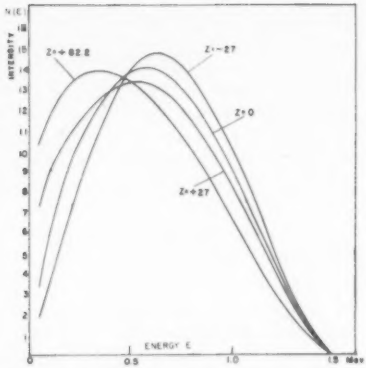

FIG. 6. Allowed simple Fermi beta-ray spectra with a maximum energy of 1.5 Mev for elements of atomic number $Z = 0$, $+27$, $+82.2$ and -27 (negative sign refers to positron emission)

electrons with increasing atomic number.

The variation of the energy-dependent part of the Fermi function $F(Z,\epsilon)$ with energy ϵ is indicated in Fig. 7 for $Z = 0$, ± 13, ± 27, ± 51 and $+82.2$; the negative Z values represent positron emitters. These curves are based on an approximation given by Nordheim and Yost (*16*), for which the modulus of the complex gamma function is expressed by

$$\left|\Gamma\left(s + i\frac{\alpha Z\epsilon}{\eta}\right)\right|^2 = \frac{2\pi\alpha|Z|\epsilon/\eta(3-2s)}{|e^{\pi\alpha Z\epsilon/\eta} - e^{-\pi\alpha Z\epsilon/\eta}|} \quad (18)$$

From Eqs. 17 and 18 follows, therefore, the energy dependence of the Fermi function as

$$F(Z,\epsilon) = \frac{2\pi\alpha|Z|\epsilon/\eta}{|1 - e^{-2\pi\alpha Z\epsilon/\eta}|}$$

The curve for $Z = 82.2$ has been calculated directly from a formula given by Fermi (*15*)

$$F(82.2,\epsilon) = \frac{4.5}{\sqrt{\epsilon^2 - 1}} + 1.6 \quad (19)$$

Finally the nuclear matrix element M depends only on the state of the nucleon before and after the transition; its value is not known in general. For a so-called *allowed transition*, its value is independent of the energy of the beta particles; it decreases with increasing number of neutrons and protons in the nucleus. The matrix element $|M|$ has a value different from zero, between zero and one. Furthermore, the order of magnitude of $|M|$ depends drastically on certain selection rules, which will be briefly indicated here without further explanation. According to Fermi, no change of nuclear spin should be involved in an allowed transition, *i.e.*, the initial and final nucleus should have the same spin. In addition the parities of the initial and final nucleus must be the same. However on the basis of experimental evidence, the selection rules given by Gamow and Teller (*17*) might be preferred to Fermi's. For an allowed transition, the Gamow-Teller selection rules are: no parity change and spin difference zero, plus one or minus one, (no $0 \rightarrow 0$ transition).

Half-life of Beta-ray Emitters

Since $P(\epsilon)d\epsilon$ gives the spectral energy distribution, the total disintegration probability λ (decay constant in sec^{-1}) should be

$$\lambda_{theor} = \frac{\ln 2}{t} = \int_1^{\epsilon_0} P(\epsilon)d\epsilon = \frac{m_0c^2}{\hbar}\frac{G^2}{2\pi^3}|M|^2 f(Z,\epsilon_0) \quad (20)$$

where

$$f(Z,\epsilon_0) = \int_1^{\epsilon_0} F(Z,\epsilon)(\epsilon^2 - 1)^{1/2} (\epsilon_0 - \epsilon)^2\epsilon d\epsilon \quad (21)$$

and t is the half-life in sec. By comparing the experimental decay constant with calculated decay probability λ_{theor} (Eq. 20), a numerical value for $G^2 \times |M|^2$ can be obtained. For a mirror nuclei transition, which is an allowed transition, since the initial proton and the final neutron are expected to be in the same nuclear state, $|M|^2 \approx 1$. Therefore, for example, from

the half-life $t = 125$ sec and the maximum energy $\epsilon_0 = 4.37\ m_0c^2$ of the positron emitter ${}_8O^{15}$, it follows that $G \approx 3.7 \times 10^{-12}$.

The product of $f(Z,\epsilon_0)$ times the half-life (t) of the radioisotope is often quoted as (ft). From Eq. 20, it follows that $|M|^2 \times (ft)$ is expected to be constant for the different classes of transitions (allowed, first forbidden, etc.). The matrix element for each class, however, depends on Z, and decreases with increasing complexity of the nucleus. Therefore, the (ft)-values for allowed transitions will increase with the atomic number.

Konopinski (*18*) has gathered the (ft)-values for all beta-ray emitters, so far as their energies and half-lives were known at that time. The (ft)-values for *forbidden* transitions are distinctly greater than for allowed disintegrations. The transition probability decreases with the increasing degree of forbiddenness of the transition.

Average Beta-ray Energy

Besides its maximum energy, the shape of the continuous beta-ray spectrum depends on a number of other factors discussed in the last paragraphs. Therefore, the *average* beta-ray energy released per disintegration will not be only a function of the upper limit of the beta-ray spectrum.

The average energy (kinetic plus rest energy) of the emitted beta particles, ϵ_{av} in units of m_0c^2, can be calculated (*19*) for a known emission probability $P(\epsilon)d\epsilon$ (Eq. 16) by:

$$\epsilon_{av} = \int_1^{\epsilon_0} \epsilon P(\epsilon)d\epsilon \Big/ \int_1^{\epsilon_0} P(\epsilon)d\epsilon \quad (22)$$

The average energy of each beta-ray emitter is a characteristic constant of considerable value in many problems. Thus the total number of ion pairs produced per unit time by a given amount of a beta-active substance is a linear function of its average kinetic beta-ray energy (*4*). Therefore, if the average

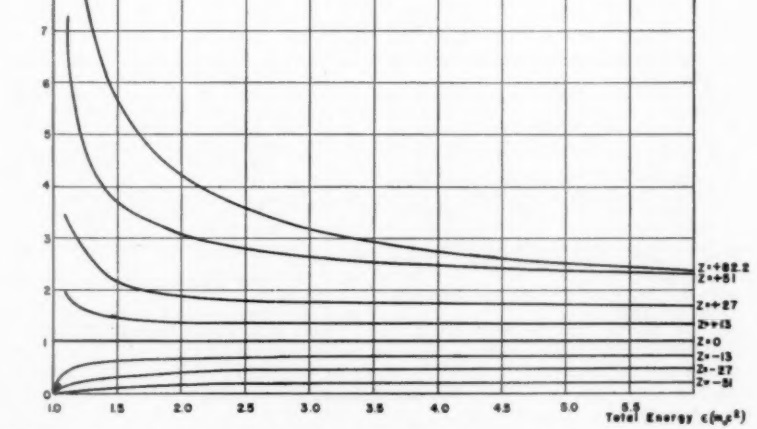

FIG. 7. Variation of the Fermi function $F(Z,\epsilon)$ with energy of the beta particles, for positron and electron emitters

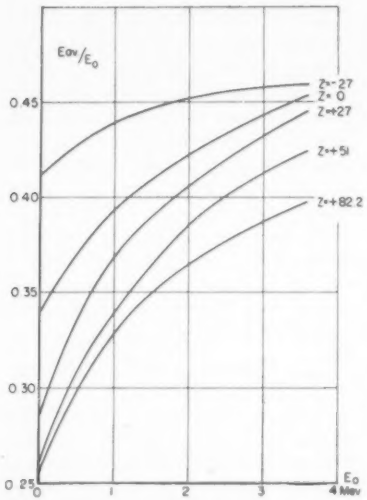

FIG. 8. Ratio of the average kinetic beta-ray energy E_{av} to the maximum energy E_0 as a function of E_0 and Z (calculated for allowed simple Fermi spectra)

energy is known, the activity of a radioactive substance can be determined by measuring the total number of ion pairs produced per unit time. Alternatively, for a calibrated source the disintegration rate can easily be calculated (*4*).

The average kinetic energy E_{av} (in units of Mev) divided by the maximum energy E_0, has been plotted in Fig. 8 for simple beta-ray spectra as a function of E_0 for elements with charge $Z = 0$, ± 27, $+51$, and $+82.2$. The calculations for these curves are based on Eqs. 16 and 22, with the values for the Fermi function $F(Z,\epsilon)$ from Fig. 7. These average kinetic energy values apply only to beta-ray spectra with the shape of an allowed Fermi distribution. The calculated and experimental values of E_{av} have been compared in a previous paper (*19*), and the experimental values for all carefully investigated beta-ray spectra have been recently reported in this journal (*4*).

The variation of the shape of allowed beta-ray spectra with E_0 and Z can be recognized from the curves of E_{av}^*/E_0 shown in Fig. 8. The energy spectrum is shifted toward the region of higher energies with increasing maximum energy as well as with decreasing nuclear charge (light elements and positron emitters).

BIBLIOGRAPHY

1. L. E. Glendenin, NUCLEONICS **2**, No. 1, 12 (1948)
2. R. G. Fluharty, NUCLEONICS **2**, No. 5, 28 (1948)
3. M. D. Kamen, "Radioactive Tracers in Biology," (Academic Press, Inc., New York, 1947)
4. L. D. Marinelli, E. Quimby, G. J. Hine, NUCLEONICS **2**, No. 4, 56 (1948)
5. E. Bleuler, W. Zünti, *Helv. Phys. Acta* **19**, 375 (1946)
6. H. A. Bethe, *Phys. Rev.* **70**, 821 (1946)
7. K. Siegbahn, *Arkiv Mat. Astron. Fysik* **30A**, No. 20 (1944)
8. L. M. Langer, C. S. Cook, *Rev. Sci. Instr.* **19**, 257 (1948)
9. C. M. Witcher, *Phys. Rev.* **60**, 32 (1941)
10. M. Deutsch, L. G. Elliott, R. D. Evans, *Rev. Sci. Instr.* **15**, 178 (1944)
11. N. Svartholm, K. Siegbahn, *Arkiv Mat. Astron. Fysik* **33A**, No. 21 (1946)
12. K. Siegbahn, *Phys. Rev.* **70**, 127 (1946)
13. I. Zlotowski, *Phys. Rev.* **60**, 483 (1941)
14. C. W. Sherwin, NUCLEONICS **2**, No. 5, 16 (1948)
15. E. Fermi, *Z. Physik* **88**, 161 (1934)
16. L. W. Nordheim, F. L. Yost, *Phys. Rev.* **51**, 942 (1937)
17. G. Gamow, E. Teller, *Phys. Rev.* **49**, 895 (1936)
18. E. J. Konopinski, *Revs. Modern Phys.* **15**, 209 (1943)
19. L. D. Marinelli, R. F. Brinkerhoff, G. J. Hine, *Revs. Modern Phys.* **19**, 25 (1947)

Design of An Improved-Yield Discharge Tube*

Used for investigating nuclear reactions, this tube is said to require less energy per nuclear reaction than present tubes. Unused kinetic energy of bombarding particles is fed back to high-voltage generator. Design and uses are discussed

By JAROSLAV PACHNER

Institute for Technical Physics, Prague Technical University
Prague, Czechoslavakia

IN THE DISCHARGE TUBES used at present only a small part of the kinetic energy of the accelerated particles is utilized for nuclear reactions, the major part of the nonutilized kinetic energy being transformed into heat which causes the temperature of the bombarded target to increase. Described in this paper is a tube in which a large proportion of the kinetic energy of those particles which have not participated in the nuclear reactions is fed back into the high-voltage generator.

The principle of this tube is based on the following considerations: Of the highly accelerated, electrically charged particles, only a certain proportion, determined by the effective nuclear cross section of the target, overcomes the repulsive forces of the Coulomb field and penetrates the nuclei. The remainder of the particles are scattered by the electrons, with the speed of the particles being successively reduced. Nuclear reaction is still possible for this second group of particles, but the probability for such a reaction, determined by the Gamow factor, decreases very rapidly with decreasing kinetic energy. It is therefore advantageous to use a very thin target to reduce to a minimum the loss of kinetic energy of the particles which pass through the target, and to feed back, by retardation in the electrostatic field, the remaining kinetic energy of these particles directly to the high-voltage generator. In this way less energy per nuclear reaction is required.

The main advantage of this tube is that the acceleration voltage can be divided into two parts—the voltage for the preliminary and the voltage for the main acceleration. The preliminary acceleration gives the particles only as much energy as they lose when passing through the target. The required voltage is determined, to a large extent, by the target thickness and can be chosen relatively low, about 100 to 300 kv. The current required for preliminary acceleration for a given number of reactions per unit time is about the same as in presently used tubes which work with a voltage of 1 to 2 megavolts. Whereas construction of a d-c generator for voltages over 1 megavolt with an output of several milliamperes is difficult, it is relatively easy to obtain up to about 1 amp d-c of 100 to 300 kv from a mercury vapor, oxide-cathode rectifier.

The voltage for the main acceleration is of the same magnitude as the voltage required for retardation. The high-voltage generator is only required to supply current for the particles which cause nuclear reactions or are so widely

* Translated from *Elektrotechnicky Obzor* No. 14, 266 (1947) by E. Gros, London, England.

dispersed on the nuclei that they would not reach the part of the tube where the retardation of the particles takes place. The current required for this purpose is very small, and it is possible to use impulse generators, which can be built without difficulty up to several megavolts. Thus high acceleration of particles, such as, up to now, has only been obtained with cyclotrons, can be produced.

The advantages more than offset the disadvantage of increased difficulty of cooling the very thin layers of target material, particularly if their melting point is low. It is likely that this difficulty will only be overcome by reduction of current density.

In the following pages the energy conditions will be analyzed quantitatively by the use of relatively simple mathematical formulas, followed by a few numerical examples. The design details of the tube, which differ from those for tubes of known design, are then described. In conclusion, the application possibilities of the tube are summarized.

Theoretical Considerations

If a mass m_2 with a charge Z_2e (e is the electron charge) moves with speed v_2 at a distance p from an initially stationary mass m_1 with a charge Z_1e, a part of the kinetic energy ΔE_2 will be transferred to the mass m_1:

$$\Delta E_2 = \frac{2}{m_1} \times \frac{(Z_1Z_2e^2)^2}{(pv_2)^2 + \left(\frac{Z_1Z_2e^2}{\mu v_2}\right)^2} \quad (1)$$

where

$$\mu, \text{ the reduced mass, } = \frac{m_1m_2}{m_1 + m_2} \quad (2)$$

Equation 1 is obtained from the formulas developed by A.v. Engel and M. Steenbeck* for the impact of two moving masses. For particles moving at a very high speed,

$$(pv_2)^2 \gg \left(\frac{Z_1Z_2e^2}{\mu v_2}\right)^2$$

Sufficient accuracy is obtained by rewriting Eq. 1:

$$\Delta E_2 \approx \frac{2}{m_1}\left(\frac{Z_1Z_2e^2}{pv_2}\right)^2 \quad (1a)$$

This equation shows that the part of the kinetic energy transferred by m_2 to m_1 is inversely proportional to the value of m_1. The bombarded target consists of electrons and considerably heavier nuclei. The whole system is quantized (Eq. 1 is developed from laws of classical physics), but the losses of kinetic energy caused by dispersion on the nuclei is negligible in comparison to the losses on the electrons. Exact quantum mechanical calculation shows that the energy loss $-dE_2$ along a distance ds is given by the relation

$$\frac{dE_2}{ds} = -\frac{4\pi Z_2^2e^4}{m_e v_2^2} \times NZ_1 \ln \frac{2m_e v_2^2}{J} \quad (3)$$

where m_e is the mass of an electron, J the mean value of the excitation energy of the atom m_1, and N the number of atoms per unit of target volume. It is advantageous to introduce into Eq. 3 the maximum potential energy E_0 of the charge Z_2e in the Coulomb field of charge Z_1e:

$$E_0 = Z_1Z_2e^2/R \quad (4)$$

and the kinetic energy E_2 of the substance m_2 measured in the coordinate system of substance m_1 and obtained after it passes through the potential difference U:

$$E_2 = \tfrac{1}{2}m_2v_2^2 = Z_2eU \quad (5)$$

Thus, we obtain

$$\frac{dE_2}{ds} = -\frac{2}{Z_1}\frac{m_2}{m_e} \times \ln\left(4\frac{m_e}{m_2} \times \frac{E_2}{J}\right)\frac{E_0^2}{E_2} \times N\sigma \quad (3a)$$

where $\sigma = \pi R^2$ is the geometric cross section of the nucleus m_1, the radius R of which is taken as being equal to the distance between the maximum potential and the center of the nucleus. If the target is very thick, it is necessary

* A. v. Engel, M. Steenbeck, "Elektrische Gasentladungen, ihre Physik und Technik," (Springer, Berlin, 1932–34; reprint: Edwards Bros., Ann Arbor, Mich., 1944).

to integrate Eq. 3*a*, which is possible by means of the logarithmic integral. After separation of the variables and slight rearrangement, we obtain

$$\left(4\frac{m_e}{m_2}\times\frac{1}{J}\right)^2\frac{E_2dE_2}{\ln\left(4\frac{m_e}{m_2}\times\frac{E_2}{J}\right)} = -\frac{E_0^2}{J^2}\times N\sigma\times\frac{32}{Z_1}\times\mu\frac{m_e}{(m_2)^2}\times ds$$

This equation is of the type

$$\frac{xdx}{\ln x} = -ads$$

The left side of this equation can be rearranged

$$\frac{xdx}{\ln x} = \frac{2xdx}{2\ln x} = \frac{d(x^2)}{\ln(x^2)}$$

and by integration of

$$\int\frac{d(x^2)}{\ln(x^2)} = -a\int ds$$

we obtain

$$\ln(x^2) = -as + \text{const.}$$

After inserting the appropriate values (E_2 is a function of s here), we obtain

$$\ln\left(4\frac{m_e}{m_2}\frac{E_2(s)}{J}\right)^2 = \ln\left(4\frac{m_e}{m_2}\frac{E_2(0)}{J}\right)^2 - \frac{E_0^2}{J^2}\times N\sigma\times\frac{32}{Z_1}\times\mu^2\frac{m_e}{(m_2)^2}\times s \quad (6)$$

The integration constant has been determined from the condition that, for $s = 0$, the energy $E_2(s) = E_2(0)$. Equation 6 can be used to determine the energy of the particles m_2 at a depth s of the target, *i.e.* the penetration depth can thus be obtained.

The logarithmic integral of Eq. 6 is not often found in tables, but an approximate integration of the appropriate differential equation (3*a*) can be obtained by considering the natural logarithm as a constant, in spite of the fact that there is a variable E_2 in the argument. As a result, we obtain the particular integral

$$E_2^2(s) \approx E_2^2(0) - \frac{4}{Z_1}\times\frac{m_2}{m_e}\ln\left(4\frac{m_e}{m_2}\frac{E_2}{J}\right)E_0^2Ns\sigma$$

or, if the range is called s_0,

$$E_2^2(s) \approx E_2^2(0)\left(1-\frac{s}{s_0}\right) \quad (6a)$$

This equation shows clearly the relation between the energy of the particles and the length of travel through the target. In the proposed tube, the target is very thin and we can therefore replace the differentials in Eq. 3*a* by differences. We obtain for the relative loss

$$\frac{\Delta E_{2E}}{E_2} = -\Lambda_1 N\sigma\Delta s \quad (7)$$

where

$$\Lambda_1 = \frac{2}{Z_1}\frac{m_2}{m_e}\left(\frac{E_0}{E_2}\right)^2\times\ln\left(4\frac{m_e}{m_2}\times\frac{E_2}{J}\right) \quad (8)$$

The index E is added to ΔE_{2E} in Eq. 7 to emphasize that the losses occur on the electrons. The length of travel of the particles inside the target is Δs. Equation 3, and also Eqs. 3*a* and 7 developed from it, give the statistical mean value of losses. The actual losses of the individual particles are dispersed around this mean value. As the value $Z_1N\Delta s$ is very high (the particles m_2 are dispersed on a great number of electrons) even for the thinnest foil, the function expressing the energy distribution of the particles will show a very steep drop to zero on both sides of the mean value. This is confirmed by α-ray photographs taken in a cloud chamber; the particles show almost equal range. In calculations, this statistical fluctuation is taken into consideration by choosing the value J (average excitation energy of the atom m_1) somewhat lower than usual. This is wrong in principle, because the average excitation energy of an atom is entirely independent of the statistical fluctuation. However, only an insignificant part of the particles m_2 will have lower losses than calculated.

In addition to loss of kinetic energy of the particles, dispersion also causes deflection of the particles from their original trajectory, and it is necessary to determine this deflection. Engel and Steenbeck have developed a formula for calculation of the deflection angle

UNIVERSITY OF MICHIGAN LIBRARIES

for simple dispersion, which is written here in a somewhat different form.

$$\tan \alpha_2 = \frac{4m_1 \frac{\mu E_2 p}{m_2 E_0 R}}{4(m_1 + m_2)\left(\frac{\mu E_2 p}{m_2 E_0 R}\right)^2 - (m_1 - m_2)} \quad (9)$$

From this

$$\frac{p}{R} = \frac{m_1 + \sqrt{(m_1)^2 + [(m_1)^2 - (m_2)^2]\tan^2 \alpha_2}}{2(m_1 + m_2)\tan \alpha_2} \times \frac{m_2}{\mu} \times \frac{E_0}{E_2} \quad (10)$$

It follows from Eq. 9 that, for dispersion on the electrons ($m_1 = m_e \ll m_2$), the maximum deflection angle is

$$\alpha_{max} = \text{arc tan} \frac{m_e}{\sqrt{(m_2)^2 - (m_e)^2}} \approx \text{arc tan} \frac{m_e}{m_2} \quad (11)$$

This deflection is so small that it can be neglected altogether. This view is confirmed by cloud chamber photographs. It is therefore unnecessary to take into consideration multiple dispersions.

The deflection angle is much larger for dispersion by the nucleus of the atom, and it is possible that a deflected particle will never reach the space where progressive retardation takes place. The limit of angle for and above which this occurs is to be determined. From Eq. 10:

$$\frac{p_0}{R} = \frac{m_1 + \sqrt{(m_1)^2 + [(m_1)^2 - (m_2)^2]\tan^2 \alpha_0}}{2(m_1 + m_2)\tan \alpha_0} \times \frac{m_2}{\mu} \times \frac{E_0}{E_2} = \sqrt{\Lambda_2} \quad (12)$$

where p_0 is the distance of the particle from the nucleus of the atom. For $m_2 \ll m_1$ we obtain the approximation

$$\frac{p_0}{R} \approx \frac{1}{2}\frac{E_0}{E_2}\cot\frac{\alpha_0}{2} = \sqrt{\Lambda_2} \quad (12a)$$

which also follows directly from the dispersion formula of Rutherford. As the mean length of the free path of the accelerated particles, $\lambda = 1/[\pi(p_0)^2 N]$, is much larger than the target thickness (*e.g.* for $\alpha_0 \approx 6°$, $E_2 \approx E_0$, $p_0 \approx R$; for $_4Be^9$, $R \approx 3.2 \times 10^{-13}$ cm, $N \approx 1.25 \times 10^{23}$ cm^{-3}, and $\lambda \approx 1$ cm, whereas the foil thickness s is only about 10^{-3} cm), it is permissible to take into consideration only the simple dispersion.

From the point of view of retardation, if a particle m_2 travels at a distance less than p_0 from the center of the atom, it loses its total energy E_2. The probability for this to occur is equal to the ratio of the area of the circle $\pi(p_0)^2$ and the area occupied by one atom $1/(N\Delta s)$. For a very large number of particles, there will be a mean value of energy loss (E_{2K}) caused by dispersion by the atom nuclei.

$$\frac{\Delta E_{2K}}{E_{2K}} = -\frac{\pi(p_0)^2}{1/(N\Delta s)} = -\Lambda_2 N\sigma\Delta s \quad (13)$$

The value Λ_2 is determined by Eqs. 12 and 12*a* and is equal to, or larger than, one. The probability of a nuclear reaction, W_R, is a combination of the probability of particle m_2 hitting a nucleus of cross section σ, the probability G (Gamow factor) that the particle will overcome the repulsive Coulomb field, and the probability w_R that the penetrating particle will cause a nuclear reaction (*i.e.* that it will not be just abnormally deflected). The total probability is

$$W_R = \frac{w}{1/(N\Delta s)} \times Gw_R = N\sigma\Delta s G w_R \quad (14)$$

As long as the energy of the particles m_1 and m_2, measured in the static system of the centers of gravity of the masses m_1 and m_2, is smaller than the maximum potential of the repulsive Coulomb field, the factor G will be smaller than one. Its value was calculated for the first time by G. Gamow, and later, more accurately by T. Sexl. The proposed tube is only advantageous if the kinetic energy of the accelerated particles is higher than the threshold of

the potential (for which the losses due to dispersion on electrons is also lower, *viz.* Eqs. 3*a*, 7, 8). Therefore, the characteristic of the G factor need not be discussed. It is sufficient to know that it is equal to one if the kinetic energy of the particles m_1 and m_2 (measured in the static point of gravity system), $\frac{1}{2}\mu(v_2)^2$, is equal to, or larger than, E_0, the maximum energy potential, or (*viz.* Eqs. 5 and 2)

$$E_2 \geqq \frac{m_2}{\mu} E_0 = \left(1 + \frac{m_2}{m_1}\right) E_0 \quad (15)$$

The value w_R is given by Weizsäcker as being of the magnitude of one, except for the reaction ${}_3Li^7(p,\alpha){}_2He^4$, for which it is about 1%.

If it is desired to obtain in the tube P reactions per unit time, the total current I_2 of the particles m_2 is given by

$$P = w_R \frac{I_2}{Z_2 e}$$

From this

$$I_2 = \frac{Z_2 e P}{w_R} = I_{PZ} \quad (16)$$

This equation gives the current taken from the d-c generator for the preliminary acceleration, I_{PZ}. As has been mentioned in the introduction the voltage required for preliminary acceleration must be high enough to give the passing particles the kinetic energy which these particles will lose by dispersion on the electrons, ΔE_{2E}. Thus, from Eqs. 5 and 7, it follows that

$$U_{PZ} = \frac{E_2}{Z_2 e} \Lambda_1 N \sigma \Delta s \quad (17)$$

The main accelerating voltage is, according to Eq. 5,

$$U_{HZ} = \frac{E_2}{Z_2 e} - U_{PZ} \quad (18)$$

and the current I_{HZ} is given by the current intensity of the particles m_2 multiplied by the probability of these particles not reaching the retardation space of the tube because of excessive dispersion on the nuclei (Eq. 13). Thus, we obtain

$$I_{HZ} = I_2 \Lambda_2 N \sigma \Delta s \quad (19)$$

The current density j_2 in the discharge tube is determined by the maximum permissible energy loss per unit target area L_0. This loss is caused by dispersion on the electrons and is equal to the power supplied by the generator for preliminary acceleration, $U_{PZ} I_{PZ}$. We obtain

$$j_2 = \frac{U_{PZ} I_{PZ}}{L_0} \quad (20)$$

I_2, the current intensity of the particles m_2, is identical with the intensity of the preliminary accelerating current, I_{PZ}, and is higher than the current intensity I_s of a standard discharge tube where the target is massive and not a thin foil. The ratio between the two current intensities can easily be determined. It has been mentioned that one of the factors determining the number of reactions P, according to Eqs. 14 and 16, is the current intensity of the particles, I_2, and the Gamow factor G, which in turn is determined by the energy E_2 and consequently (Eqs. 6 and 6*a*) by the travel s of the particle in the target:

$$P = N \sigma w_R \frac{I_2}{Z_2 e} \int_0^s G(s) ds$$

To obtain in the new tube the same number of reactions as is obtained in the types used at present, it is necessary to fulfill the relation

$$I_2 \int_0^{\Delta s} G(s) ds = I_s \int_0^{s_0} G(s) ds$$

which follows from the preceding relation (after division of both sides of the equation by $N \sigma w_R / Z_2 e$). As long as the kinetic energy, E_2, of the particles m_2 is higher than the maximum energy potential, E_0, as is the case in the new tube, the Gamow factor G is constant and equal to one, and the following approximate relation is applicable:

$$\frac{I_2}{I_s} = \frac{\int_0^{s_0} G(s) ds}{\int_0^{\Delta s} G(s) ds} \approx \frac{s_0}{\Delta s} \quad (21)$$

Comparison of Current Intensities and Voltages in Proposed Tube with Those in Present Tubes

Reaction	$10^3\Delta s$ cm	m_2E_0/μ Mv	E_2 Mv	Gw_R	I_{PZ} ma	U_{PZ} kv	I_{HZ} A	U_{HZ} Mv	$F \times 10^{-4}$ Mev	$(\eta - 1) \times 10^4$	$\frac{I_{PZ}}{I_z}$	$\frac{I_{HZ}}{I_z}$ %
Ia	1.0	1.9	0.8	0.55	2.4	500	3.60	0.30	7.4	2.0	1.16	0.17
Ib	1.0	1.9	3.0	1	1.3	160	0.13	2.84	1.3	11.0	9.7	0.10
IIa	0.5	2.2	3.0	1	0.8	300	0.28	2.70	1.5	2.8	5.3	0.19
IIb	0.2	2.2	3.0	1	2.0	120	0.28	2.88	1.5	2.8	13.0	0.18
IIc	0.5	2.2	10.0	1	0.8	100	0.016	9.90	0.5	8.2	50.0	0.10
III	0.2	5.2	6.0	1	2.0	240	0.25	2.76	6.0	0.9	6.7	0.08

In reality this relation is not a favorable one, because, for $E_2(s) < E_0$ (this only occurs at the end of the trajectory in present tubes), the Gamow factor decreases. Inserting into Eq. 21 values from Eq. 6*a*, we obtain, after slight rearrangement, the sought relation

$$\frac{I_2}{I_z} = \frac{I_{PZ}}{I_z} = \frac{1}{1 - \left(\frac{E_2(\Delta s)}{E_2(0)}\right)^2} = \frac{1}{1 - \left(\frac{U_{HZ}}{U_{HZ} + U_{PZ}}\right)^2} \approx \frac{1}{2}\left(1 + \frac{U_{HZ}}{U_{PZ}}\right) \quad (22)$$

From a summary of the results obtained it follows that, for a number of reactions in the new tube equal to that in normally used ones, the current I_2 of the particles m_2 is equal to the current intensity of the preliminary acceleration I_{PZ} and is higher by the ratio given in Eq. 22 than the current intensity in the normal tubes, whereas for the main acceleration the current intensity is considerably lower. The ratio is

$$\frac{I_{HZ}}{I_z} = \frac{I_{HZ}}{I_{PZ}} \times \frac{I_{PZ}}{I_z} \approx \frac{1}{2}\left(1 + \frac{U_{HZ}}{U_{PZ}}\right)\frac{I_{HZ}}{I_{PZ}} \quad (23)$$

To permit better judgment of the performance of the new tube, two additional terms must be introduced—tube utilization and tube efficiency. Utilization factor of the tube, F, is the energy required to produce one nuclear reaction.

$$F = \frac{\Delta E_{2E} + \Delta E_{2K}}{w_R} \quad (24)$$

Inserting the appropriate values from Eqs. 7, 13, and 14, we obtain:

$$F = \frac{\Lambda_1 + \Lambda_2}{Gw_R} \times E_2 = \frac{\Lambda_1{}^x\Lambda_2{}^x}{Gw_R} \times E_0 \quad (24a)$$

where

$$\left.\begin{aligned} \Lambda_1{}^x &= \frac{E_0}{E_2}\Lambda_1 = \frac{2}{Z_1} \times \frac{m_2}{m_e} \times \frac{E_0}{E_2} \ln\left(4\frac{m_e}{m_2} \times \frac{E_2}{J}\right) \\ \Lambda_2{}^x &= \frac{E_0}{E_2}\Lambda_2 = \left[\frac{m_1 + \sqrt{(m_1)^2 + [(m_1)^2 - (m_2)^2]\tan^2\alpha_0}}{2(m_1 + m_2)\tan\alpha_0} \times \frac{m_2}{\mu}\right]^2 \frac{E_0}{E_2} \end{aligned}\right\} \quad (25)$$

The tube efficiency (η) is defined as the ratio of the consumed energy F plus the freed energy E_R to the consumed energy.

$$\eta = \frac{F + F_R}{F} \quad (26)$$

Inserting the values from Eqs. 24*a* and 25, we obtain

$$\eta = 1 + \frac{Gw_R}{\Lambda_1 + \Lambda_2} \times \frac{E_R}{E_2} = 1 + \frac{Gw_R}{\Lambda_1{}^x + \Lambda_2{}^x} \times \frac{E_R}{E_0} \quad (26a)$$

The value η is larger than unity for all exothermic reactions, *i.e.* those in which more thermic energy is freed than

electrical energy consumed. As the efficiency of transformation of thermic into electrical energy is always less than unity, utilization of atomic energy would only be of practical interest for tube efficiencies approaching two.

The above theoretical considerations are supplemented by a few numerical examples in the table on page 48. The calculations are based on the assumption that the number of reactions per second, P, is equal to 10^{11}. The reactions are designated as follows:

I. ${}_3Li^7(d,n){}_4Be^8$
II. ${}_4Be^9(d,n){}_5B^{10}$
III. ${}_4Be^9(\alpha,n){}_6C^{12}$

The following values were assumed: For Li, the number N of atoms per cubic cm $\approx 4.7 \times 10^{22}$ cm^{-3}; the geometrical cross section of the nucleus $\sigma \approx 2.6 \times 10^{-25}$ cm^2. Similarly for Be (reactions II and III) $N \approx 1.25 \times 10^{23}$ cm^{-3}, $\sigma \approx 3.2 \times 10^{-25}$ cm^2. The indexes a, b and c designate various conditions of the same reaction.

Comparison of the figures for the first two reactions, which differ only in the values of E_2, shows that the tube does not offer any advantage as long as the kinetic energy of the accelerated particles is lower than the maximum energy potential of the repulsive Coulomb field. According to S. Flügge, 1 ma of deuteron current at an acceleration voltage of 0.8 Mv produces, in an ordinary discharge tube, about 10^{11} neutrons per second, whereas for the proposed tube, at $U_{VB} + U_{HB} = 0.8$ Mv, 2.4 ma and 500 kv are necessary to obtain the same number of reactions. It is problematical to consider this advantageous. The situation is entirely different if the voltage for the main acceleration is increased to about 3 Mv. The advantage of requiring only 1.3 ma at 160 kv for the preliminary acceleration and 0.13 ma at 2.84 Mv for the main acceleration offsets the disadvantage whereby the tube has to be built for a voltage sufficiently high to produce a source of neutrons of the same intensity as is obtained in the above-mentioned tube. The above examples are given only for comparison of the performances of the new tube and the ones used at present, as it is unlikely that a lithium foil could be produced with a thickness of only 10^{-8} cm. Also the very low melting point (180°C) would only allow a very low loss per unit area.

In practice beryllium would be used for the target, because its melting point is much higher (1,278°C) but the manufacture of foils of 2 to 5×10^{-4} cm presents certain difficulties. The reactions II*a* and II*b* differ only in the thickness of the beryllium target foil. For a thicker foil less current but higher voltage is required for the preliminary acceleration, and the current and voltage values for the main acceleration remain unchanged. If the main accelerating voltage is increased to 10 Mv (reaction II*c*), the current taken from the generator drops to its lowest value (*i.e.* all particles which did not produce a nuclear reaction reach the retardation space of the tube); the current consumption for the preliminary acceleration is the same as for reaction II*a* (same thickness of target foil), but the voltage drops to a third of the value of II*a*. Simultaneously the power consumption per reaction, F, also drops to a third of the value of the previous reaction.

The reaction III in the table is produced by α-particles. If compared with the reaction II*b*, which differs only in that it uses deuterons instead of helium nucleii as bombarding particles, it can be readily recognized that only the preliminary acceleration voltage and the tube utilization values differ, the other differences being unimportant. In the last two columns the current consumption for preliminary acceleration, I_{PE}, and main acceleration, I_{HE}, are compared with the current con-

sumption, (I_x), of a current tube for the same number of reactions.

The current consumption for the preliminary acceleration is, in only two cases, higher than ten times the value in current tubes, but for the main acceleration the current consumption is in no case higher than 0.2% I_x, the reduction of I_{HZ} being greater than 500 times.

Design Details

The design of this tube is done according to the same principles as the design of ordinary tubes for nuclear reactions. Therefore only those points which differ from conventional considerations are dealt with here.

The particles emanating from the ion source 1 (see illustration) are first accelerated in the electrostatic field preceding electrode 2. The main acceleration is between the following electrodes, 3, 4 and 5 (only three of these electrodes are shown in the figure). The shape of the electrodes should be such that their electrostatic field, particularly that preceding electrode 2, acts like a lens with a suitable focus length. The accelerated particles pass through the target, a thin foil, where the desired nuclear reaction occurs. The particles are then retarded in the electrostatic field between electrodes 5, 6, 7 and 8 and reach the recombination space 8 with only a low speed. After recombination to neutral atoms, they are sucked into a reservoir by a high vacuum pump or fed through a sufficiently long high-vacuum tube back into the ion source 1. Sufficient attention must be paid to the electrostatic field between the electrodes 5 and 6 and to the correct placing of the target foil, so that a maximum number (if not all) of the particles dispersed on the nuclei of the foil are refocused and made to reach the recombination space 8 after absorption of their kinetic energy by retardation. Condensers A and B act as voltage dividers and maintain a constant voltage. The voltage for preliminary acceleration is impressed on terminals X, and that for the main acceleration on terminals Y.

The particles which bombard the target foil, lose, because of dispersion on the electrons, the part of the energy they gained during preliminary acceleration, and this loss is transformed into heat which increases the foil temperature. Cooling is effected by convection and radiation. If the melting point of the foil is low, the foil must be placed perpendicular to the axis of the discharge tube, because heat transfer is mainly effected by convection and the distance to be covered should be as small as possible. Because of the thinness of the foil, this cooling is not good enough, but if the melting point of the target is high (over 1,000°C), *e.g.* for beryllium (if the tube is used as a source of neutrons), the foil can have a sufficiently high temperature to allow cooling to be predominantly by radiation. The total radiation of a black body is:

$$E_s = 5.75 \times 10^{-12} T^4$$

watts per sq cm

As the melting point of beryllium is 1,278° C (1,551° K) the maximum permissible temperature is about 1,415° K. Taking into consideration that heat radiation takes place on both sides of the target foil, we obtain for the heat radiation of the target, $E_s' \approx 46$ watts per sq cm. This value applies only to a black body, and if it is assumed that the absorption is about one fourth (the actual value depends on the temperature of the radiating body and the frequency of the radiation and can only be determined experimentally), the heat radiation of the foil can be assumed to be $E_s^x \approx 10$ watts per sq cm. If the target is placed in a direction perpendicular to the axis of the tube, this value represents the maximum permissible loss per unit area L_e. If the

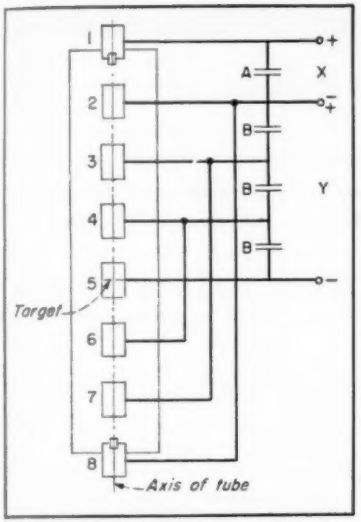

Diagram of discharge tube showing electrodes and power connections

target foil is placed oblique to the tube axis, this value is increased to

$$L_o = \frac{E_s^2}{\sin \omega} \qquad (27)$$

where ω is the angle between the foil plane and the axis of the tube (see figure). It follows from Eq. 27 that it is advantageous to place the target at an oblique angle to the tube axis, because the permissible current density is thereby increased, but a thinner foil has to be used in this case, because the distance of travel of the particles in the target is also increased.

$$\Delta s = \delta / \sin \omega \qquad (28)$$

where δ is the foil thickness and s the length of travel of the particles in the target. The disadvantage of placing the target at an oblique angle is that a larger number of particles dispersed on the nuclei do not reach the electrostatic field between the electrodes 5 and 6 and are lost for retardation and recombination.

As regards the design of the impulse generator for the main acceleration voltage and the condensers B, it is necessary to bear in mind that the voltage on the condensers must not fluctuate too much. This purely electrical problem can be solved, because the voltage is very high and the current intensity is extremely low. Either electrode 5 and the target, or the source of ions 1 can be grounded. If the target is grounded, the current for the ion source and for both generators has to be fed through an insulation transformer, or it has to be produced by a small synchronous generator at ground potential and driven by a motor through an insulated shaft. If the ion source is put at ground potential, these difficulties are dispensed with, but the safe operation of the collection of the particles (neutrons) which result from nuclear reaction in the target is difficult.

Applications of the Tube

The tube is very suitable for use as a source of neutrons. Relatively simple impulse, electrostatic or cascade generators can be used as a source of the main acceleration voltage (the intensity of the neutrons for equal voltage and 1 ma is up to 500 times that of ordinary tubes).

It is also possible to obtain acceleration of particles hitherto possible only in cyclotrons because impulse generators can be built for voltages up to 10 Mv. Tube design would not be easy for such high voltages, but it is likely that the difficulties can be overcome.

The tube is unsuitable for direct utilization of the energy of light elements, because the particles would require a kinetic energy of about 10^4 Mev to bring the losses caused by dispersion on the electrons into a reasonable relationship with the freed energy, and this is not possible (*viz.* Eq. 25, 26*a*).

Application of the design principles of this tube to the isotron would considerably increase its efficiency.

UNIVERSITY OF MICHIGAN LIBRARIES

Measurement of P^{32} and I^{131} Radiations with Dental Film

More exact determination of phosphorus and iodine* radiation dosage is obtained by the establishment of net density versus roentgen relationships for monitor-type dental film

By F. Hermann Rudenberg, Russell F. Cowing, and Charles K. Spalding†
New England Deaconess Hospital, Harvard Cancer Commission, Boston, Massachusetts

MONITOR FILMS provide a convenient method for measuring the radiation doses encountered by the worker using radioisotopes. When worn by the worker, the film, which is sensitive to ionizing radiations, becomes exposed and its density, as measured by a densitometer, can then be compared to "known" values to determine the amount of radiation received.

The purpose of the study‡ described below was to find the "known" values.

In our laboratory a packet of DuPont Dental Film No. 552-2 in a metal holder is worn by all those handling radioactive materials. It is worn for a week before it is developed. The upper part of the holder consists of a cadmium strip with a number punched in it for use in coding the film. The lower part has a window to permit soft radiation to impinge upon the film. Each packet contains two films, the more sensitive one having a range from 0 to 3 roentgens and the other from 0 to 20 roentgens (*1*).

For these studies, only fresh film that was stored under favorable conditions was used; for each batch processed fresh developer was used as recommended by DuPont for this particular film. Developing lasted exactly six minutes at 68° F. With each batch, at least one unexposed film was developed for background effects to arrive at the net densitities of the exposed films by the subtraction of the background density. Densities were read on an Ansco-Sweet photo-cell type of densitometer. The average value was taken of the exposed area of the film, except where, at the outer fringe of that area, scatter phenomena from the edge of the window in the metal holder, or cutting effects on the film edge, may have increased the densities. We were concerned only with the film in front, the more sensitive one, since it covered the dosage range in which we were most interested, and since we were measuring soft as well as hard radiation.

Films were exposed simultaneously and placed alternately, one with holder and one without, along arcs of set radius from the center of the source, a dehydrated radioactive solution. The maximum number of films radiated was kept within an angle of about 45° and were placed so that each would be radiated from the total surface of the source. The source was placed in one position in a ring stand (and not rotated

---

* The radioactive phosphorus and iodine used in this investigation was supplied by the Oak Ridge National Laboratory and obtained on allocation from the U. S. Atomic Energy Commission.

† The authors wish to thank Egilda De-Amicis and Kathryn H. Haley for their assistance in preparing this paper.

‡ Supported in part by N5, ORI-76 Project, Order VII, NR-171-105.

throughout the entire experiment) and was oriented in such a fashion that the center of the source dish faced, and was approximately at the height of, the films to be exposed. Both the films, with and without holders, were held in place 2.6 cm above the floor by means of cork stoppers, thus placing the center of the exposed part of the film 4 to 4.5 cm from the floor.

Films were exposed at every 5 centimeters from 10 to 50 cm from the source, and at 60, 70, and 80 cm, for periods of from ½ to 48 hours to obtain values of 0.05 to 1.0 roentgen.

To improve the accuracy of the above distance readings, a position chart was drawn on a large piece of paper for use throughout the work. Since this permitted both film and source to be placed with an accuracy of 0.1 cm, errors of from ±1.0 to ±0.125% were encountered, depending on the distance. Similarly, the error in timing was determined as having a range of ½ minute in 30 minutes to 2 minutes in 48 hours, or from ±1.67 to ±0.07% (see also Table 1).

Because all exposures were made in a room in which no one was working and all surfaces except the floor were sufficiently far away to avoid scatter phenomena, only the scatter effects of the floor and the dish were encountered. Reflection from the dish did not influence our results since we were comparing instrument readings to film densities. Variation in radiation over the arc of exposure was checked both by the use of films and by the use of an Instrument Development Laboratories* portable Geiger-Müller beta-gamma counter tube having a glass wall of 30 mg/cm² approximately 0.12 mm thick.† The variation measured by films agreed with that measured by the Geiger tube. This was probably due to the unequal distribution of radioactive material over the face of the dish. It should be noted, however, that this error also includes the variation in distance readings, film development, and densitometer readings.

Frequently during this study the strength of the source at the above distances was measured by a Beckman Model MX-2 (Zeus) air ionization chamber with a nylon window for measuring soft as well as hard radiation. The chamber window measures approximately 17 cm long and 11 cm high. It was located about 3 cm above the floor. In measuring distances from the center of the source to the middle of the horizontal anode bar centered in the ionization chamber, a correction factor of 3 cm was allowed from the anode to the front of the unshielded ionization chamber. By this means any slight inaccuracy of the use of the inverse square law was avoided.

The readings of the ionization chamber were compared to those of the Geiger counter tube after both instruments, with shields to absorb beta radiation, has been calibrated against the gamma radiation of a 25-mg needle of radium. This calibration was checked during the course of the study and was found not to vary within the accuracy of the instruments. The calibration was performed on the basis that a 1-mg radium needle with 0.5 mm platinum wall produced ionization equivalent to 0.84 mr/hr (0.00084 r/hr) at a distance of one meter and with appropriate calculations in accordance with the inverse square law.

Since our interest lay in the measurement of all soft and hard radiation, the intensity of ionization at each distance of film placement was measured directly with the ionization chamber every second day so that the amount of radiation the film packets actually received could

* Manufactured by Nuclear Instrument & Chemical Corporation, formerly Instrument Development Laboratories, Inc.

† Black paper was placed around the tube to cut out the ultraviolet effects which were encountered.

UNIVERSITY OF MICHIGAN LIBRARIES

TABLE 1

Percent Errors

Source	*Units*	*Percent*
Beckman ionization chamber reading reported in catalog and estimated due to fluctuation in temperature and humidity		±10
Beckman ionization chamber reading, visual fluctuation of needle	±1 division in 50	±2.0
Instrument Development Laboratories Geiger-Müller tube counter reading including variation due to temperature and humidity (estimated)		±5
Geiger counter tube reading when in vertical position (used to measure variation over field of radiation)	±0.1 mr/hr	±0.7
Geiger counter tube reading when in horizontal position (used to measure vertical variation of radiation at center of field)	±0.2 mr/hr	±1.5
Horizontal distance readings for films and source, and ionization chamber or Geiger counter tube	±0.1 cm from 10 to 80 cm	±1.0 to ±0.125
Vertical distance reading for Geiger counter tube when measuring vertical variation in radiation at center of field	±0.2 cm from 2 to 15 cm	±10.0 to ±1.33
Calibration by radium (estimated)		±1.0
Time of placing and removing films	½ min in 30 min to 2 min in 48 hr	±1.67 to ±0.07
Variation due to developing	Small, because a control was developed to count background and other effects; also film was fresh and had been stored under favorable conditions.	
Densitometer reading	±0.02 from 0.25 to 2.20	±8.0 to ±0.9
Mathematical dropping of third place		±10.0 to ±0.4

be determined with greater accuracy. It was found that the inverse square law was not followed exactly but that the exponential decay curve was followed within the accuracies of the instrument and of the distance measurement.

Table 1 lists the units as well as the percent error (plus or minus) which was allowed for each of the various steps where inaccuracies may have resulted. These errors were determined, unless otherwise noted, by visual observation. The over-all error was estimated to be ±20%, which agreed with the experimental error found. The errors caused by developing were small since a control film was developed with each batch and net densities rather than actual densities were plotted. It must be kept in

mind that each batch of film developed may have been drawn from different boxes and, consequently, that variation in film emulsions of undeterminable amount must be considered. However, the manufacturer's error is low compared to the errors that slight changes in temperature during developing may have produced. We attempted to minimize this error by measuring the background density in the shielded area of each film exposed in a holder.

By exposing films over the whole range of time values and by making use of the decay of the source, it was possible to cover a large range of roentgen values at each distance. To establish which of our resultant values were most accurate, graphs were drawn, in the first case, of values of common distance and varying time, and in the second, of constant time and varying distance. Rather than drawing curves between these values, they were connected by straight lines. This permitted a better evaluation of the accuracy of each specific series of points. We were able to note how many hours of irradiation were needed for stable results to appear as well as at what distance from the source our results were significant. Obviously this also showed us where the various possibilities of error were large enough to appear and where the error, compared to the over-all amount, was too small to become visible.

A third graph was then plotted of all the "good" points, as found by the method described above. From this plot the final curve was drawn. All the other points were then entered on the graph and the percent error at 0.5 r and at 1.0 r was calculated for:

a) the points closest to the curve (as determined visually rather than on an approximate percentage error basis),

b) all the "good" points and any others within their over-all range,

c) all the points.

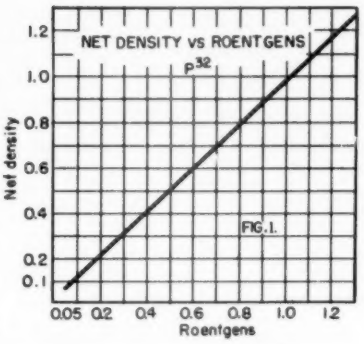

Studies with Phosphorus-32

A 0.5 millicurie source of radioactive phosphorus, P^{32}, was made by evaporating an appropriate amount of a solution of the salt $KH_2P^*O_4$, as it comes from Oak Ridge, in a metal dish 4.3 cm in diameter and 1 cm in depth. This was placed in a vertical position with the center of the face of the dish 5.4 cm from the floor and the required distance from the films. The P^{32} layer was assumed to be less than 0.2 mm in thickness but it was not evenly distributed over the face of the dish [see Table 2 (*B,C*)].

Since P^{32} emits only beta particles, which have a maximum energy of 1.7 Mev (*2*) and an average energy of 0.700 Mev (*3, 4*), the resulting curve (see Fig. 1) is almost linear. From our plot of lines connecting the points of constant time and varying distance, we found that exposures of 5 hours and more (29 points) fall along the curve, that exposures of 3 and 4 hours (11 points) have a maximum error of +20% at 1 r, but only +10% at 0.5 r, and that exposures of ½, 1, and 2 hours vary too greatly above the curve to be of significance in determining its position.

The plot of lines connecting the points of constant distance and varying time shows that exposures at 35 cm and be-

TABLE 2

Phosphorus-32

A. Comparison of Beckman ionization chamber with Instrument Development Laboratories Geiger-Müller counter tube.

Distance	*Beckman*	*Inst. Dev. Labs.*
48 cm	31.0 mr/hr	20 mr/hr
57	20.5	15
68	13	10
88.5	6.5	5

B. Intensity variation from center line at various distances from the source, measured with Geiger tube vertical and window centered 10.4 cm above table.

Distance from source	*Intensity at center line as measured by Geiger tube*	*Percent intensity measured at points of reference and their angles with center line at the source*	
50 cm	19.5 mr/hr	98%	20°
60	13.6	95	20
70	9.7	96	20

C. Intensity variation from center line at various distances from the source, as measured by film density and by Beckman ionization chamber.

Distance from source	*Intensity at center line as measured by Beckman*	*Net film density at center line for exposure of 17 hr*	*Percent net film density measured at points of reference and their angle with center line at the source*	
40 cm	65 mr/hr	1.07	95%	20°

D. Vertical variation of intensity at center line measured with Geiger tube at 60 cm from source and with tube horizontal over center line.

Height from table	*Intensity at center line*
3 cm	13.2 mr/hr
6	13.8
8	13.9
10	14.0
12	13.7
14	13.5

yond (40 points) fall within ±7% at 1 r and ±12% at 0.5 r of the curve while those exposures made at 30 cm and closer to the source (29 points) for the most part are too varied to be of significance in determining the final curve. Thus all exposures of 5 hours and more at 35 cm from the source and beyond are defined as "good" points.

The errors that attend the maximum deviation from the final curve are listed in Table 3 for the 69 pairs of films irradiated.

The variation between the film in the holder and that with no holder was found to average out, the variation usually being so slight that it can probably be attributed to variation in expo-

TABLE 3

Errors for Figure 1

	At 1 r	*At 0.5 r*
All 69 points at 10 cm from the source and beyond	±26%	±35%
54 "good" points and those within their over-all range	±18	±22
41 points closest to the curve (determined visually)	± 7	± 9

sure time and distance, processing, and densitometer reading.

The variation along the arc at one distance as measured with the Geiger tube agrees with that measured with the exposed films [Table 2 (*B,C*)]. Although the films were not placed along the path of strongest ionization [Table 2 (*D*)], they did receive approximately that much exposure; the Geiger tube was centered on that path. In comparing the Geiger tube with the ionization chamber [Table 2 (*A*)], it must be remembered that the wall thickness of the tube absorbed all impinging beta particles which had insufficient energy to pierce the glass window.

Studies with Iodine-131

A one millicurie source of radioactive iodine was made by evaporating to dryness a silver iodide precipitate compounded in a glass dish to prevent the oxidation found in metal dishes. By combining the I^{131} (received from Oak Ridge, in $NaHSO_3$ solution of *p*H 8) with $NaHSO_3$ and $AgNO_3$, Cowing and DeAmicis (*5*) showed that the sublimation of iodine in solution is prevented. The glass source dish of 0.1 cm thickness had a diameter of 4.2 cm and was 1.2 cm deep. It was placed in a vertical position 5.8 cm from the table when facing the films to be irradiated and 9 cm from

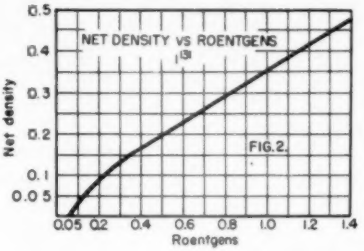

the table when its ionizing strength was measured [Table 4 (*A,D*)]. In this way, since the source was not rotated throughout the study, all measurements and exposures were made close to the path of greatest ionization. The thickness of the AgI* layer was assumed to be 0.5 mm but it was not uniform. Variation in the amount of radiation over the angle of exposure is shown in Table 4 (*B,C*) in terms of direct measurements. Cowing and DeAmicis (5) concluded that neither the silver atoms nor the residual non-radioactive salts will cause appreciable scatter at the source.

Since I^{131} emits both beta particles and gamma rays, the net density vs roentgen relationship (see Fig. 2) is not linear. The beta particles have an average energy of 0.205 Mev (*4*) and a maximum energy of 0.60 Mev (*2*) while the gamma rays have maximum energies of 0.080 and 0.367 Mev (*4, 2*). The decay of the I^{131} source was found to follow the exponential decay law within the accuracies of our instruments. However, the inverse square law was followed only up to approximately 20 cm from the source; beyond this the intensity readings, as measured by both the ionization chamber and the Geiger tube instruments, fall off rapidly [see Table 4 (*A,B*)]. This was probably due to absorption of radiation in the air.

The plot of lines connecting the points of constant distance and varying time shows that exposures at 35 and 40 cm (22 points) approximate the curve in

TABLE 4

Iodine–131

A. Comparison of Beckman ionization chamber with Instrument Development Laboratories Geiger-Müller counter tube.

Distance	*Beckman*	*Inst. Dev. Labs.*
38.5 cm	159 mr/hr	20 mr/hr
43.1	108	15
49.2	68	10
65.3	22	4.4

B. Intensity variation from center line at various distances from the source, measured with Geiger tube vertical and window centered 10.4 cm above table.

Distance from source	*Intensity at center line as measured by Geiger tube*	*Percent intensity measured at points of reference and their angles with center line at the source*	
25 cm	16.5 mr/hr	69%	37°
30	10.2	82	31
35	6.6	82	31
40	4.4	91	20

C. Intensity variation from center line at various distances from the source, as measured by film density and by Beckman ionization chamber.

Distance from source	*Intensity at center line as measured by Beckman*	*Net film density at center line for exposure of 17 hr*	*Percent net film density measured at points of reference and their angles with center line at the source*	
60 cm	25.9 mr/hr	0.22	82%	20°
35	55	0.35	82	31

D. Vertical variation of intensity at center line measured with Geiger tube at 25 cm from source and with tube horizontal over center line.

Height from table	*Intensity at center line*
3 cm	15.7 mr/hr
4	16.2
7	16.4
9	16.0
11	15.5
13	14.6
15	13.8

Fig. 2; that exposures at 10 to 30 cm (35 points) fall for the most part (23 points) above the curve (the other 12 points being much closer and below the curve); and that exposures at 45 to 80 cm (34 points) fall below the curve (except for 10 points which are close to and above the curve). For equal amounts of radiation there is a general trend for the net density values to be lower the farther the films from the source.

It is noted from the plot of lines connecting the points of constant time and

varying distance that exposures of 6 to 48 hours, if between 30 and 45 cm distance (21 points defined as "good"), fall within ±16% of the curve in Fig. 2 (see Table 5) (closer to the source the densities run high, farther away they run low); that all exposures of 1 to 4 hours (41 points) are erratic, mostly above the curve; and that exposures beyond 45 cm for 24 and 48 hours (6 points) are below the curve. It is interesting, too, to observe that 5 films exposed for ½ hour at 15 to 35 cm have densities that fall close enough to the curve to be significant in determining its position.

The errors for the 91 pairs of films irradiated are listed in Table 5 with respect to maximum deviation from the final curve.

The differences in the exposure of the film in the holder and that with no holder are found to average out, as in the case of P^{32} exposures. The slight variation observed may be due to variation in exposure time and distance, processing, and densitometer reading rather than to variation of ionizing strength of the source along the arc of irradiation. As is seen in Table 4 (*B,C*), the variation along the arc at one distance as measured with the Geiger tube agrees astonishingly well with that measured with the exposed films, other possibilities of error being included here.

Since the beta particles from I^{131} have such low energy, the protective paper around the films in the film packet probably absorbs them before they strike the more sensitive film in front. This front film absorbs the radiation to such a degree that the less sensitive film behind it shows so little net density deviation that it can not be relied upon should the film in front accidentally be overexposed. It is noted from Fig. 2 that a very slight fluctuation in densitometer reading (which in this study varies ±0.02 units from 0.25 to 0.75 units) may account for an error of

TABLE 5

Errors for Figure 2

	At 1 r	*At 0.5 r*
All 91 points at 10 cm from the source and beyond	±26%	±40%
44 "good" points and those within their over-all range	±16	±15
42 points closest to curve (determined visually)	± 6.4	± 8.8

±8.0% in the low readings to ±2.7% in the high ones.

Accuracy of Results

An attempt was made in both of these studies to achieve conditions as close as possible to those found in laboratories in order that the reported values can be matched with those of films of unknown amount of exposure with reasonable accuracy. This is within ±10%. Since the instruments used may be expected to vary as much as this, any errors within ±20% are acceptable. This margin takes into account also the inaccuracy resulting from the expanded scale for net density in Figs. 1 and 2.

BIBLIOGRAPHY

1. Russell F. Cowing, Charles K. Spalding. Photographic Effect of Various Radiations on Special Dental Packets, *Radiology* (in press)
2. Robley D. Evans. Radioactivity Units and Standards, NUCLEONICS **1**, No. 2, 32–43 (1947)
3. L. R. Zumwalt, C. V. Cannon, G. H. Jenks, W. C. Peacock, L. M. Gunning. Comparison of the Determination of the Disintegration Rate of Radiophosphorus by Absolute Beta Counting and Calorimetric Measurement, *Science* **107**, 47 (1948)
4. L. D. Marinelli, Edith H. Quimby, G. J. Hine, Dosage Determination with Radioactive Isotopes—II. Practical Considerations in Therapy and Protection. *Am. J. Roentgenol. Radium Therapy* **59**, 260 (1948)
5. Russell F. Cowing, Egilda DeAmicis. Variations in Total Counts of P^{32} and I^{131} for Dishes of Different Atomic Number, *Science* **108**, 187 (1948)

UNIVERSITY OF MICHIGAN LIBRARIES

NUCLEONIC EVENTS

Atomic Energy Work in Britain

By M. H. L. PRYCE
Department of Physics, University of Oxford, England

THE START-UP of Britain's second atomic pile at the Atomic Energy Research Establishment at Harwell, Berkshire, was announced recently in the press. The first British pile went into operation at Harwell last year. These are the only working piles so far outside the American continent. They are outward signs of the resumption of active work in Britain on the development of atomic energy, interrupted during World War II by the pooling of the research effort of Britain, Canada and the United States, and its concentration for military reasons in North America, with emphasis on atomic bombs.

Shortly after World War II, Britain's research workers began to return to their former employment, and the establishment at Harwell, originally a Royal Air Force airfield, began to take shape as a new kind of scientific and technological laboratory under the Ministry of Supply. Britain has a long tradition of research in atomic and nuclear physics, centered particularly about the Cavendish Laboratory in Cambridge, and associated with the names of J. J. Thomson, Rutherford, Chadwick and Cockcroft. It is natural, therefore, that the practical application of these researches should be actively pursued in Britain, with Sir John Cockcroft as director at Harwell.

The development of atomic energy can be said to start with the discovery that neutrons, discovered by Chadwick in 1932, caused fission of the nuclei of uranium atoms. In fission energy is released and several additional neutrons are ejected. It became at once apparent that this discovery opened the way to a self-sustaining nuclear reaction, which might lead to the development of power on an unprecedented scale.

Weapon of Unprecedented Power

The realization of the implications could hardly have come at a more dramatic time. Shortly after the declaration of World War II in September, 1939, a few scientists in Britain saw that there might be a possibility of adapting the process to the manufacture of an atomic bomb of explosive power enormously greater than any previous bomb. Independently, Sir James Chadwick and two refugees from Nazi Germany, Professor Peierls and Professor Frisch, reported the possibility to the Government. At the time too little was still known about fission to say for certain that the atomic bomb would work. What was certain was that if it did, it would be a weapon of unprecedented power. Its exploration, therefore, was a military necessity. There was the obvious danger that the same idea had occurred to German scientists and that the Germans might develop an atomic bomb before Britain did. As it happened, the German scientists never thought of the essential step (the use of separated U-235 or plutonium) and what development of uranium fission did take place in Germany would not have led to any

effective weapon. In fact, German research on the application of fission was on so unsatisfactory a basis that it had led to no practical result when Germany was overrun by the Allies in 1944. But this comforting knowledge only emerged in 1944.

The Government appointed a scientific committee under the chairmanship of Sir George Thomson to follow up the suggestion. At this stage the problems were essentially of the kind for which university physics laboratories are suited, such as to find out more precisely how many neutrons are formed in a fission, what fraction of neutrons actually produce fissions and the average distance traveled by a neutron in uranium before it produces a fission. On the other hand, most of the British physicists had left the universities to work on such war projects as radar. It was out of the question to recall them until the possibility of the atomic bomb was more firmly established. Fortunately, some were left, notably Sir James Chadwick, and in addition there were a number of foreign physicists with specialized knowledge in the field, refugees from the Germans. These men, being aliens, had not been absorbed into radar and other secret projects. There thus arose the paradoxical situation in which British research on the most secret military development of World War II was largely undertaken by foreign scientists. The work was principally carried out in the universities of Oxford, Cambridge, London, Liverpool and Birmingham.

Four Years

By the summer of 1941 it had become clear that in principle an atomic bomb would work, and that its production would involve large-scale industrial processes of a novel kind, in particular the separation of the uranium isotopes. It was estimated that it would take four years and a large amount of Britain's productive effort. A number of prominent industrial firms had already been brought in to lay the foundations of the industrial development. In August, 1941, Winston Churchill, then Prime Minister, was advised to this effect.

At the time Britain was being bombed and was an unsuitable location for such a vast undertaking. Manpower was very short. It appeared better to locate the effort in one of the Commonwealth countries or in the United States. Through lend-lease the United States, though not actively in World War II, was effectively Britain's ally, and there was full interchange of information between Britain and America on all war projects. This extended to the atomic bomb. Scientists in the United States had approached their Government in 1939, and set up an investigating committee, in much the same way as had been effected in Britain, although, not being at war, they had not pressed the matter so urgently. The findings of the British committee, reinforced by their own investigations, acted as a powerful stimulus, and in November, 1941, President Roosevelt suggested to Mr. Churchill that the work should be co-ordinated. As a consequence, the industrial development was concentrated in the United States, and later, in 1943, the greater part of the scientists connected with the pioneering work in Britain went to America, headed by Sir James Chadwick.

Alternative Lines

It had been realized from an early stage that there were two ways of proceeding to an atomic bomb. One was to separate the uranium isotopes, to obtain U-235 from which a bomb could be manufactured. The other was to use the fission process in unseparated uranium to produce, as a by-product, the new element plutonium, and con-

UNIVERSITY OF MICHIGAN LIBRARIES

struct the bomb of plutonium. Britain's resources were such that only one of these methods could be adopted for large-scale development, and the separation process had been chosen as being the most certain from the facts known in 1941. Nevertheless, there was a team in Cambridge working on the alternative lines, headed by two pioneers in the field of fission reactions, Dr. Halban and Dr. Kowarski, who had escaped to Britain from Paris when France was invaded. This team continued to work in Britain for a time; later it moved to Canada, where its work was conducted as a joint American-British-Canadian effort. When, towards the end of World War II in Europe, it was found possible to release scientists from other war projects, many of Britain's scientists were sent to work in the Canadian project.

At the end of World War II the Harwell establishment was set up. The nucleus of the staff there was drawn from the British members of teams in the United States and Canadian projects.

The Work at Harwell

During World War II the emphasis in atomic energy development was necessarily on the atomic bomb. This does not mean that the techniques for peacetime applications were altogether neglected, for many of these led to the formation of new elements such as plutonium which play an important part in both the military and industrial applications. In fact, the work of the Canadian project, where the bulk of Britain's scientists was employed, was mainly directed towards long-term developments which could only have had a military significance had World War II lasted several years longer, but which have been very valuable in laying the foundations for industrial development of atomic energy. If, in the future, atomic power plays an important part in the economy of the world as a substitute for coal, it will almost certainly be used in such a way that plutonium and the artificial isotope 233 of uranium play an important part. The present atomic piles in Briain use natural, uranium—that is, without any separation of the isotopes—and although they do not produce power on the scale required, it is conceivable that piles built on these lines could be made to do so. On the other hand, this would be extremely wasteful of uranium and would exhaust the available stocks in a short time. This is why techniques using plutonium and U-233 are so important.

Plutonium Production

The two piles at the Atomic Energy Research Establishment, Harwell, Berkshire, are experimental tools, partly for laying the foundation of future developments, and partly for pure scientific research. In addition to Harwell, Britain's Government is undertaking the construction of a pile for the production of plutonium. The plutonium would be available for future power developments, and if necessary for making bombs. The big pile will not be located at Harwell, which is to be preserved as a strictly experimental establishment, but in a remote spot where the hazards of an accident are less serious.

It is one of the functions of Harwell, at the present time, to study the factors involved in the building of such a pile and this in turn involves a heavy research program with the experimental piles, the testing of materials, and experimental work on novel lines of mechanical and chemical engineering, not to mention medical research on the biological effects of radiations produced in nuclear reactions.

Scope for Creative Work

Pile engineering requires men with a specialist knowledge of atomic and nuclear physics such as in the past were only to be found in the research laboratories of universities. Partly in order to train more such men, and partly because it is recognized that the last word in atomic energy has not been said, and it is necessary to keep abreast of all developments in atomic physics, the Atomic Energy Research Establishment is also pushing ahead with a program of academic research, involving the construction of machines such as cyclotrons, high voltage generators, betatrons, synchrotrons, etc., which play such a large part in modern physical research. This has the advantage that it attracts to the staff students from the universities, who feel that they will have scope for creative work. There is no secrecy about this research, the results of which are published in the same way as the work of university laboratories. Secrecy is only maintained on technological matters which could give away information leading to the manufacture of atomic bombs.

Up to now atomic energy has not been used to generate useful power, although it is reported that an atomic electricity station is under construction in the United States. This is because much patient development is still necessary, stage following stage. Plans for machines driven by atomic power are being investigated at Harwell, and the future lines of development are kept under constant review. Actual demonstration of machines run on atomic power, on an experimental scale, may be expected in a few years. But this will only be a beginning.

Results for Medical Science

One of the most important uses of the two piles at Harwell is for the production of artificial radioactive substances for medical research. Before the start-up of the first Harwell pile the supply of tracers was solely from the United States. Since then there has been a steady trickle of tracer elements from Harwell to the medical research laboratories in Britain and overseas. The output from Harwell, when it gets fully underway with two piles, should prove adequate to satisfy the needs of the medical laboratories of all Europe. In this way atomic energy, whose first use was for such destructive purposes, is now showing that it can be a benefit to mankind.

MIT BUILDS 12-MEV ELECTROSTATIC GENERATOR

Construction of a 12,000,000-volt electrostatic generator, a project of the Laboratory for Nuclear Science and Engineering, has been started at the Massachusetts Institute of Technology, according to an announcement by George R. Harrison, dean of science.

The generator will be contained in a steel tank slightly more than 12 feet in diameter and approximately 32 feet high, the total weight of which will be 93 tons. The weight of the insulating gas within the tank is 10 tons. The machine will be shielded by a cylindrical concrete silo two feet thick and separated from the generator by an air space of three feet. Beneath the generator will be a laboratory 40 feet by 50 feet with walls two feet thick to provide ample shielding against stray radiation.

The upper section of the building is in the form of a tower connected to a bridge which will give access to the interior of the generator and will be equipped with a crane capable of removing the 17-ton generator cover and parts of the machine. Access to this bridge is by elevator and stairs in the tower. A machine room will house accessory equipment, compressor motor, generator and batteries.

The structure will be built of rein-

UNIVERSITY OF MICHIGAN LIBRARIES

forced concrete for the laboratory room and silo. The tower and bridge sections will be steel framed and covered with corrugated asbestos, while the shop and office wing walls are to be built of masonry faced with the light colored brick used in other Institute buildings.

RADIOLOGICAL SOCIETY HOLDS ANNUAL MEETING

The thirty-fourth annual meeting of the Radiological Society of North America was held this month in San Francisco.

Among the papers presented were the following:

"Wet clinic" on radioactive isotopes, W. E. Chamberlain, Philadelphia, presiding; R. R. Newell, San Francisco, Edith H. Quimby, New York; Earl R. Miller, San Francisco; R. H. Chamberlain, Philadephia; and George C. Henny, Philadelphia.

Recent developments in radioisotope distribution, P. C. Aebersold, Oak Ridge, Tenn.

Instrumentation for therapeutic radioisotope application, S. L. Warren, Los Angeles.

Relationships between chemical and biological effects of ionizing radiations, R. E. Zirkle, Chicago.

Comparative studies on the biological effects produced by radiation and chemical agents, Leon O. Jacobsen, Chicago.

Studies of apparent submicroscopic structural changes in bone matrix associated with the ionizing radiations from metabolized radium, Frank E. Hoecker, Lawrence, Kansas; Paul G. Roofe, Lawrence, Kansas.

The nature of radiation injury as seen by the geneticist, H. J. Muller, Bloomington, Ind.

Further studies on the relation between radiation effects, cell viability, and induced resistance to malignant growth, Anne Goldfeder, New York.

Tentative dose units for mixed radiations, H. M. Parker, Richland, Wash.

The problems of dosage measurements for radiations produced by the betatron, Lauriston S. Taylor, and Harold O. Wyckoff, Bethesda, Md.

The depth dose of electrons from the betatron, L. S. Skaggs.

29 PAPERS GIVEN AT NATIONAL ACADEMY OF SCIENCES

Twenty-nine papers were presented at the meeting of the National Academy of Sciences held at the University of California, Berkeley, last month.

Among the papers presented were the following:

New systematics in alpha radioactivity, Glenn T. Seaborg, University of California, Berkeley; *The magnetic moments of light nuclei*, F. Bloch, Stanford University; *The cyclotron: a progress report*, E. O. Lawrence, University of California, Berkeley; *The Berkeley linear accelerator*, L. W. Alvarez, University of California, Berkeley; *Some results obtained with the 184-inch cyclotron*, E. M. McMillan, University of California, Berkeley; and *Relative rates of hydrolysis of urea containing* C-14 *and* C-12, F. Daniels and A. L. Myerson, University of Wisconsin.

AEC AWARDS 18 HEALTH PHYSICS FELLOWSHIPS

Eighteen fellowships in health physics have been awarded to student scientists from twelve states by the Atomic Energy Commission. These are the first such awards to be made.

Ten of the fellows are studying at the AEC's Oak Ridge National Laboratory, Oak Ridge, Tenn., under the direction of Karl Z. Morgan, director of the health physics department; and eight are studying at the University of Rochester School of Medicine and Dentistry, Rochester, New York, under the direction of Henry A. Blair, director of the atomic energy project there. The courses, which are at the post-graduate level, began November 1.

Winding the coils for the Carnegie Institute of Technology 400 million volt synchro-cyclotron. The work is being done at the Brooklyn Navy Yard

SHIPMENT OF STEEL AND COILS FOR CARNEGIE TECH SYNCHROCYCLOTRON CREATES UNUSUAL TRANSPORTATION PROBLEMS

Design of the 400 million volt synchrocyclotron now being erected at the Carnegie Institute of Technology has created unusual problems of construction and hauling.

For example, in order to have fewer gaps and a higher average density in the steel frame, the some three million pounds of steel which have been poured into this part of the cyclotron have been put into only twelve pieces—some of these weighing as much as 240,000 pounds. This technical improvement will make for greater operating efficiency, but it also made it necessary for the men in charge of moving these pieces from the United States Steel mill where they were poured and machined to scour the nation for two of the six freight cars in existence which can handle such a load.

And, with one mile of highway to travel from the railroad freight station to the Nuclear Research Center at Saxonburg, Pennsylvania, this pouring of larger-than-usual steel parts made it difficult to locate motor trucks capable of carrying these pieces.

A further transportation and assembly problem will be presented soon by the cyclotron coils. Unlike the coils of other cyclotrons (which are shipped in sections), each of the coils for the Carnegie machine will be transported and will have to be placed into position as one piece. As with the steel parts, this one-piece plan will bring research advantages—but it also eliminated the otherwise most logical means of transportation, by rail, since the magnet coils are too high for railroad tunnels and, if loaded horizontally, too wide to pass other trains enroute. The coils, which weigh approximately 95 tons each and have a 20-foot o.d., must be transported from the Brooklyn Navy Yard. They will probably be shipped by sea and up the Mississippi and Ohio Rivers.

UNIVERSITY OF MICHIGAN LIBRARIES

AIR FORCE ANNOUNCES DETAILS OF RAND CORP.

Details of the nature of the Rand Corporation, a non-profit organization set up to apply scientific effort to improvement of national security, have been announced by the Air Force.

Rand (derived from Research and Development) was set up in March, 1946, as a separate department at Douglas Aircraft Co. Its work since then has been done under a contract with the Air Force. Executives of Douglas and of three other aircraft companies—Boeing, Northrop and North American—worked with the Air Force in setting policy and lending support to the project.

Rand does not develop new weapons or inst uments, as such. Its main purpose is to shorten the gap between scientific theory and military reality.

The corporation is financed entirely by private sources. Directing an eleven man board of trustees is F. R. Collbohm, a prominent engineer from Douglas. Other members of the board are: C. Dollard, president, Carnegie Corp. of N. Y.; L. A. Dubridge, president, California Institute of Technology; H. R. Gaither, Jr., Rand Corp.; L. J. Henderson, Jr., Rand Corp.; J. A. Hutcheson, director, research laboratories, Westinghouse Electric Corp.; A. L. Loomis, scientist, N. Y.; P. M. Morse, department of physics, Massachusetts Institute of Technology; F. F. Stephan, Princeton University; G. D. Stoddard, president, University of Illinois; and C. Williams, director, Battelle Memorial Institute, Columbus, O.

GE BUILDS MOBILE BETATRON FOR NAVY

A mobile, 10-million-volt betatron, whose radiations are capable of penetrating 16 inches of steel, is now being installed at the Naval Ordnance Laboratory, White Oak, Maryland, according to a Navy announcement.

Built for the Bureau of Ordnance by the General Electric Company, Schenectady, N. Y., the machine will be placed in operation some time after the first of the year. The betatron, which can be aimed in any direction, will be used at White Oak principally for studying the internal assemblies of mines, torpedoes, and other items of Naval ordnance.

MIT TO EXPAND NUCLEAR FACILITIES

A new laboratory building and field station for nuclear science and engineering are among the projects proposed in a $20,000,000 development program announced last month at the Massachusetts Institute of Technology.

The proposed building for nuclear science, which will house the interdepartmental Laboratory for Nuclear Science and Engineering organization already operating at MIT, will contain 60,000 square feet of floor space. Present plans call for five floors above the ground and two well-shielded floors underground.

The building will furnish laboratories together with office and shop space for graduate instruction and research. It will house such large nuclear equipment as does not have to remain decentralized throughout the campus for reasons of safety.

The plans outlined by the committee also included the development of a nuclear field station on land leased by the Institute at Fort Devens, 35 miles from Cambridge. Terrain, power, water, waste disposal facilities, and privacy are said to make this site especially suited to nuclear work.

The building is estimated to cost $2,000,000, according to present plans; more than $1,000,000 of this amount is already available. The field station, including its equipment as now proposed, will cost $800,000 more.

FACKENTHAL TO HEAD ASSOCIATED UNIVERSITIES

Frank D. Fackenthal, former acting president of Columbia University, has been named president of Associated Universities, Inc., the management corporation which operates Brookhaven National Laboratory, Upton, L. I. Fackenthal, who will continue as chairman of the trustees' committee on education of Columbia University, will succeed Edward Reynolds, vice president of Harvard University, in this non-salaried post.

PHYSICS NOBEL PRIZE AWARDED TO BLACKETT

The 1948 Nobel Prize for physics has been awarded to P. M. S. Blackett, British nuclear physicist and authority on radar, cosmic rays and experimental physics. He received the award for his improvement of the Wilson cloud chamber and for various cosmic ray discoveries. Professor of physics at the University of Manchester, Blackett found that cosmic rays left traces in the cloud chamber similar to those left by radioactive particles, and he invented a device to make better photographs of the trails. He also discovered the positive electron.

A recently published book by Professor Blackett, "Military and Political Consequences of Atomic Energy," has become a center of international controversy. In it, Blackett attacks the Baruch plan for the control of atomic energy and calls for a re-examination of the two different viewpoints confronting the United Nations.

PUBLICATIONS AVAILABLE

Handbook of Radioactivity and Tracer Methodology. Prepared by the Air Materiel Command of the Air Force, this comprehensive volume covers some of the fundamental concepts of nuclear physics, isotope production, instrumentation and tracer techniques. The three main divisions of the handbook are: Nuclei and Radioactivity, Measurement of Isotopes, and Biological and Medical Applications of Isotopes. Orders are now being taken for the 900-page handbook, which will cost $20. Requests accompanied by check or money order payable to the Treasurer of the United States, should be addressed to the Office of Technical Services, Department of Commerce, Washington 25, D. C.

American and British Atomic Energy Reports. Two bibliographies, covering subject matter on atomic energy freed from security restrictions by American and British agencies, are available from the Office of Technical Services at the above address. List PB 87782-S contains 13 pages and costs $.50 per copy; list PB 87782 contains 29 pages and costs $.75.

Publications of the National Bureau of Standards. Circular 460, which lists all Bureau publications from 1901 to June 30, 1947, is available from the Superintendent of Documents, U. S. Government Printing Office, Washington 25, D. C. at a cost of $.75 per copy. The 375-page circular also contains brief abstracts for the publications issued from January 1, 1942, to June 30, 1947.

Measurement of Radioactive Isotopes. This 12-page pamphlet gives detailed directions for use of radioactive standards and calibrated samples of radioisotopes issued by the National Bureau of Standards. Among the topics treated are basic principles of measurement, units, the use of radioactive standards, preparations of working standards, and corrections for change in radioactivity with time. Written by L. F. Curtiss, circular 473 can be obtained from the Superintendent of Documents at the address above.

UNIVERSITY OF MICHIGAN LIBRARIES

PRODUCTS and MATERIALS

SCALER

El-Tronics, Inc., 2647 N. Howard St., Philadelphia 33, Pa. The Model LS-100 scaler, which measures 11 in. × 9 in. × 18 in., uses a direct-reading decimal system. It contains hermetically sealed components and has available a scale-of-100 or 1,000.

GEIGER COUNTER

Nuclear Instrument and Chemical Corp. (formerly Instrument Development Laboratories), 223 W. Erie St., Chicago 10, Ill. The main feature of this counter, especially designed for the detection of soft ionizing radiation similar to that from C^{14} or S^{35}, is its use of "Q-Gas." This gas is said to permit operation of the counter at atmospheric pressure over a wide temperature range, with an anode potential of 1,450 volts. The pulse output operates a scaling unit with an input sensitivity of 0.25 volt.

BETA-GAMMA SCALER

Kelley-Koett Mfg. Co., Covington, Ky. The Model K-280 beta-gamma scaler is 27 in. × 11 in. × 15 in. deep and weighs 47 pounds. Incorporated in the scaler are a scale-of-256, scale selector, autocount and autotime. More detailed information can be obtained by writing Dept. B, Instrument Division.

BATTERY

Vitamite Co., 227 W. 64 St., New York 23, N. Y. The Model 2A-3.00 rechargeable, non-spill wet cell battery weighs 6 ounces and measures $1\frac{3}{16}$ in. × $3\frac{3}{16}$ in. × $1\frac{7}{16}$ in. It has a 4 ampere capacity and is said to operate well under low temperature and pres-

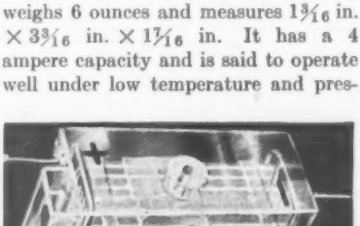

sure conditions. Other models are available from 1 ounce to 1 pound in weight.

BINARY SCALER

General Electric Co., Syracuse, N. Y. The Model 4SN1A1 binary scaler, for counting speeds up to 200 kc, in either binary or decade operation, is designed to provide a scale-of-2 in a self-contained, plug-in unit. A 5–20 volt negative input pulse of 1 μsec duration

and 0.1 minimum rise time will produce an output pulse from the scaler of 50 volts, peak to peak. The 50-volt signal has a rise time of 0.1 μsec. The unit has a resolution time of 5 μsec and an output impedance of 27,000 ohms. The specified power supply is 210 volts d-c ± 20% at 7 ma, filament 6.3 volts at 0.3 amp.

BETA-GAMMA COUNTER

Victoreen Instrument Co., 5806 Hough Ave., Cleveland 3, O. This beta-gamma counter tube (RMA No. 1B85) has an aluminum wall of 30 mg/cm². thickness. It operates at 900 volts, has a plateau which is said to be not less than 200 volts and a plateau slope no greater than 3% per 100 volts. The

Thyrode 1B85 is designed to have a nominal recovery time of 100 μsec and a minimum operating life of 10^8 counts.

SURVEY METER

Precision Radiation Instruments, Inc., 1101 N. Paulina St., Chicago 22, Ill. This portable beta-gamma survey meter (Model 101) uses a plug-in unit, which incorporates the major components, to facilitate ease of part replacement.

The meter measures 5⅜ in. × 6½ in. × 4½ in. and weighs less than 7½ pounds. The probe and cable assembly are designed to be light in weight and weatherproof.

What Can Be Patented and How

By WILLIAM R. BALLARD*

If you stop in at the corner shop and buy a shirt the transaction corresponds in its fundamental characteristics with the transaction involved in the issuing of a United States patent for an invention. In each case there is a voluntary exchange of certain recognized values and in each case each party to the deal gets a full and unencumbered property right in the thing he receives, that is to say, what he receives is entirely for his own benefit—to do with as he pleases.

When you bought the shirt your five dollars was worth more to the dealer than the shirt, and the dealer's shirt was worth more to you than the five dollars. If the deal was honest both parties profited by it, as they should. When an inventor applies for a patent under our laws and the Government, acting for the public, issues the patent, it is because the certainty of full control of his invention for a few years is worth more to the inventor than a perhaps longer but quite precarious hold on it by secrecy; and, to the public, the assurance of full and free possession of the invention after the patent term expires is worth more than the vague chance that it might sooner come into possession of the invention in some other way. As in the case of the shirt, it is nothing against the transaction to show that the inventor may make a good profit out of his invention during the life of the patent. Indeed if we were somehow to make certain that patentees could make no profit—or only a little profit—then we might as well repeal the patent laws for it is the hope of substantial profits that makes the patent system work, just as it is the main spring for all the rest of our free enterprise economy. It was the power of this incentive to promote the useful arts by leading people to invent new things and sell them to the public which the framers of the Constitution had in mind when they wrote into Article I, Section 8, "Congress shall have power . . . to promote the progress of science and the useful arts *by securing* for limited times to . . . inventors the exclusive right to their respective . . . discoveries" (emphasis supplied).

The fact that the sale of the shirt and the issuing of the patent correspond also in giving a full and unencumbered ownership in each case, as mentioned above, does not mean that a patent right must in the nature of the case represent such an unencumbered ownership. Patents in our country give this full control of the invention during the term of the patent merely because the authors of the Constitution arranged to have it that way. In many foreign countries the patent right is conditioned upon such things as the granting of licenses by the patentee to others to use the invention, upon the putting of the invention into commercial use or upon the paying of periodic fees.

The *sine qua non* for a successful patent system is that the value of the patent right granted should be sufficient to induce people to invent and disclose their inventions to the public.

What Is Patentable

The Constitution gave Congress the power to provide for patents but did not require it to do so. Congress, however, promptly exercised its power by enacting a law specifying certain classes

* Formerly, General Patent Attorney, American Telephone and Telegraph Co., now retired.

of things that might be patented and it has from time to time amended the laws on the subject.

Up to 1842 a thing could be patented only if it was an "art, machine, manufacture or composition of matter" and these are still the most important classes whether judged by numbers of patents or by commercial value. (The names of these four classes are fairly self-explanatory with the exception of "art." Patentably speaking an art is a method or process of making or treating something—an act or series of acts performed upon some physical object to change its character or condition.) In 1842 Congress provided that an ornamental design for an article of manufacture might be patented; and in 1930 it provided that an "asexually reproduced plant other than a tuber propagated plant" might be patented.

Anything that does not fall within one of these six statutory classes cannot be patented no matter how novel or valuable it may be. Thus a newly discovered law of nature cannot be patented, nor a form of government nor a newly coined language, phrase or word nor a plan of travel.

Besides falling in a statutory class a thing, to be patentable, must be "new" and "useful" and be the product of "invention."

"New" means new to the fund of public knowledge in this country, which includes the contents of printed publications and patents in foreign countries but does not include mere use in a foreign country (provided the inventor here does not copy but believes himself to be the original inventor when he files his application for patent). Novelty is thus a question of fact.

The presence of "invention" is determined by comparing the new thing with what was known before and deciding whether the step taken from the old to the new is one requiring the special creative ingenuity which we associate with the idea of invention or is merely a step which one familiar with the subject would normally take if faced with the need which the new thing supplies. The presence of invention is thus a question of judgment. Despite the fact that no sharp definition of "invention" has ever been devised (as might be guessed from the attempted explanation above) and despite the fact that human judgments are seldom identical on any given state of facts, reasonably satisfactory working conclusions are reached in actual practice. The judgments are made in the first instance by those who examine the applications for patent filed in the Patent Office, and their judgments are reviewable by the Courts. Those who handle the cases in the Patent Office become highly experienced in distinguishing invention from the ordinary skill of the art, and the courts, if not always experienced in this, have the benefit of witnesses pro and con who are familiar with the particular field involved. It should be noted that in comparing the new thing with the old to determine whether invention was involved, the "old" which is used as the basis of comparison is not the old as known to the inventor but as known to the public. Thus it may well happen that the step taken beyond that of which the inventor was aware was indeed a long one actually requiring the exercise of invention, and yet he will still fail to get his patent because the step beyond what was known to the public was but a short one which anyone skilled in such things could have taken. Therefore it is not a thing for which the public should pay by granting a patent.

The "usefulness" required for patentability is seldom the subject of controversy. If a thing is not utterly frivolous or dangerous or injurious to public health or morals, utility is ordinarily assumed. If brought in question a showing of a modicum of usefulness

UNIVERSITY OF MICHIGAN LIBRARIES

serves to support patentability. As indicated above there is no need to vary the character of the grant in any way to try to match it to the degree of utility of an invention. If the utility is so slight that the public benefit is small, it will also be true that the patentee's exclusive control will be but a slight burden upon the public; thus the balance of values remains.

It must be observed, further, that an invention has not been made within the meaning of the patent law until the inventor has a complete and operative idea of a means for accomplishing the desired result. A clear idea of the result to be attained is not enough, nor is even a general idea of how it can be accomplished. To deserve a patent the inventor must be in a position to teach the public exactly how to make and use the invention after the patent expires. On the other hand, if the inventor has a complete and operative idea of means, it may be patented although the means is crude, provided the means described in his application is the best within his knowledge at the time. Few inventions are made that are not improved later and it is seldom that an inventor, in the disclosure of his application, can hit upon the best commercial form in all details of design.

Now if an inventor has something—or thinks he has something—which satisfies the foregoing requirements, he is ready to apply for a patent, provided he believes that the prospects of profit from exploiting the invention or selling the patent or the reputation of being an inventor justifies the preliminary expense. This amounts to $60 or more in Government fees plus attorney's fees, the exact amount depending upon the intricacy of the invention and upon whether the case has smooth or rough sailing in the Patent Office. An inventor may prepare and prosecute his own application if he so desires but this is not advisable unless he is thoroughly familiar with the requirements of law and Patent Office procedure.

Briefly the mechanics of getting a patent are as follows: Application for the patent must be made in writing to the Commissioner of Patents, Washington, D. C. A complete application includes (*1*) a brief, formal "petition" asking that the patent be granted on the basis of the annexed papers, (*2*) a "specification" which is a complete and accurate description of the invention and its mode of operation, (*3*) an "oath" stating that the invention was made by the applicant and that to the best of his knowledge and belief it is new, and denying the existence of certain statutory bars, and (*4*) a "drawing" illustrating the invention when its nature permits such illustration. The specification ends with one or more brief summaries called "claims" which must exactly define the element or combination of elements which the inventor believes constitutes his invention. These are what the Patent Office Examiner compares with the known things to determine novelty and invention. They may be phrased in varying degrees of detail, those with less detail being, of course, the broader and the more valuable since they will cover more equivalent structures or procedures.

When such a complete application is received in the Patent Office it is given a date and serial number which determine its order of precedence among the cases waiting to be examined and fixes its *prima-facie* standing on priority of invention if it should happen that one or more other applicants are found claiming the same invention.

When the examiner reaches the case and completes his examination of the existing knowledge relating to the invention disclosed he writes the applicant a letter stating his conclusions on novelty and invention with respect to each of the "claims" in the application and pointing out any defects in the

several parts of the application papers. In almost all cases there will be a "rejection" of at least the broader claims, not infrequently of all the original claims. The applicant may then amend his case, including the claims, in the light of the office action, pointing out how he avoids the grounds of rejection, or he may stand pat and appeal if the rejection is repeated. Should the examiner in reply cite new grounds of rejection the applicant may amend again. All amendments made must fall within the four corners of the disclosure as originally filed. No "new matter" whatever may be added.

Since our law authorizes a patent only for the first inventor, a decision on priority as between rival claimants must be made by the Patent Office when two or more applicants are found to be claiming the same thing. This is done by an "interference proceeding." Many of these are disposed of upon the basis of the respective filing dates and the facts given by each party in an ex parte sworn "preliminary statement" required of each claimant. Where the asserted dates of invention are close, interpartis testimony may be required and in such cases the proceeding is apt to be long and expensive. Of course any party may drop out if he prefers not to press his claim.

If the examiner finally rejects an applicant's claims, or some of them, the latter may appeal, first to the Board of Appeals within the Patent Office and, if the decision is still adverse, to the court. When the office notifies an applicant that his case is in condition for allowance, he must pay the final Government fee within the next six months whereupon the patent will be prepared and issued within three months from the receipt of the fee.

Atomic Energy Commission Publications

THE FOLLOWING AEC DOCUMENTS have been added to the list of publications which the AEC has made available for sale to the public through its Document Sales Agency. This tabulation combines Document Sales Agency Lists Nos. 5 and 6 and supplements NUCLEONICS' previous listings of these documents. At the prices indicated, these publications can be obtained by sending a money order or check made payable to the Treasurer of the United States to the **Document Sales Agency, P. O. Box 62, Oak Ridge, Tennessee.**

MDDC or *AECD**		*Price*
Biology and Medicine		
401	Review of Water Monitoring Procedures at Clinton Laboratories (*10 pp*)	$.10
554	Industrial Health and Medical Rehabilitation at an Atomic Energy Laboratory (*15 pp*)	.10
583	Histopathological Studies on Mice Following External β-ray Treatment (*17 pp*)	$.10
1000	Metabolism of Fission Products. Radiocerium (Ce^{140}), Radiostrontium (Sr^{89}), and Decontamination Studies (*28 pp*)	.15
1012	Radiation Hazards of Bremsstrahlung (*8 pp*)	.10
1022	Study of Plutonium Metabolism in Bone (*99 pp*)	.35
1142	Metabolism of [Fission] Products. Progress Reports for month ending March 15, 1943 (*12 pp*)	.10

* Documents with numbers 1 through 1779 carry the prefix *MDDC* (Manhattan District Declassification Code); for those numbered 1780 and above, the prefix of *AECD* (Atomic Energy Commission Document) applies.

A notation in italics after a title indicates if the document is a circuit diagram (*c.d.*) or shows how many pages or drawings it contains.

MDDC or AECD		Price
1143	Metabolism of Fission Products. Progress Report for period ending February 15, 1943 (*20 pp*)	$.15
1185	A New Dominant Autosomal Mutant Affecting Coat Color in the Mouse, Mus Musculus (*4 pp*)	.05
1209	On the Association of Certain Hematomas With Myelencephalic Blebs in the Mouse (*3 pp*)	.05
1219	Control of Hemorrhagic Syndrome and Reduction in X-Irradiation Mortality With a Flavonone (*3 pp*)	.05
1224	Inherited *Situs Inversus Viscerum* in Mice (*3 pp*)	.05
1309	A Study of the Hands of Radiologists (*18 pp*)	.10
1488	The Lack of an Effect of Aging on Mutation Rate Induced by Irradiation (*3 pp*)	.05
1492	Influence of 24-Hour Gamma-Ray Irradiation at Low Dosage on the Mutation Rate in Drosophila (*6 pp*)	.10
1914	Metabolism of Plutonium in the Rat (*23 pp*)	.15
2015	Biochemical Studies on Workers Exposed to Beryllium (*10 pp*)	.10
2027	The Mass Spectrometer Analysis of Volatile Products of Metabolism (*2 pp*)	.05
2143	The Effect of Uranyl-Chloride on the Respiration and Photosynthesis of Chlorella Pyrenoidosa (*5 pp*)	.05

Chemistry

400	A Table of Radioactive Isotopes Arranged According to Half-Lives (*112 pp*)	.40
478	The Radiography of Heavy Radioactive Metals (*20 pp*)	.10
511	Spectrochemical Analysis: 1. The Copper Spark Method (*14 pp*)	.10
529	Microgas Analysis (*8 pp*)	.10
588	Vacuum Properties of Plastic Materials (*20 pp*)	.10
626	Segré Chart (Revised 1946)	.60
691	A Method for the Determination of Certain Metals Present in Minor Concentration in Various Substances, Electrodeposition in Mercury; Mercury Distillation and Polarographic or Colorimetric Estimations (*20 pp*)	.10
715	Standardization of the pD scale (*9 pp*)	.10
724	The Purification of Some Laboratory Gases (*10 pp*)	.10
763	An Introduction to Nuclear Chemistry Lecture Series (*48 pp*)	.20
777	Purification of Uranium Oxide (*4 pp*)	$.05
790	Some Exchange Experiments Involving Ferrocyanide and Ferricyanide Ions (*4 pp*)	.05
847	Determination of Anodic Current Efficiency in the Counter-flow Electrolysis of Uranyl Chloride Solutions (*16 pp*)	.10
851	Pyrolysis Method for Detection of Traces of Fluorocarbons in Air (*5 pp*)	.05
854	Apparatus for Rapid Analysis of Boron-10 (*5 pp*)	.05
855	Four New Methods of Industrial Gas Analysis (*8 pp*)	.10
856	The Addition of Methyl Alcohol to Fluoroethylenes (*4 pp*)	.05
870	The Theory and Properties of Low Voltage Radiation Counters (*45 pp*)	.20
878	The Number of Neutrons Emitted by Ra + Be Source (*6 pp*)	.10
906	Chemistry of Plutonium (V). 1. Potential of the Plutonium (V)/(VI) Couple Ionic Species of Plutonium (V) in Acidic Solutions (*7 pp*)	.10
910	A Comparison of Analytical Methods for the Determination of Uranium (*5 pp*)	.05
941	Determination of Small Amounts of Beryllium by Fluorescence Measurement (*13 pp*)	.10
971	A Rapid Method for the Determination of Nitrogen Oxides in Air (*3 pp*)	.05
1027	The Dark Reductions of Photosynthesis (*2 pp*)	.05
1030	Vapor Pressure of Beryllium Oxide (*8 pp*)	.10
1038	A Method for Handling and Purifying UF_6 in Glass Vessels by Means of Alkali Fluoride Getters (*2 pp*)	.05
1039	Note on the Separation of Hydrogen Fluoride from Uranium Hexafluoride (*3 pp*)	.05
1040	Note on the Use of Silica-Free Glasses for Handling Anhydrous Hydrogen Fluoride and Uranium Hexafluoride (*3 pp*)	.05
1041	UF_6. A New Fluoride of Uranium (*2 pp*)	.05
1044	Use of A Zinc Spiral in the Titrimetric Determination of Uranium (*2 pp*)	.05
1087	Chemical Problems in Stable Isotope Separation (*8 pp*)	.10
1110	The Fluorination of Polychloroheptanes With Hydrogen Fluoride (*27 pp*)	.15
1123	Potentiometric Titration of Uranium With Ferric Sulfate (*1 p*)	.05

MDDC or AECD		Price
1161	Alkaline Condensations of Fluorinated Esters With Esters and Ketones (*6 pp*)	$.10
1165	The Crystal Structure of Zirconium Oxysulfide: ZrOS	.05
1190	Cobalt-62 Radioactivity (*1 p*)	.05
1195	The Natural Abundance of Isotopes of Stable Elements (*18 pp*)	.10
1303	A Method of Assay for C^{14} (*24 pp*)	.15
1311	The Exact Masses of the Zirconium Isotopes (*2 pp*)	.05
1347	A 4y Lanthanum Sub-Group Activity (*6 pp*)	.10
1349	Slow-Neutron Disintegration of Boron; ^{10} Search for the Formation of Be^{10} and Estimate of the Mean Life of Be^{10} (*4 pp*)	.10
1402	Capture of Electrons by Ions (*2 pp*)	.05
1419	Neutron Absorption in Samarium (*1 p*)	.05
1454	Determination of Water in Perfluordimethylcyclohexanese —I. Potentiometric Titration with Karl Fischer Reagent	.10
1455	Determination of Water in Perfluordimethylcyclohexanese —II. Absorption by Phosphorus Pentoxide (*8 pp*)	.10
1456	Physical Properties of Chlorotrifluoroethylene Polymers as a Function of Molecular Weight—I. Molecular Weight of Chlorotrifluoroethylene Polymer (*13 pp*)	.10
1657	The Electrodeposition of Plutonium	.10
1706	The Chemical Identification of Isotopes Formed in the Bombardment of Uranium with High-Energy Particles (*41 pp*)	.20
1707	The Determination of Silica in Beryllium Metal Powder	.05
1724	Physical Properties of Chlorotrifluoroethylene Polymers as a Function of Molecular Weight—II. Molecular Fractionation, Density, Viscosity, Molecular Weight and the Correlation of these Properties of Chlorotrifluoroethylene Polymers (*36 pp*)	.20
1732	Effects of Electron Beams on Aqueous Dichromate Solutions (*3 pp*)	.05
1824	Survey of Studies on the Valence States of Some Secondary Fission Products (*10 pp*)	.10
1859	Color Production in Lithium Fluoride by Radiation (*7 pp*)	.10
1909	Exchange Reactions of Uranium Ions in Solution (*8 pp*)	.10
1910	The Radiocolloidal Properties of Some Fission Products	.10
1933	Isolation of Actinium (Ac^{227}) (*4 pp*)	$.05
1947	Preparation of Low Activity Radiocobalt-Ray Sources	.05
2098	Disintegration of Mesotrons in B^{10} (*2 pp*)	.05
2111	Segré Chart (Revised April 1948)	.60
2124	Investigation of Plutonium Hydride (*2 pp*)	.05

Instruments

194	Process Monitor, Mark 10, Model 20 (*c.d.*)	.20
346	Differential Pressure Indicator (*47 pp*)	.25
557	Neutron Spectrometer Circuits (*23 dwgs*)	2.75
594	Model 260 Sweep (*1 dwg*)	.15
794	Mercury Slug Flowmeter	.05
839	A Fast Coincidence Circuit with Pulse Height Selection (*5 pp*)	.05
1052	A Combined Shutter and Projection Device for the Alignment of Electrodes in Spectrographic Analysis (*4 pp*)	.10
1065	Photographic Film as a Pocket Radiation Dosimeter (*7 pp*)	.10
1099	Ionization Chamber for Carbon-14 Measurements (*4 pp*)	.05
1331	Walkie-Poppie—A Portable Battery-Operated Proportional Type Alpha Survey Counter (*10 pp*)	.10
1502	The Clinton Walkie-Talkie and Scale of Two (*8 pp*)	.10
1646	Tungsten Wire Straightener (*2 pp*)	.05
1856	A Pressure Ionization Chamber for the Measurement of Neutron Fluxes At Tolerance Level in Portable Instruments (*12 pp*)	.10
1972	A Radiation Dose Integrator of High Sensitivity (*8 pp*)	.10
1978	RC Ohmmeter (*4 pp*)	.05
2004	Special Container (*3 dwgs*) Los Alamos	.80
2025	Recording Type Automatic Geiger Tube Calibrator (*7 pp*)	.10
2049	An Investigation of the Input Grid Current of the Type 959 Acron Tube Used as an Electrometer Tube	.10

Metallurgy and Ceramics

776	Method for the Preparation of Butt-Welded Thermocouples Using 3-Mil Diameter Wire (*6 pp*)	.10
1163	Ceramics and Nucleonics	.05
1333	Fabrication of Gold-Beryllium Alloys (*4 pp*)	.05
1448	Crushing Strength of Aluminum Tubes (*6 pp*)	.10

MDDC or AECD		Price
1880	The Preparation of Very Thin Plastic Films (*3 pp*)	$.05
1851	Uranium, Thorium, and Beryllium Melting and Fabrication (*9 pp*)	.10

Physics

512	The Slow Neutron Cross Section of Water as a Function of Energy (*4 pp*)	.05
626	Berkeley Isotope Chart	.60
639	Boron Absorption of Resonance Activation (*1 p*)	.05
729	University of California Synchrotron Drawings (*7 dwgs*)	1.45
730	Internal Cyclotron Targets (*8 pp*)	.10
743	The Introduction to the First Issue of Applied Mathematical Series of the National Bureau of Standards (*2 pp*)	.05
768	Ultra Short Duration Flash Radiographs (*5 pp*)	.05
770	Transient Response of Damped Linear Network with Particular Regard to Wideband Amplifiers (*20 pp*)	.10
782	Van de Graaff Ion Source with Axial Magnetic Field (*3 pp*)	.05
792	Atomic Power Engineering (*20 pp*)	.10
841	Meteorological Equipment of the Hanford Engineer Works (*14 pp*)	.10
846	The Slowing Down of Neutrons in Air (*7 pp*)	.10
872	The Total Netron Cross Section of Rhenium and Neodymium (*6 pp*)	.10
879	The Absolute Measurement of Thermal Neutron Density (*4 pp*)	.05
1034	Cosmic-Ray Induced Fission (*3 pp*)	.05
1035	Reflection Spectra of Neutrons From Crystals (*9 pp*)	.10
1036	The Diffraction of Neutrons by Crystals II (*21 pp*)	.10
1080	Los Alamos Fast Reactor (*1 p*)	.05
1086	Graphical Surface Area Calculations (*18 pp*)	.10
1088	Activation in Unimolecular Reactions (*2 pp*)	.05
1145	Some Excitation Functions of Alphas and Deuterons on Bismuth (*2 pp*)	.05
1162	The Trochotron—A Crossed-Field-Type Mass Spectrometer (*10 pp*)	.10
1292	Inelastic Scattering of Fast Neutrons (*1 p*)	.05
1307	The Outgassing of Materials in a Vacuum (*4 pp*)	.05
1310	Drift Tube Design in Linear Proton Accelerator (*6 pp*)	.10
1323	Methods of Driving A High *Q* Cavity With Many Self-Excited Oscillators (*3 pp*)	.05

MDDC or AECD		Price
1350	Alpha-Particle and Deuteron Tracks in Eastman NTA Photographic Plates (*4 pp*)	$.10
1351	Differential D(*d,n*)He^3 Cross Section for 10 Mev Deuterons (*4 pp*)	.05
1358	An Anomaly in the Study of Dielectric Constant (*1 p*)	.05
1420	"Shielded Contact" Grounding Key for Electrometers (*2 pp*)	.05
1424	Water Boiler (*3 pp*)	.05
1428	Apparatus for Measuring Young's Modulus and Decrement of Graphite and Metals (*12 pp*)	.10
1491	Advancement in Industrial Radiography (*3 pp*)	.05
1704	Summary Report on Neutron Counter Work (*17 pp*)	.10
1834	The Thermodynamics of Gaseous, Cuprous Chloride Monomer and Trimer (*15 pp*)	.10
1853	Half-Scale Model Tests on the Three Quarter Wave R. F. System for the 184-Inch Frequency Modulated Cyclotron (*28 pp*)	.15
1889	Scintillation Counting with Anthracene (*6 pp*)	.10
1932	Stopping of Fission Fragments (*6 pp*)	.05
1943	Neutron Density, Point Source and Plane Source (*7 pp*)	.10
1973	Photographic Neutron Dosimetry II (*7 pp*)	.10
2111	Segré Isotope Chart (*Revised*)	.60
2131	Comparison of the Variation-Theory and End-Point Results for Tamped Spheres (*2 pp*)	.05
2173	Calculations for use with the Fast Neutron Meter (*4 pp*)	.05

Abstracts

The *Nuclear Science Abstracts* are now available at a semiannual subscription rate of $3.75 for twelve (12) issues (one volume, including the cumulated subject and author index) starting with the July 1, 1948 issue. Single copies are 30¢ each. Individuals who have previously purchased single issues may subscribe for the remainder of the volume on a pro rata basis.

Vol. I, No. 1.	Nuclear Science Abstracts (*76 pp*) (July 15, 1948) AECD 2024–2064	.30
Vol. I, No. 2.	Nuclear Science Abstracts (*60 pp*) (July 30, 1948) AECD 2065–2083	.30
Vol. I, No. 3.	Nuclear Science Abstracts (*67 pp*) (August 15, 1948) AECD 2084–2103	.30
Vol. I, No. 4.	Nuclear Science Abstracts (*52 pp*) (August 30, 1948) AECD 2104–2141	.30
Vol. I, No. 5.	Nuclear Science Abstracts (*64 pp*) (September 15, 1948) AECD 2142–2168	.30

ABSTRACTS

CHEMICAL PUBLICATIONS

Natural variations in the isotopic content of boron and its chemical atomic weight, H. G. Thode, J. MacNamara, F. P. Lossing, C. B. Collins (McMaster Univ., Hamilton, Ontario), *J. Am. Chem. Soc.* **70,** 3008–3011 (1948). The isotopic constitution of boron obtained from widely separated geological deposits was measured using mass spectrometers equipped with automatic recording devices. The samples, obtained as borates, were converted to boric acid and then to boron trifluoride. The ratio of B^{11}/B^{10} was found to vary from 4.27 to 4.42, or about 3.5%, depending on the boron source. The chemical atomic weight of boron was found to vary from 10.82078 to 10.82580.

A synthesis of isoguanine labeled with isotopic nitrogen, A. Bendich, J. F. Tinker, G. B. Brown (Sloan-Kettering Inst. for Cancer Research, New York), *J. Am. Chem. Soc.* **70,** 3109–3113 (1948). Described is a synthesis of isoguanine, starting with malononitrile and thiourea, which permits the introduction of N^{15} in the 1 and 3 positions. Synthetic isoguanine was compared in detail with natural isoguanine. 2-Thioladenine, 2-carboxymethylthioladenine, 2,6-diaminopurine, and adenine were also synthesized.

Reactions of ions in aqueous solution with glass and metal surfaces, J. W. Hensley, A. O. Long, J. E. Willard (Univ. of Wisconsin, Madison), *J. Am. Chem. Soc.* **70,** 3146–3147 (1948). The sorption of sodium, silver, and cesium ions on glass and various metals was studied by immersing small flat samples in a solution of the radioactively tagged ion, removing, rinsing, drying and counting the residual activity. Soft glass samples flamed prior to immersion showed a much greater rate of sorption than those cleaned only by water and vapor degreasing. The apparent activation energy was the same, however (approximately 10,000 cal/mole).

Photo-disintegration of deuterium and beryllium by thorium C″ γ-rays, D. J. Allan, M. J. Poole (Atomic Energy Research Estab., Harwell, England), *Nature* **162,** 373–374 (1948). By placing 300 mc of radium-thorium in the center of spheres of beryllium and heavy water, respectively, the ratio between the photo-disintegration cross sections for beryllium and deuterium for 2.62-Mev γ-rays was found to be 0.35 ± 0.01. The neutron flux from the sources was measured by slowing the neutrons down in a large water tank and measuring the β-activity of manganese detectors placed in the tank. A second determination using a long counter in the water tank gave a cross section ratio of 0.36 ± 0.03.

Formation of hydrogen peroxide in water irradiated with X- and α-rays, P. Bonet-Maury, M. Lefort (Institut du Radium, Paris), *Nature* **162,** 381–382 (1948). The effect of 0.9-A.U. X-rays and polonium or radon α-rays on water was studied, and the effect of dissolved oxygen and temperature on the yield of hydrogen peroxide was determined. The results are in agreement with the theory that for X-rays the hydrogen atoms formed by the ionizing radiation remain near the hydroxyl groups formed. In the absence of oxygen, they combine to form water but, with oxygen, hydrogen peroxide is formed. Along the trajectory of an α-particle, the hydroxyl groups remain isolated from the hydrogen atoms and hence react to produce hydrogen peroxide whether or not oxygen is present.

Isotopic assignment of the α-activity of samarium, N. Feather (Univ. of Edinburgh, Scotland), *Nature* **162,** 412 (1948). Recent work indicates that the α-activity previously assigned to Sm^{148} should really be assigned to Sm^{152}. Feather points out that this new result is more compatible with other evidence than is the old conception.

Spectrum of helium-3, L. C. Bradley, H. Kuhn (Clarendon Lab., Oxford Univ., England), *Nature* **162,** 412–413 (1948). The arc spectra of samples enriched in He^3 were investigated using a technique which permits the investigation of faint satellites very close to strong lines. The He^3 line was found to have a separation of 0.83 ± 0.03 cm^{-1} from the He^4 line. The theory of isotope shifts of two-electron spectra due to mass effects gives for the line $2^1S—3^1P$ a shift of 0.77 cm^{-1}.

Evidence of geological age against decay of tin-115 to indium-115 by electron capture, L. H. Ahrens (Univ. of Cambridge, England), *Nature* **162,** 413–414 (1948). Only a doubtful trace (equal to or less than 0.0001% indium) was found by

UNIVERSITY OF MICHIGAN LIBRARIES

spectrographic analysis in the oldest known specimen of cassiterite ($2{,}100 \times 10^6$ yr). This indicates that the relative abundance of In^{115} in natural indium, and the paucity of Sn^{115} in natural tin cannot be attributed to electron capture decay of Sn^{115} during earth periods. The half-life for such decay, if it occurs, is equal to or greater than 5.0×10^{12} yr.

Observations on slow mesons of the cosmic radiation, U. Camerini, H. Muirhead, C. F. Powell, D. M. Ritson (Oxford Univ., England), *Nature* **162,** 433–438 (1948). Experiments are described which indicate that the negative mesons of mass $\sim 200 m_e$ present in cosmic radiation even when captured by heavy atoms, rarely, and perhaps never, produce disintegrations of nuclei with the emission of heavy charged particles. The observations made give support to the theory that the capture of light negative mesons leads to the emission of a neutron and a neutretto. The mean life-time of heavy mesons is calculated to be $6 \pm 3 \times 10^{-9}$ sec.

Oxidation of ferrous ions in aqueous solutions by X- and γ-radiation, N. Miller (Univ. of Edinburgh, Scotland), *Nature* **162,** 448–449 (1948). The rate of oxidation of ferrous ions in dilute sulfuric acid solution by X- and γ-radiation is independent of the concentration of ferrous ions in the region 10^{-3} to $10^{-4} M$, and does not depend on the wavelength of the radiation over a wide range of wavelengths. The average ionic yield (number of Fe^{++} ions oxidized per 32.5 ev expended in the solution) for solutions containing dissolved oxygen was 5.5, and for oxygen-free solutions was found to be 2.2.

Decay and capture of slow mesons in dielectrics, H. Fröhlich, R. Huby, R. Kolodziejski, R. L. Rosenberg (Univ. of Bristol, England), *Nature* **162,** 450–451 (1948). Fermi, Teller and Weisskopf have estimated that negative mesons having an energy of about 1000 ev take approximately 10^{-13} sec to reach the K-orbit of an atomic nucleus, losing energy in the process. In this paper, reasons are given for believing that in dielectrics the time required for a meson to reach the K-orbit is longer than estimated by Fermi *et al.*, but it is not possible on theoretical grounds to say whether or not this time is of the same order ($\sim 2 \times 10^{-6}$ sec) as the meson decay time.

Relation between the masses of mesons, J. Destouches (Univ. de Paris), *Nature* **162,** 451–452 (1948). The principle of associated particles proposed by Destouches-Février leads to the possibility of the existence of two particles of spin 1 or 0 and of masses more than 900 m_e. Experimental results agree with the relation between the meson masses m_μ and m_π given by this principle.

Thorium and uranium content of the Velence Mountains, Hungary, A. Szalay (Univ. of Debrecen, Hungary), *Nature* **162,** 454–455 (1948). Using portable battery-operated G-M counting equipment, the acid eruptive rocks of the Velence Mountains were found everywhere to contain similar concentrations of thorium and uranium, namely, about 8–9 gm uranium per 1000 kg rock, and 40–60 gm thorium per 1000 kg rock. These deposits cannot be worked economically at present. The age of the rocks may be determined by the thorium and uranium content.

Radiations and health, A. S. McFarlane, *Nature* **162,** 480–481 (1948). The importance of keeping down accumulated radiation dosage both to tissue and reproductive cells is stressed. A review is given of the symposium on the therapeutic applications of radioactive isotopes held at the recent Cambridge meeting of the British Medical Association.

. . . I. W. RUDERMAN

LIFE SCIENCE PUBLICATIONS

The urinary excretion of radioactive iodine as an aid in the diagnosis of hyperthyroidism, J. McArthur, R. Rawson, R. Fluharty, J. Means (Thyroid Clinic, Massachusetts General Hosp., Cambridge), *Ann. Internal Med.* **29,** 229–237 (1948). The finding of a low urinary excretion of radioiodine aided in establishing the diagnosis of Graves' disease in clinically equivocal cases. The finding of a high urinary excretion of radioactive iodine was of assistance in excluding Graves' disease in borderline cases in which a truly basal metabolic rate could not be obtained. The exclusion of Graves' disease has been facilitated in patients exhibiting hypermetabolism due to alcoholism, anxiety, compensated hypertensive cardiovascular disease, parkinsonism, pheochromocytoma and thyrotoxicosis factita. The diagnosis of Graves' disease in those patients exhibit-

ing an intermediate excretion of radioactive iodine must be established by other clinical and laboratory findings. Use of a G-M counter following administration of a tracer dose of radioiodine enables the location of thyroid tissue to be established when doubt exists.

The use of radioactive isotopes in immunological investigation—I. Precipitin reactions with ovovitellin containing P^{32}, G. Francis, A. Wormall (Medical College of St. Bartholomew's Hospital, London), *Biochem. J.* **42,** 469–474 (1948). P^{32}-labeled vitellin and lipovitellin were isolated from eggs laid by hens injected with inorganic phosphate labeled with P^{32}, and were used in precipitin reactions. The amount of antigen in the specific lipovitellin-antivitellin precipitates can easily be determined by use of these labeled antigens. In other experiments P^{32}-labeled egg lipid was used to determine the role of egg phosphatides in the lipovitellin-antivitellin reaction. Evidence was obtained that lipovitellin-antivitellin precipitates contained a much higher ratio of phosphatide P^{32} to protein P^{32} than did the lipovitellin antigens. This preferential carrying down of phosphatide by the precipitate is specific, and it does not occur in the precipitin reactions unrelated to vitellin such as the precipitation of human serum proteins by their antibodies.

Lethal effect of absorbed radioisotopes on plants, J. Spinks, E. Cumming, R. Irwin, T. Arnason (Univ. of Saskatchewan, Saskatoon), *Can. J. Research* **26,** 249–262 (1948). The lethal dose of radiophosphorus and radiostrontium for wheat barley and sunflower seeds is approximately 1.4 microcuries per seed (0.05 rd). The distribution of phosphorus in a five-week wheat plant as indicated by radioautograph is fairly uniform. The distribution of radiostrontium is very uneven with practically all of the isotope being concentrated in the first two leaves.

The effect of vitamin deficiencies upon the metabolism of cardiac muscle in vitro—II. The effect of biotin deficiency in ducks with observations on the metabolism of radioactive carbon-labeled succinate, R. Olson, O. Miller, Y. Topper, F. Stare (Harvard School of Public Health and Harvard Med. School, Boston), *J. Biol. Chem.* **175,** 503–514 (1948). Oxygen consumption of heart slices of biotin-deficient ducks was less than that of pair-fed controls. The conversion of pyruvate to non-lactate products was reduced 48% in heart slices from biotin-deficient ducks. $C^{14}O_2$ production from carboxyl-labeled succinate in heart slices from biotin-deficient ducks was decreased 55% from that of pair-fed controls. Prior intraperitoneal administration of biotin-deficient ducks restored respiration and pyruvate utilization of heart slices to normal.

Synthesis of carboxyl-labeled DL-tryptophan from hydantoin containing isotopic carbon, H. Bond (Exptl. Biol. and Med. Inst., Natl. Inst. of Health, Bethesda, Md.), *J. Biol. Chem.* **175,** 531–534 (1948). Isotopic hydantoin has been prepared in 57% yield from C^{13} potassium cyanide. DL-Tryptophan labeled in the carboxyl group has been prepared from C^{13}-hydantoin in 59% yield.

The metabolism of americium in the rat, K. Scott, D. Copp, D. Axelrod, J. Hamilton (Univ. of California, San Francisco and Berkeley), *J. Biol. Chem.* **175,** 691–704 (1948). No appreciable absorption took place in the digestive tract after administration of americium by stomach tube. Twenty-four hours after parenteral administration, 55% of the total amount absorbed from the site of injection was deposited in the liver and 20% in the skeleton. Americium was heavily deposited in the region of the trabecular bone below the epiphysis at the endosteal and periosteal surfaces of the shaft and throughout the cortical bone in the region of small blood vessels. Two plates are presented.

The deposition of uranium in bones—I. Animal studies, M. Neuman, W. Neuman, B. Mulryan (School of Medicine and Dentistry, Univ. of Rochester, N. Y.), *J. Biol. Chem.* **175,** 705–709 (1948). The deposition of injected uranium in bone was found to be directly related to growth activity. Young rats of both sexes showed a greater concentration than older animals of uranium in bone.

The deposition of uranium in bone—II. Radioautographic studies, M. Neuman, W. Neuman (School of Medicine and Dentistry, Univ. of Rochester, N. Y.), *J. Biol. Chem.* **175,** 711–714 (1948). Radioautographs of bone showed U^{235} to be deposited only in the mineral portions and to be especially concentrated on surfaces adjacent to circulation and areas of calcification. Little redistribution occurred. As growth and calcification continued, new bone accumulated over the lines of

UNIVERSITY OF MICHIGAN LIBRARIES

deposition, and resorption of bone was inhibited to some extent because of the insolubility of uranium-impregnated bone salt. Several plates are shown.

The deposition of uranium in bone—III. The effect of diet, W. Neuman, M. Neuman, E. Main, B. Mulryan (School of Medicine and Dentistry, Univ. of Rochester, N. Y.), *J. Biol. Chem.* **175,** 715–720 (1948). Alkaline and acidic diets did not affect the rate of mobilization of skeletal uranium in rats. A rachitogenic diet increased the rate of mobilization. The half-life of skeletal uranium in rats was around 50 to 60 days.

The urinary excretion of citrate in uranium poisoned rats, F. Haven, C. Randall (School of Medicine and Dentistry, Univ. of Rochester, N. Y.), *J. Biol. Chem.* **175,** 737–743 (1948). Urinary excretion of citrate rose 3 to 4 times normal in 3 days when rats were given a single intraperitoneal dose of uranium nitrate. Return to normal level was followed by a secondary rise of equal magnitude. Tolerance to uranium could be acquired and was explained on the basis of the formation of a soluble complex with citrate within the kidney tubule, thus protecting against toxic action.

Biosynthesis of penicillins—II. Utilization of deuterophenylacetyl-N^{15}-DL-valine in penicillin biosynthesis, O. Behrens, *et al.* (Lilly Research Laboratories, Indianapolis, Ind.), *J. Biol. Chem.* **175,** 765–770 (1948). Preparation of deuterophenylacetyl-N^{15}-DL-valine is given. Benzyl penicillin was isolated following use of this as a precursor. The phenylacetyl portion of the precursor was incorporated directly into the penicillin molecule. Very little N^{15} on the other hand was found in the penicillin. Thus the role of the amide portion is still unknown.

On the absorption of phospholipides, C. Artom, M. Swanson (Bowman Gray School of Med., Wake Forest College, Winston-Salem, N. C.), *J. Biol. Chem.* **175,** 871–882 (1948). Labeled phospholipides were fed by stomach tube to rats. Part of the phospholipide was split off in the gastrointestinal tract, so that the phosphate radical was absorbed in inorganic form. Evidence is presented that a detectable portion of the ingested phospholipides can be absorbed as the intact molecule.

Evidence against the occurrence of a tricarboxylic acid cycle in Azotobacter agilis, J. Karlsson, H. Barker (Div. of Plant Nutrition, Univ. of California, Berkeley), *J. Biol. Chem.* **175,** 913–922 (1948). The enzymes involved in the substrate oxidation in *Azotobacter agilis* are in general adaptive. The existence of a reaction chain from α-ketoglutarate through succinate, fumarate, malate, and pyruvate to acetate is supported by the finding that each of the more reduced compounds causes adaptation to all the more oxidized ones. But since the lower compounds do not cause adaptation to the higher ones as the tricarboxylic acid theory would require, this cycle cannot be operative for pyruvate or acetate in this organism.

The utilization of carbon dioxide by the mature rat in the formation of fatty acids, J. Schubert, W. Armstrong (Dept. of Physiolog. Chem., Univ. of Minnesota, Minneapolis), *Science* **108,** 286 (1948). The incorporation of labeled carbon dioxide into fatty acids of rats was studied. It was shown that a very small fraction of the administered carbon dioxide was incorporated into the saturated fatty acids and, to an even lesser extent, into unsaturated fatty acids. The carboxyl carbon isotope concentration of the saturated fatty acids was approximately two times as high as the average of the rest of the fatty acid carbons. The specific activities of C^{14} in the glycerol portion of the fat molecule was about ten times greater than those of the corresponding mixed fatty acids. It was indicated that the C^{14} derived from labeled carbon dioxide is present on the odd carbon atoms of the fatty acids. The mechanism of the incorporation is derived from the tricarboxylic acid cycle.

The path of carbon in photosynthesis—II Amino acids, W. Stepka, A. Benson, M. Calvin (Radiation Lab., Dept. of Chem., and Div. of Plant Nutrition, Univ. of California, Berkeley), *Science* **108,** 304 (1948). The amino acid constituents of the green algae Chlorella and Scenedesmus D-3 were examined after exposure to $C^{14}O_2$. The radioactive amino acids photosynthesized by Scenedesmus in 30 seconds include aspartic acid predominantly and some alanine. When the radioactive amino acids were synthesized in the dark (1 minute) by preilluminated (10 minutes) Scenedesmus and separated, the predominant radioactive product was aspartic acid with some alanine. Corresponding results were obtained when Chlorella was used. The positive determination of the absence of radioactive glutamic acid is taken as evidence against

the participation of the tricarboxylic acid cycle in the anabolic path of carbon dioxide in photosynthesis.

The quantitative theory of autoradiography illustrated through experiments with P^{32} in the chick embryo, H. Branson, L. Hansbrough (Graduate School, Howard Univ., Washington, D. C.), *Science* **108,** 327–328 (1948). The autographic technique was used to determine the distribution of P^{32} between the embryo and blastoderm. The techniques and interpretation of results reveal that the procedure is capable of giving quantitative results.

Radiocardiography: A new method for studying the blood flow through the chambers of the heart in human beings, M. Prinzmetal, E. Corday, H. Bergman, L. Schwartz, R. Spritzler (Institute for Med. Research, Cedars of Lebanon Hosp., Los Angeles), *Science* **108,** 340–341 (1948). The passage of radioactive substances through the cardiac chambers can be graphically recorded by a specially constructed ink-writing Geiger-Müller counter. The method consists of placing a carefully shielded G-M tube over the pre-cordium, rapidly injecting 0.1 to 0.2 mc of radiosodium into one of the antecubital veins, and recording the counts by means of a newly devised direct-writing counter. The curve records the concentration of the radiosodium in the structures underlying the tube. Radiocardiograms are shown of a normal patient and of two patients with rheumatic heart disease, mitral and aortic valvulitis.

The formation of monoiodotyrosine from radioiodine in the thyroid of rats and man, K. Fink, R. Fink (Birmingham Veterans Administration Hosp., Van Nuys, Calif.), *Science* **108,** 358–359 (1948). Investigation of the multiple radioactive substances found in the filter paper chromatograms of thyroid hydrolysates indicates that monoiodotyrosine acts in the metabolism of iodine by the thyroid gland.

. . . BERNARD KANNER

PHYSICAL PUBLICATIONS

The angular distribution of D-D neutrons scattered by deuterons, J. F. Darby, J. B. Swan (Univ. of Melbourne, Australia), *Australian J. Sci. Research* **1A,** 18–27 (1948). The method used included a cloud chamber in which the recoil deuteron tracks from heavy methane (CD_4) were observed. The bombarding neutron energies were in the vicinity of 2.5 Mev (produced by a D-D reaction). The procedure in reducing the observations eliminates tracks hitting the walls and includes correction for possible proton recoils. The back-scattering maximum is found to be six times the minimum, which occurs at a scattering angle of 90–100°, and the distribution in angle agrees somewhat better with the results expected from ordinary than with those from exchange forces as calculated by Buckingham and Massey.

Ein beta-spectrometer hoher lichtstarke, W. Zunti (Univ. of Zurich, Switz.), *Helv. Phys. Acta* **21,** 179–180 (1948). A discussion of the resolution and intensity of magnetic lens beta-spectrometers. Use of a ring focus gives a resolving power of 1.3% for transmission of 2.7%.

Origine de l'effect de température sur le tube de Geiger-Müller á alcool-argon, G. Joyet, M. Sunion (Univ. of Lausanne, Lausanne, Switz.), *Helv. Phys. Acta* **21,** 180–183 (1948). The effect of a temperature change on the plateau curves of counters is traced to absorption of the alcohol in various materials in the counter.

Sur la mesure de la concentration en uranium des plaques Ilford D, imprégnées et la determination de sections efficaces de fission, C. Haenny, O. Rochat (Univ. of Lausanne, Lausanne, Switz.), *Helv. Phys. Acta* **21,** 186–188 (1948). A study was made of the fission tracks in photographic plates as a method of measuring the cross section for the process under study, especially with weak sources of neutrons. Slow neutrons gave a value of 4.9×10^{-24} cm^2 ($\pm 30\%$).

Anregungs-niveaux des Au^{197}-kernes, O. Huber, R. Steffen, F. Humbel (Univ. of Zurich, Switz.), *Helv. Phys. Acta* **21,** 192–194 (1948). The various gamma rays emitted are investigated by means of their conversion electrons in a beta spectrometer. A 77-kev gamma is emitted with a 65-hr half-life. A 25-hr *K*-capture is coupled with the emission of 135 and 165-kev gammas. Conversion coefficients are given.

Der zerfall der goldisotope Au^{194}, Au^{195} und Au^{196} durch electroneneinfang, R. Steffen, O. Huber, F. Humbel, W. Zunti (Univ. of Zurich, Switz.), *Helv. Phys. Acta* **21,** 194–197 (1948). Disintegration schemes are given on the basis of electron spectra and conversion lines observed.

Relative wirkungsquerschnitte fur den (γ,n)-prozess mit der lithium-gamma-strahlung (quantenenergie $h\nu$ = 17.5 Mev), H. Waffler, O. Hirzel (Univ. of Zurich, Switz.), *Helv. Phys. Acta* **21,** 200–203 (1948). The relative cross sections for the photoneutron effect using 17.5-Mev gamma rays was found for 36 nuclei from N^{14} to Au^{197}, using the beta activity of the residual nucleus for detection. The counter readings were corrected for self-absorption in the irradiated sample. An approximate value of the absolute cross section is given for Cu^{63}, taken as 100 on the relative scale.

Kernphotoeffect an kohlenstoff unter aussendung von alphateilchen, H. Hanni, V. L. Telgadi, W. Zunti (Univ. of Zurich, Switz.), *Helv. Phys. Acta* **21,** 203–204 (1948). The reaction $C^{12} + h\nu \rightarrow 3He^4$ is discussed with respect to the energy distribution of the alpha particles. It may occur in two steps, with $Be^{8*} + He^4$ being the intermediate one. The cross section for the process is of the order of 10^{-29} cm^{-2}.

Untersuchung der n-p reaktion an phosphor, F. Metzger, F. Alder, P. Huber (Univ. of Basel, Switz.), *Helv. Phys. Acta* **21,** 278–288 (1948). The reaction P^{31} (n,p)S^{31} was investigated using P_2O_5 in an ionization chamber irradiated with 3-Mev neutrons. The Q value for transition to the ground state was -0.97 ± 0.13 Mev, with an excited state 0.7 Mev above. The cross section for 3-Mev neutrons was $(7.4 \pm 1.5) \times 10^{-26}$ cm^2 and, by varying the angle of the D-D neutrons used, the variation with neutron energy was found.

Measurements on the east-west asymmetry of cosmic-rays at Lahore, India (22° N.), O. P. Sharma, H. R. Sarna (Government College, Lahore, India), *Indian J. Phys.* **22,** 19–25 (1948). A triple-coincidence counter telescope was used at a number of zenith angles, the asymmetry being greatest at an angle of 30° with the zenith.

A study of the RaE β-spectrum from absorption measurements, N. N. Das Gupta, A. K. Chaudhury (Univ. College of Science, Calcutta, India), *Indian J. Phys.* **22,** 27–38 (1948). The spectrum is obtained by varying the absorber thickness between the sample and the counter. With the range-energy relation and the stopping power of the absorber, the number of electrons of various energies can be calculated from the number penetrating the absorbers. The spectrum, plotted as a function of energy, agrees better with the Konopinski-Uhlenbeck than with the Fermi theory.

Resolution of devices actuated by random events, P. G. Klemens (Univ. of Sydney, Australia), *Phil. Mag.* **39,** 656–660 (1948). An investigation was made of the behavior of a device that uses (1) a time t_1 following a recorded event during which no event can be recorded, and (2) a time t_2 following the failure to record an event before which none can be recorded. Thus the ensuing recovery time may be either lengthened or decreased.

Ranges in air and mass identification of plutonium fission fragments, S. Katcoff, J. A. Miskel, C. W. Stanley (Los Alamos Scientific Lab., N. Mex.), *Phys. Rev.* **74,** 631–638 (1948). Fission fragments, obtained by neutron irradiation of plutonium, collimated, and passed through various distances of air at 12 or 14 cm pressure, deposited themselves on the nearest of a series of very thin Zapon films (of low stopping power compared with the air). Differential and integral range curves were plotted for each of the activities exhibited by radiochemical analysis of the films for individual fission products. Extrapolated ranges in air at 15° C and 76 cm vary from 2.90 cm for mass 83 to 1.95 cm for mass 157. The range-mass curve allows the definite assignment of certain masses to corresponding activities.

Proton stopping power of solid beryllium, C. B. Madsen, P. Venkateswarlu (Univ. of Copenhagen, Denmark), *Phys. Rev.* **74,** 648–649 (1948). The energy loss of protons in penetrating beryllium foils was measured by the change in accelerating potential required to give resonance radiation from a thin aluminum target. The gamma-ray yield from the targets as a function of accelerating voltage with and without the interposed beryllium foil gave the specific stopping power for protons of Be. The experimental points fit with a curve (theoretical) corresponding to an average ionization energy of 64 $\pm$ 5 ev.

Mass spectrographic mass assignment of radioactive isotopes, R. J. Hayden (Univ. of Chicago, Ill.), *Phys. Rev.* **74,** 650–655 (1948). A more efficient ion source utilizing the heating of oxides of active fission products on a tungsten filament is incorporated into a mass spectrograph. The types of ionic emission are described for various elements. The spectrograph gives the mass of the radioisotopes, using a counter to determine activity along the photographic plate which acts as detector.

Some measurements of gamma-ray energies, F. N. D. Kurie, M. Ter-Pogossian (Washington Univ., St. Louis, Mo.), *Phys. Rev.* **74,** 677–682 (1948). Isotopes which appear to decay by *K*-capture may actually give off very slow positrons which are annihilated in the *K*-shell. An examination of the gamma radiation of such elements was therefore instituted. In the course of spectrometer calibration by Cu^{64} annihilation radiation, the Compton distribution indicated the presence of annihilation radiation from positrons in flight. Be^{7} and Cr^{51} gave off gammas of 485 and 320 kev, respectively, sufficiently far from the annihilation radiation energy to preclude the possibility of their representing the suggested process.

The beta- and gamma-rays of Rb^{86}, D. J. Zaffarano, B. D. Kern, A. C. G. Mitchell (Indiana Univ., Bloomington), *Phys. Rev.* **74,** 682–686 (1948). An ion-exchange column was used to separate the Rb^{86} from Cs^{134}. The beta- and gamma-ray spectra of the Rb isotope were investigated by using a magnetic-lens spectrometer and photoelectrons ejected from a lead radiator to locate the energy of the gamma. This proved to be 1.081 Mev. Two beta-ray groups were inferred from the Fermi plot, with endpoints of 1.822 and 0.716 Mev, the latter presumably in cascade with the gamma. Deviation from linearity in the Fermi plot at the high-energy end of the spectrum is attributed to the second forbidden nature of the transition.

On the β-decay of mesons, J. J. Horowitz, O. Kofoed-Hansen, J. Lindhard (Univ. of Copenhagen, Denmark), *Phys. Rev.* **74,** 713–717 (1948). The possible methods of beta decay of cosmic-ray mesons are discussed—and in particular the alternative of decay into an electron-neutrino plus a neutral meson. This process lends itself to treatment on the same basis as beta decay of nuclei, the *ft* value (where *f* is the Fermi integral and *t* the half-life) being of the same order of magnitude as for the lightest beta-active nuclei. The calculations are compared with experimental data on the energy of decay electrons from cosmic-ray mesons and the masses of the mesons.

Short-lived isomers of nuclei, S. DeBenedetti, F. K. McGowan (Oak Ridge National Lab., Tenn.), *Phys. Rev.* **74,** 728–735 (1948). A search was made for short-lived isomeric states (half-lives from 10^{-3} to 10^{-6} sec), using two Geiger counters in a delayed coincidence circuit of variable delay time. One counter counts the gamma rays from the isomeric state (or the conversion electrons resulting from them); the other counter counts the beta rays emitted in going to this isomeric state. The isotopes investigated were, therefore, limited to those resulting from a beta decay. In these cases the gamma rays will be strongly converted because of the high degree of forbiddenness of the transition from the metastable (isomeric) state. The excited states found in this region of half-life are Ta^{181*} (22 μsec) Re^{187*} (0.65 μsec), Tm^{169*} (1 μsec) and, Tm^{171*} (2.5 μsec). A list is also given of isotopes giving negative results.

Radioactive Kr isotopes, L. L. Woodward, D. A. McCown, M. L. Pool (Ohio State Univ., Columbus), *Phys. Rev.* **74,** 761–764 (1948). Alpha-particle bombardment of enriched Se^{74} produces an activity of 1.1-hr half-life, assigned to Kr^{77}. It decays by positron emission, *K*-capture, and gamma emission. The 1.42-day isotope of Kr is produced by an (α,n) reaction on enriched Se^{76}, and is assigned to Kr^{79}. This isotope is also found to give positrons and gamma rays and to decay by *K*-capture as well. The cross-section ratio for production of the two isotopes by alpha-particle bombardment of selenium is given. Kr^{85} has been produced by a $Se(\alpha,n)$ reaction.

On the angular distribution in nuclear reactions and coincidence measurements, C. N. Yang (Univ. of Chicago, Ill.), *Phys. Rev.* **74,** 764–772 (1948). General theorems regarding the angular distribution from nuclear reactions and disintegrations are derived on the basis of invariance of the processes under inversion and rotation. The theorems give the general form of the outgoing angular distribution as a function of the orbital angular momentum of the incoming waves, and similar relations. In particular, the correlation between the electron and neutrino in beta decay, as well as that between successive gammas and a successive beta- and gamma-ray from a given nucleus, is derived for various order multipoles. Extension can be made to mesons and to relativistic velocities.

The isotopic constitution of europium, gadolinium, and terbium, D. C. Hess (Univ. of Chicago, Ill.), *Phys. Rev.* **74,** 773–778 (1948). Using a circuit which varied the magnetic field in the mass spectrometer, the ion current was measured as the mass number axis was scanned. By measuring the height for a

UNIVERSITY OF MICHIGAN LIBRARIES

given mass number at different times, the variation of ion emission was determined. The accuracy of the proportionality of peak height to isotopic abundance was better than one percent. The abundances of two europium, one terbium, and seven gadolinium isotopes were measured, and an upper limit set to the existence of others.

Polarization and direction of propagation of successive quanta, D. R. Hamilton (Princeton Univ., N. J.), *Phys. Rev.* **74,** 782–788 (1948). The correlation between the polarization of one quantum and the direction of propagation of another, successively emitted, is derived. Methods of finding transitions of quadrupole and dipole character from coincidence measurements are discussed, and assignment of relative parities of the three levels can be made.

Elastic scattering of high energy nucleons by deuterons, G. F. Chew (Univ. of Chicago, Ill.), *Phys. Rev.* **74,** 809–816 (1948). The *n-d* and *p-d* elastic scattering cross sections (total and angular distribution) are calculated for energies of 90 and 350 Mev, using the Born approximation as applied to Serber's mixed potential. At 90 Mev this may overestimate the total cross section by 30%, while at 350 Mev, relativistic corrections will be serious. The total *n-d* cross section, found to be about half of *n-p* cross section at the same energy, is sharply confined to small angles. It is concluded that the cross sections for nucleons in light nuclei are not additive, and that the elastic scattering is never negligible, so that one cannot neglect the deuteron binding.

Some probability distributions connected with recording apparatus, C. Domb (Cambridge Univ., England), *Proc. Cambridge Phil. Soc.* **44,** 335–341 (1948). By use of the Laplace transform, the probable number of counts recorded by a recording apparatus of finite resolving time for a given intensity of radiation is calculated and extended to the case of a variable dead time.

A note on the calculation of the spacing of energy levels in a heavy nucleus, I. N. Sneddon, B. F. Touschek (Univ. of Glasgow, Scotland), *Proc. Cambridge Phil. Soc.* **44,** 391–403 (1948). With a model of two Fermi-Dirac gases (neutrons and protons) corresponding to the assumption of an interaction that is small compared to the kinetic energies, distribution of a given excitation energy among the nucleons and the density of the energy levels is calculated without using thermodynamic relations. Application is made to the spherical shell model of the nucleus.

The half-life of thorium C′, J. M. Hill (Cambridge Univ., Cambridge, England), *Proc. Cambridge Phil. Soc.* **44,** 440–446 (1948). By use of a coincidence circuit including a delay line instead of a variable resolving time, the effect of random delay times in the alpha and beta counters used was eliminated, as was the effect of different delay times for the different particles. (Indications from the experiment were that the alpha particles are recorded with slightly less delay.) By variation of the time in the delay line, the difference in times between the emission of alphas and betas was established and the half-life was determined as $(3.0 \pm 0.15) \times 10^{-7}$ sec.

Design study for a ten-Bev magnetic accelerator, W. M. Brobeck (Univ. of California, Berkeley), *Rev. Sci. Instr.* **19,** 545–551 (1948). The design of a proton synchrotron to reach an energy of ten billion electron volts is discussed. It includes a well-focused steady beam injected by a Van de Graaff generator at an energy of 4 Mev, and betatron action prior to the start of synchrotron action to bring the protons to one-third the velocity of light (55-Mev energy). The protons can thus be kept in an orbit of approximately constant radius by using a three-to-one frequency ratio in synchrotron operation. Radiation losses from protons at these energies are negligible. The magnet design proposed includes a gap of eight inches and a width of four feet for a ring-type magnet of eighty-foot radius. The flux density variation cycle is given, the central flux change required for betatron action being provided by an auxiliary coil around the inner leg.

Technique for observing nuclear disintegrations and scattering in small gas volumes, R. F. Taschek (Los Alamos Scientific Lab., N. Mex.), *Rev. Sci. Instr.* **19,** 591–594 (1948). A non-planar scattering chamber of small gas volume (less than 3 cm^3) is described. It contains an associated Faraday cage and proportional counter, which is mounted on a ground joint to vary the angle of observation. The geometry is extensively discussed and use of the chamber as a neutron source is pointed out. A differential pulse height

(Continued on page 91)